

# SANDIA REPORT

SAND2015-4123

Unlimited Release

Printed May 26, 2015

# High Fidelity Forward Model Development for Nuclear Reactor Spent Fuel Technical Nuclear Forensics

Matthew R. Sternat

Prepared by  
Sandia National Laboratories  
Albuquerque, New Mexico 87185 and Livermore, California 94550

Sandia National Laboratories is a multi-program laboratory managed and operated by Sandia Corporation, a wholly owned subsidiary of Lockheed Martin Corporation, for the U.S. Department of Energy's National Nuclear Security Administration under contract DE-AC04-94AL85000.

Approved for public release; further dissemination unlimited.



**Sandia National Laboratories**

Issued by Sandia National Laboratories, operated for the United States Department of Energy by Sandia Corporation.

**NOTICE:** This report was prepared as an account of work sponsored by an agency of the United States Government. Neither the United States Government, nor any agency thereof, nor any of their employees, nor any of their contractors, subcontractors, or their employees, make any warranty, express or implied, or assume any legal liability or responsibility for the accuracy, completeness, or usefulness of any information, apparatus, product, or process disclosed, or represent that its use would not infringe privately owned rights. Reference herein to any specific commercial product, process, or service by trade name, trademark, manufacturer, or otherwise, does not necessarily constitute or imply its endorsement, recommendation, or favoring by the United States Government, any agency thereof, or any of their contractors or subcontractors. The views and opinions expressed herein do not necessarily state or reflect those of the United States Government, any agency thereof, or any of their contractors.

Printed in the United States of America. This report has been reproduced directly from the best available copy.

Available to DOE and DOE contractors from

U.S. Department of Energy  
Office of Scientific and Technical Information  
P.O. Box 62  
Oak Ridge, TN 37831

Telephone: (865) 576-8401  
Facsimile: (865) 576-5728  
E-Mail: [reports@adonis.osti.gov](mailto:reports@adonis.osti.gov)  
Online ordering: <http://www.osti.gov/bridge>

Available to the public from

U.S. Department of Commerce  
National Technical Information Service  
5285 Port Royal Rd.  
Springfield, VA 22161

Telephone: (800) 553-6847  
Facsimile: (703) 605-6900  
E-Mail: [orders@ntis.fedworld.gov](mailto:orders@ntis.fedworld.gov)  
Online order: <http://www.ntis.gov/help/ordermethods.asp?loc=7-4-0#online>



# **High Fidelity Forward Model Development for Nuclear Reactor Spent Fuel Technical Nuclear Forensics**

Matthew R. Sternat  
International Nuclear Threat Reduction  
Sandia National Laboratories  
P.O. Box 5800  
Albuquerque, New Mexico 87123-1136

## **Abstract**

The fidelity of the forward model within a spent fuel forensic analysis system was improved by using two unique methodologies. The first consisted of developing a system to create accurate one-group neutron cross-section libraries for any user specified reactor system. In such, a detailed model is developed using the depletion code MONTEBURNS. During MONTEBURNS execution, cross-section libraries are generated at every user specified burnup step in time. These libraries could be developed for many reactor systems, then housed in a database and used for analyzing unknown fuel samples. The forensic analysis system for spent fuel resulted in higher accuracy at predicting the initial uranium isotopic compositions and burnup from spent fuel samples. Using this method, the error in results was reduced from the order of 1-6% down to less than 1% when recovering a fuel sample's burnup and initial uranium isotopic composition.

The second method consisted of implementing 2D/3D reactor depletion codes as the forward model within the system's framework. This method would allow the usage of potentially recoverable geometric information from an unknown sample. No predetermined cross-section library is required for the system using this method, therefore potentially reducing model error associated with the neutron flux spectrum. The accuracy of the recovered initial uranium isotopic compositions and burnup from spent fuel samples was also improved using this method, even more so than the first. For MTR reactors, the error using this method was significantly reduced and was driven to below 0.5%. However, additional research may be required to determine the ideal fission yield and recoverable energy per fission for cases where significant amounts of  $^{239}\text{Pu}$  are bred and burned throughout the life of the fuel.

INTENTIONALLY LEFT BLANK

# CONTENTS

ABSTRACT.....	3
CONTENTS.....	5
FIGURES.....	7
TABLES.....	9
NOMENCLATURE.....	10
1 INTRODUCTION.....	11
1.1 Inverse problems .....	11
1.2 Nuclear Reactors .....	11
1.3 Nuclear Forensics .....	12
1.3.1 Spent Reactor Fuel Forensics .....	13
2 FORWARD MODELS.....	14
2.1 Reactor Depletion Code Systems .....	14
2.1.1 ORIGEN .....	14
2.1.2 MCNP6/CINDER .....	14
2.1.3 MONTEBURNS .....	15
3 SPENT REACTOR FUEL INVERSE ANALYSIS SYSTEM.....	17
3.1 Previous Work.....	17
3.1.1 Analytic Initial Uranium Isotopic Composition and Fuel Burnup Prediction....	17
3.1.2 Iterative Numerical Optimization .....	20
3.1.3 Fuel Age .....	21
3.2 Improvements to System Accuracy: Higher Fidelity Forward Models.....	22
4 FORWARD MODEL DEVELOPMENT .....	24
4.1 ORIGEN Cross-Section Library Development.....	24
4.1.1 ORIGEN 2.2 Reactor Libraries Included with Code .....	24
4.1.2 Library Creation Algorithm and Code .....	26
4.1.3 Data Management and Compilation .....	28
4.2 2D and 3D Forward Model Implementation.....	31
4.2.1 Input Parameter Analysis .....	31
4.2.2 Code Execution.....	32
5 BENCHMARKS AND RESULTS .....	35
5.1 Materials Test Reactor – Oak Ridge Research Reactor.....	35
5.1.1 ORR Information .....	35
5.1.2 MTR Cross-Section Library Forward Model Benchmarks .....	37
5.1.3 MTR 0D Inverse Analysis Results .....	49
5.1.4 MTR 2D/3D results.....	53
5.2 Pressurized Water Reactor – AP1000.....	55
5.2.1 AP1000 Information.....	56
5.2.2 PWR Cross-Section Library Forward Model Benchmarks .....	60
5.2.3 PWR 0D Inverse Analysis Results .....	68
5.2.4 PWR 2D Reconstruction results .....	70
6 CONCLUSIONS.....	72
7 REFERENCES .....	73
9 DISTRIBUTION LIST.....	75

## FIGURES

Figure 1. Worldwide Map of Countries With Research Reactors .....	12
Figure 2. Worldwide Map of Civilian HEU Inventory by Country.....	12
Figure 3. Spent Research Reactor Fuel ICP-MS Spectrum.....	13
Figure 4. Proof of Concept Spent Fuel Inverse Analysis System from Previous Work .....	17
Figure 5. Schematic of Forensic Inverse Analysis.....	23
Figure 6. Cross-section Library Development Schematic.....	27
Figure 7. ORIGEN Execution Script .....	29
Figure 8. ORIGEN Data Compilation Code.....	30
Figure 9. Spent Fuel Forensics Main Input File .....	32
Figure 10. Spent Fuel Forensics Cross-Section File .....	32
Figure 11. Placeholder Text Example from MONTEBURNS ".inp" File .....	33
Figure 12. Placeholder Text Example from MCNP File.....	33
Figure 13. ORR XY Plane Assembly Dimensions (Expressed in mm) .....	35
Figure 14. ORR Axial Assembly Profile.....	36
Figure 15. ORR Example Core Configuration .....	37
Figure 16. ORR MTR Reactor Full Core Model XY-Plane at Z=0 .....	38
Figure 17. MTR $^{235}\text{U}$ mass variance based on beginning to end of life neutron spectrum changes .....	40
Figure 18. MTR $^{235}\text{U}$ mass difference between ORIGEN simulations using 1-group cross-section libraries created at various burnups in MONTEBURNS 3D model, resulting standard deviation is 0.161%.....	41
Figure 19. MTR $^{238}\text{U}$ mass variance based on beginning to end of life neutron spectrum changes .....	42
Figure 20. MTR $^{137}\text{Cs}$ mass variance based on beginning to end of life neutron spectrum changes .....	43
Figure 21. MTR $^{137}\text{Ba}$ mass variance based on beginning to end of life neutron spectrum changes .....	43
Figure 22. MTR $^{148}\text{Nd}$ mass variance based on beginning to end of life neutron spectrum changes .....	44
Figure 23. MTR $^{148}\text{Sm}$ mass variance based on beginning to end of life neutron spectrum changes .....	45
Figure 24. MTR $^{139}\text{La}$ mass variance based on beginning to end of life neutron spectrum changes .....	46
Figure 25. MTR $^{145}\text{Nd}$ mass variance based on beginning to end of life neutron spectrum changes .....	48
Figure 26. MTR $^{146}\text{Nd}$ mass variance based on beginning to end of life neutron spectrum changes .....	48
Figure 27. MTR $^{145}\text{Nd}$ and $^{146}\text{Nd}$ mass standard deviations from spectrum perturbations.....	49
Figure 28. Error in Reconstructed Burnup using Neutron Spectra at Various Burnup Levels .....	52
Figure 29. Error in Reconstructed $^{234}\text{U}$ Enrichment using Neutron Spectra at Various Burnup Levels .....	52
Figure 30. Error in Reconstructed $^{235}\text{U}$ Enrichment using Neutron Spectra at Various Burnup Levels .....	53
Figure 31. 2D ORR MTR Type Reactor Model XY Plane .....	54

Figure 32. AP1000 Fuel Assembly .....	57
Figure 33. AP1000 Reactor Core Map.....	57
Figure 34. AP1000 Fuel Shuffling Scheme.....	59
Figure 35. Depletion Sequence for AP1000 Equilibrium Core.....	60
Figure 36. PWR $^{235}\text{U}$ mass variance based on beginning to end of life neutron spectrum changes .....	61
Figure 37. PWR $^{238}\text{U}$ Mass variance based on beginning to end of life neutron spectrum changes .....	62
Figure 38. PWR $^{137}\text{Cs}$ Mass variance based on beginning to end of life neutron spectrum changes .....	63
Figure 39. PWR $^{137}\text{Ba}$ Mass variance based on beginning to end of live neutron spectrum changes .....	63
Figure 40. PWR $^{148}\text{Nd}$ Mass variance based on beginning to end of life neutron spectrum changes .....	65
Figure 41. PWR $^{139}\text{La}$ Mass variance based on beginning to end of life neutron spectrum changes .....	66
Figure 42. PWR $^{145}\text{Nd}$ Mass variance based on beginning to end of life neutron spectrum changes .....	67
Figure 43. PWR $^{146}\text{Nd}$ Mass variance based on beginning to end of life neutron spectrum changes .....	67
Figure 44. PWR $^{145}\text{Nd}$ and $^{146}\text{Nd}$ resulting standard deviations.....	68
Figure 45. 2D AP1000 PWR Pincell Model XY plane.....	71

## TABLES

Table 1. ORIGEN 2.2 Reactor Cross-Section Libraries .....	24
Table 2. ORIGEN Cross-Section Data Sources .....	26
Table 3. ORR MTR Simulation Power History.....	38
Table 4. MTR Inverse Analysis Results Using 0D Forward Model with Thermal Cross Sections .....	50
Table 5. MTR Inverse Analysis Results Using 0D Forward Model with 79.02 GWd/MTHM Cross Sections.....	50
Table 6. MTR Inverse Analysis Results Using 0D Forward Model with 158.0 GWd/MTHM Cross Sections.....	50
Table 7. MTR Inverse Analysis Results Using 0D Forward Model with 237.0 GWd/MTHM Cross Sections.....	51
Table 8. MTR Inverse Analysis Results Using 0D Forward Model with 315.9 GWd/MTHM Cross Sections.....	51
Table 9. MTR Inverse Analysis Results Using 0D Forward Model with 394.7 GWd/MTHM Cross Sections.....	51
Table 10. MTR Inverse Analysis Results Using 2D Forward Model.....	55
Table 11. MTR Inverse Analysis Results using 3D Forward Model.....	55
Table 12. AP1000 Design Parameters .....	56
Table 13. AP1000 Reactor Core Dimensions.....	58
Table 14. AP1000 Multiplication Factor Results .....	59
Table 15. Burnup and Batch Duration Results for AP1000 Equilibrium Core .....	60
Table 16. AP1000 PWR Simulation Power History.....	60
Table 17. PWR Inverse Analysis Results Using 0D Forward Model with PWRU Cross Sections .....	68
Table 18. PWR Inverse Analysis Results Using 0D Forward Model with 4.995 GWd/MTHM Cross Sections.....	69
Table 19. PWR Inverse Analysis Results Using 0D Forward Model with 19.53 GWd/MTHM Cross Sections.....	69
Table 20. PWR Inverse Analysis Results Using 0D Forward Model with 29.81 GWd/MTHM Cross Sections.....	69
Table 21. PWR Inverse Analysis Results Using 0D Forward Model with 47.32 GWd/MTHM Cross Sections.....	70
Table 22. PWR Inverse Analysis Results Using 0D Forward Model with 52.84 GWd/MTHM Cross Sections.....	70
Table 23. PWR Inverse Analysis Results Using 2D Forward Model.....	71

## NOMENCLATURE

ABR	Advanced Burner Reactor
AP1000	Westinghouse Electric Company Reactor
DOE	U.S. Department of Energy
DU	Depleted Uranium
ENDF/B	Evaluated Nuclear Data Files – Basic
GWd	Gigawatt Days
HEU	Highly Enriched Uranium
HTGR	High Temperature Gas Reactor
HTR	High Temperature Reactor
HTTR	High Temperature Test Reactor
HM	Heavy Metal
IAEA	International Atomic Energy Agency
INL	Idaho National Laboratory
LEU	Low Enriched Uranium
LWR	Light Water Reactor
MCNP	Monte Carlo N – Particle
MCNPX	Monte Carlo N – Particle Extended
MT	Metric Tons
MTHM	Metric Tons Heavy Metal
PWR	Pressurized Water Reactor

INTENTIONALLY LEFT BLANK

# 1 INTRODUCTION

## 1.1 Inverse problems

In numerical analysis, a standard system is simulated with what is defined as a forward model. In such, a series of differential equations is approximated and based on a set of initial conditions the system parameters are calculated or iterated progressing through a phase space. The phase space may span across parameters such as time, position, direction, or energy. In all cases, you begin with initial conditions and end up with a final solution or system response. A basic example is a system where a ball is dropped from a known height, drag function, and gravitational force. Progressing forward from the time the ball is dropped, the time and velocity expected once it reaches the ground may easily be calculated.

Inverse problems differ such that the system initial conditions are unknown, potentially in addition to system parameters or characteristics. The observable information available is only the final solution or system response. This may be in the form of measurements or observations made where numerous techniques exist to recover information pertaining to the system. In the example of the ball dropping, an inverse problem could exist such that only the velocity of the ball is measured when hitting the ground. The inverse problem would be to recover the time and height of when it was dropped, and potentially the gravitational force and fluid drag function. Unique solutions are not guaranteed with inverse problems, due to the fact that numerous initial conditions may exist to generate the same final measurable conditions or observables.

## 1.2 Nuclear Reactors

Many research reactors exist worldwide with large ranges in operating power, initial enrichment, fuel material form, fuel type, moderator type, coolant type, and purpose. In addition to tremendous variety, the reactors generally operate very dynamically, causing standardized safeguard systems to be troublesome [1]. The spent fuel produced from this dynamic operation has the potential to possess a large variance in output isotopic composition.

There is a total of 678 research reactors worldwide, 241 operating, 413 shutdown, and a few more in either construction phase or unverified status. Twenty percent of all research reactors are located in underdeveloped countries including 40% of operating reactors in 2011 [1]. Figure 1 shows a map displaying countries with research reactors [1].

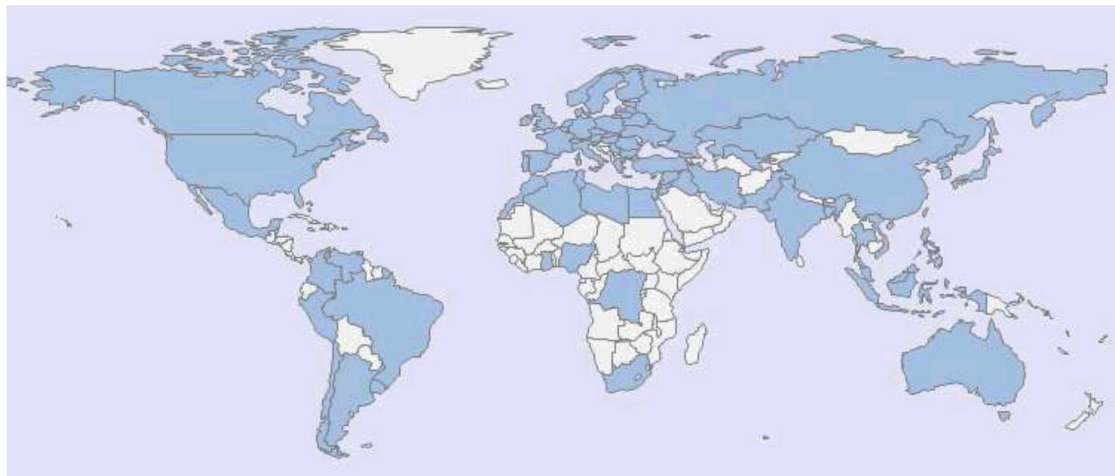


**Figure 1. Worldwide Map of Countries With Research Reactors**

With research reactors, highly enriched uranium (HEU) also becomes a concern. Approximately 130 research reactors operate on highly enriched uranium with enrichments over 90% in  $^{235}\text{U}$  [2]. A map of the worldwide civilian HEU inventory is shown in Figure 2 [2].

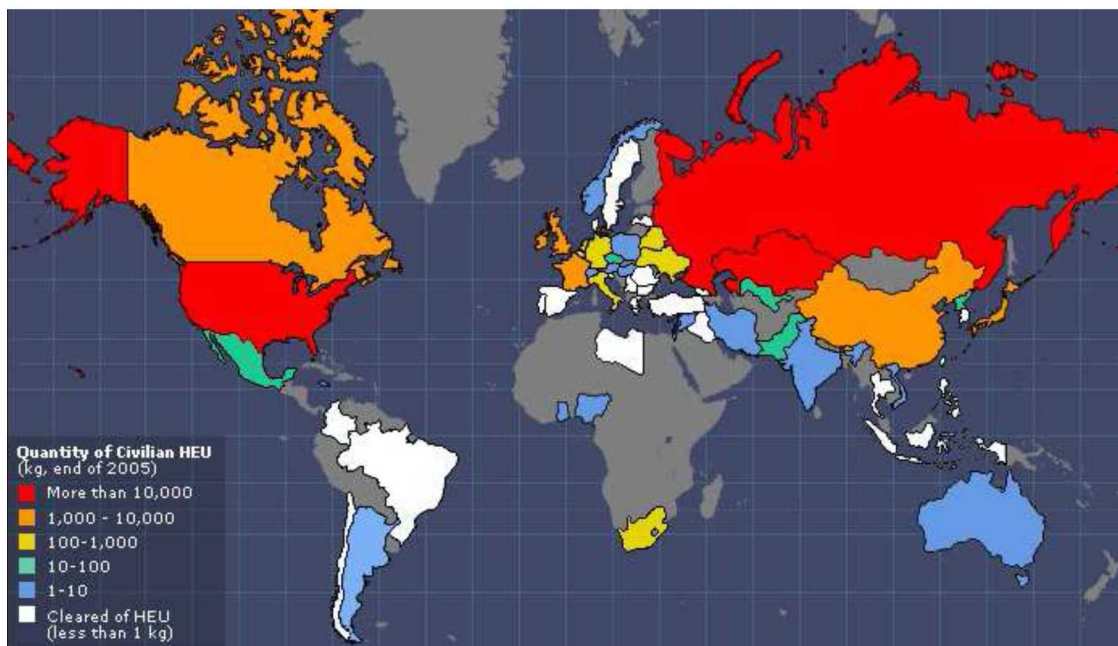


**Figure 2. Worldwide Map of Civilian HEU Inventory by Country.**

Power reactors are also of interest. While power reactor assemblies are significantly larger and heavier than typical research reactor fuel elements, diversion scenarios involving these materials are not impossible. The 434 power reactors worldwide mostly consist of pressurized water reactors (273) or boiling water reactors (81). Nuclear reactors produce around 13% of the world's electricity [3].

### 1.3 Nuclear Forensics

Technical nuclear forensics is a means of how nuclear material is characterized and interpreted through various measurement techniques [4]. This process may include obtaining representative samples of material, laboratory analyses, simulations, and comparison to databases. There are many laboratories in the United States capable of performing nuclear forensic analyses.

Upon completion of a forensic measurement analysis, a sample may be well characterized and the results used to reconstruct identifying information about the sample. Typical nuclear forensic measurements include mass, atomic emission, gamma, and alpha spectrometry. For nuclear forensics purposes, trace nuclides are often desired and can be measured in quantities ranging from nanograms to picograms using mass spectrometry [5]. An example of an inductively coupled plasma mass spectrometry (ICP-MS) analysis for research reactor spent fuel is shown in Figure 3 [9].

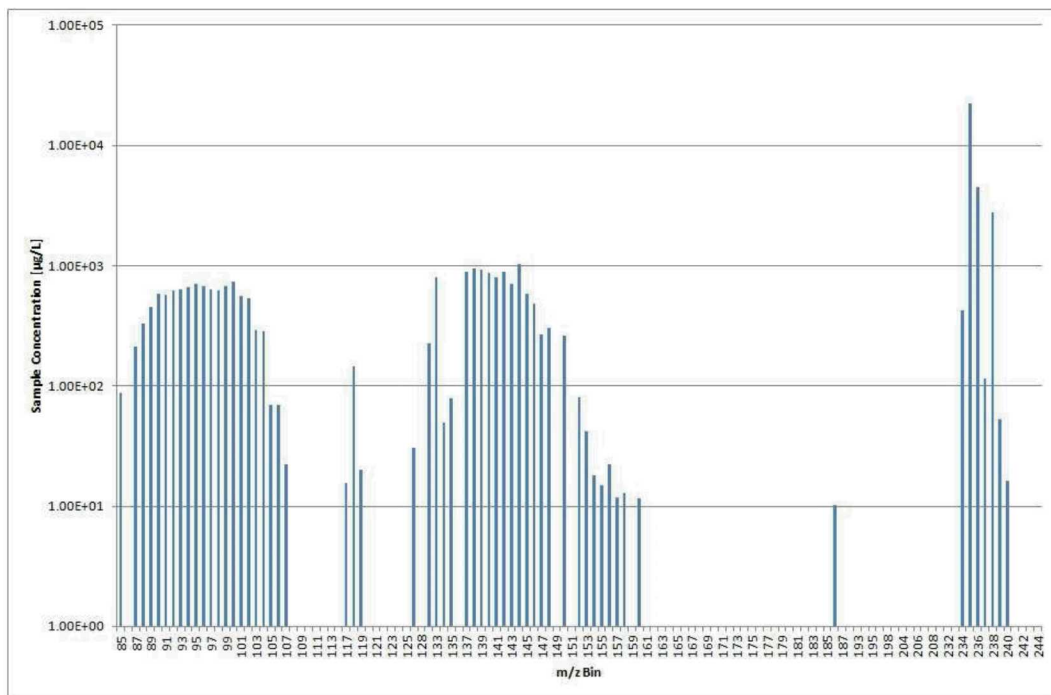


Figure 3. Spent Research Reactor Fuel ICP-MS Spectrum

### 1.3.1 Spent Reactor Fuel Forensics

If spent fuel is found out of regulatory control and is to be analyzed, a representative sample must be acquired. Depending on the nature of the fuel found, it may be challenging to acquire a sample and drilling may be required. Nuclear reactors often do not have spatially flat neutron flux, so precision, expertise, and planning is required in determining a sample acquisition procedure. Upon sample acquisition, the fuel sample will be dissolved in acid and then is able to be analyzed by destructive assay and nondestructive assay techniques.

## 2 FORWARD MODELS

### 2.1 Reactor Depletion Code Systems

State-of-the-art computer code systems were utilized to minimize the error that differs a model from reality. Several code systems were used in this project, each with unique features and advantages. These depletion codes are a type of forward model, where a set of initial conditions for a nuclear system are known. Then progressing forward in time, the system computes the expected changes in material compositions from neutron irradiation, fission, and decay of radioisotopes.

#### 2.1.1 ORIGEN

ORIGEN 2.2 is a code developed by Oak Ridge National Laboratory to burn and decay nuclear fuel. The code utilizes collapsed one group cross sections which are provided for approximately 30 different reactor types. Unfortunately, this cross section library does not contain any specific research reactors; however, a generic thermal library is included. Input materials are broken down into two classes including actinide and non-actinide isotopes which are separate for normalized burnup calculations. An input isotopic vector may be decayed or burned with either constant power or constant flux to any user specified burnup or time period [6].

The resulting spent fuel has many options for output printing which is separated into three classes of isotopes: activation products, actinides, and fission products. While there are approximately 27 different print options for each of these classes of isotopes, only output isotopic masses and activities are useful in this work.

Many research reactors are used for their high flux magnitude capabilities. There are several methods and positions for experimentation to be exposed to this high flux. Unlike reactors that are used for producing power, the flux profile across a research reactor core is not very flat. There is no way to account for spectrum changes or flux shapes when using ORIGEN and a more detailed calculation may be desired [6].

#### 2.1.2 MCNP6/CINDER

MCNP6 is a Monte Carlo transport code that combines features from the MCNPX code with MCNP5, which added charged particle transport along with a variety of other features including CINDER 90 depletion capabilities. Using CINDER in MCNP6 only requires the addition of a BURN card with depletion parameters in a standard MCNP style input. Cell volumes may be required to be added if they cannot be determined by the code. This package performs similar to MONTEBURNS, using alternating depletion and transport calculation steps, but has a few notable differences. CINDER uses Markov chains to solve the series of differential decay equations while ORIGEN 2.2 uses the matrix exponential method [7]. A fractional importance is used in a similar way to MONTEBURNS, but is only based on mass fraction.

In MCNP6/CINDER, only one input file is required. A similar MCNP input is used, but a BURN card is added providing the model depletion parameters. Instead of explicitly listing all isotopes which are to be placed in the output file, one of three tiers of isotopes is chosen. Tier 1 is a basic list compromised of a few common fission products, uranium isotopes and plutonium isotopes. Tier 2 adds additional fission products and actinides to the tier 1 list, while tier 3 includes a very large list of isotopes [7]. MCNP6 was originally considered for implementation into the inverse analysis software, but due to time constraints focus was placed on MONTEBURNS.

### 2.1.3 MONTEBURNS

MONTEBURNS links MCNP to ORIGEN 2.2 and consists of a Perl script and a Fortran executable. Other software requirements for execution include ORIGEN 2.2 and MCNP5; however, simple modifications may be made for usage with MCNPX or MCNP6. During execution, the software package alternates between ORIGEN 2.2 depletion steps and MCNP5 neutron transport calculations. Operation is performed using data saved in text files when passing between codes and calculations. Running the software requires two input files: a MONTEBURNS input file, which contains depletion parameters, and a standard MCNP model using certain format ensuring proper read in from the Perl script [6-8].

A third optional input file, a feed file, may be used for user specified variable time steps, operating power, and input/output of isotopic vectors. Without usage of a feed file, the code burns the fuel the desired time length in equally spaced steps. Variable length time steps are often desired to account for  $^{135}\text{Xe}$  accumulation and other similar effects.

In the MONTEBURNS input file, an ORIGEN 2.2 starting collapsed one-group cross-section library is required. This collection does not include libraries for research reactors, so the thermal library or some representative library is often chosen. In the MCNP steps of execution, reaction rate tallies are performed in addition to total flux tallies. Cross sections are effectively updated in one energy group spectrum collapsed form by calculating the ratio of the MCNP tallied reaction rate to total flux.

The user manual states that up to 49 materials may be burned simultaneously within a model. Multiple materials are desired to create accurate neutron flux and depletion profiles throughout a model in both two and three dimensional simulations. This limit was established by the numbering system for flux tallies in the version of MCNP available during MONTEBURNS development. The present day numbering system allows for significantly more tallies, but an update to the code has not been released yet. Upon testing, the RSICC released version 2.0 only allows for a maximum of 40 materials due to a potential bug in the tally numbering system [7-8].

The code uses a fractional importance system to determine which isotopes produced are critical to include in the transport calculations. In addition to any user specified isotopes, additional isotopes are added based on mass fraction, atomic fraction, absorption cross sections or fission cross sections. When any of these parameters fractionally exceeds the importance factor, that particular isotope is included in the next step's transport calculation but detailed information is not included in the output file. Only user specified isotopes listed on the MONTEBURNS input file are included in the output [8].

### *MCNP5 Version 1.51*

The last working version of MCNP that is usable with MONTEBURNS without modification to the source code is MCNP5 Version 1.51 [8]. Any later version of MCNP has changes in the spacing and control characters in the output file. These changes do not allow the MONTEBURNS code to acquire data from the MCNP outputs.

### 3 SPENT REACTOR FUEL INVERSE ANALYSIS SYSTEM

#### 3.1 Previous Work

Previous work by the project principal investigator developed a proof of concept spent fuel inverse analysis system. The primary goal of the original work was to utilize numerical optimization techniques in an iterative method to recover initial conditions of spent fuel samples. A schematic of the original system is shown below [9].

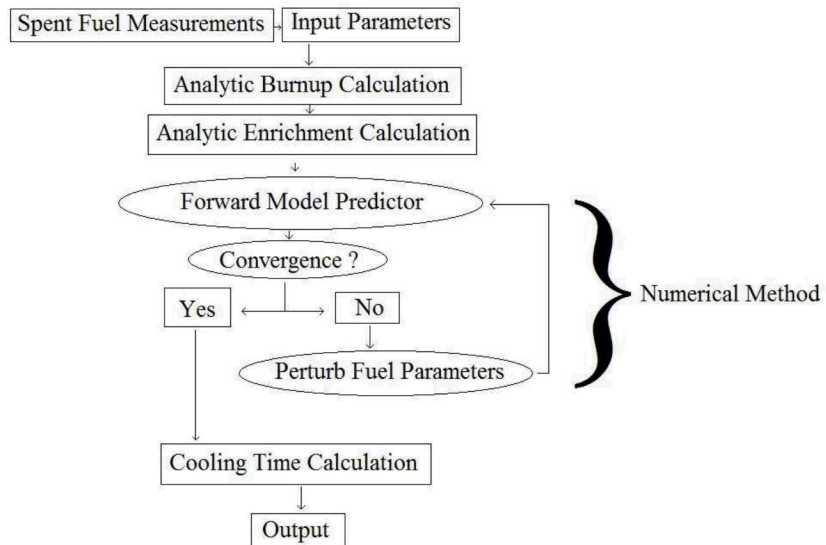


Figure 4. Proof of Concept Spent Fuel Inverse Analysis System from Previous Work

In this system, the forward model predictor used was ORIGEN 2.2 and was severely limited by the accuracy of ORIGEN 2.2's ability to predict spent fuel characteristics with a limited set of cross-section libraries. The iterative numerical system performs an ORIGEN fuel depletion calculation using an initial guess for the original uranium isotopic compositions and the fuel's burnup. Analytic predictors were utilized to improve the system's initial conditions and likelihood of convergence [9].

##### 3.1.1 Analytic Initial Uranium Isotopic Composition and Fuel Burnup Prediction

Spent fuel burnup is defined as the amount of energy produced per initial unit mass of heavy metal fuel. This is most commonly reported in units of GWd/MTHM. For research reactors, burnup is often reported as a percentage of the initial  $^{235}\text{U}$  load. For example a reactor starting with 100g  $^{235}\text{U}$  and ending with 60g  $^{235}\text{U}$  would be referred to as having a 40% burnup. In an inverse analysis, the initial heavy metal fuel load is unknown, so standard burnup units are used. Burnup reconstruction begins by calculating the fission reaction rate,  $RR_f(t)$ , and performing a series of approximations and unit conversions to arrive at Equation 1,

$$BU(T) = \left[ \frac{N^B(T)}{N^{U238}(T)} \right] \left[ \frac{N^{U238}(T)}{N_0^U} \right] \frac{N_a E_R}{M_U Y_B}, \quad (1)$$

where  $N_a$  is Avogadro's constant,  $E_R$  is the average recoverable energy per fission,  $M_U$  is the average molecular mass for uranium in the sample, and  $N_0^U$  is the initial uranium atom concentration. The ratio  $\frac{N^B(T)}{N^{U238}(T)}$  is measured by mass spectrometry,  $N_a$ ,  $E_R$ , and  $Y_B$  are constants, and the final term  $\frac{N^{U238}(T)}{N_0^U}$  is unknown and must be solved for iteratively with  $BU(T)$  [9].

$$\frac{N_0^U}{N^{U238}(T)} = \frac{\frac{N^U(T)}{N^{U238}(T)} + \frac{N^{Np}(T)}{N^{U238}(T)} + \frac{N^{Pu}(T)}{N^{U238}(T)} + \dots}{1 - \frac{M_0^U BU(T)}{N_a E_R}}. \quad (2)$$

A system of two equations (Equations 1 and 2) and two unknowns ( $BU(T)$  and  $\frac{N_0^U}{N^{U238}(T)}$ ) is established. Due to the nonlinearity of the system, an iterative method is used to solve this. The iterations process begins by solving for  $\frac{N_0^U}{N^{U238}(T)}$  with an initial guess of  $BU(T) = 0$ . Alternating steps between 1 and 2 converge after several steps. Larger burnup and higher enrichment lead to slower convergence, but the method is stable regardless [9].

After a sample's burnup is reconstructed, its initial  $^{235}\text{U}$  enrichment can be calculated. This is done by calculating the initial  $^{235}\text{U}$  concentration based on fissioned, transmuted, and measured contributions. Several assumptions are made and the sample's initial  $^{235}\text{U}$  enrichment is calculated using Equation 3:

$$e_0 = \frac{Z^{235} - \frac{\bar{\sigma}_f^{U238}}{\bar{\sigma}_a^{U238}} Z^{238} - \frac{\bar{\sigma}_f^{Pu239}}{\bar{\sigma}_a^{Pu239}} Z^{239} - \frac{\bar{\sigma}_f^{Pu240}}{\bar{\sigma}_a^{Pu240}} Z^{240} - \frac{\bar{\sigma}_f^{Pu241}}{\bar{\sigma}_a^{Pu241}} Z^{241}}{1 - \frac{\bar{\sigma}_f^{U238}}{\bar{\sigma}_a^{U238}} - \frac{\bar{\sigma}_f^{Pu239}}{\bar{\sigma}_a^{Pu239}} \frac{\bar{\sigma}_\gamma^{U238}}{\bar{\sigma}_a^{U238}} - \frac{\bar{\sigma}_f^{Pu240}}{\bar{\sigma}_a^{Pu240}} \frac{\bar{\sigma}_\gamma^{Pu239}}{\bar{\sigma}_a^{Pu239}} \frac{\bar{\sigma}_\gamma^{U238}}{\bar{\sigma}_a^{U238}} - \frac{\bar{\sigma}_f^{Pu241}}{\bar{\sigma}_a^{Pu241}} \frac{\bar{\sigma}_\gamma^{Pu240}}{\bar{\sigma}_a^{Pu240}} \frac{\bar{\sigma}_\gamma^{Pu239}}{\bar{\sigma}_a^{Pu239}} \frac{\bar{\sigma}_\gamma^{U238}}{\bar{\sigma}_a^{U238}}}} \quad (3)$$

where,

$$Z^{235} = \frac{N^{U238}(T)}{N_0^U} \left[ \frac{N^{U235}(T)}{N^{U238}(T)} + \frac{N^{U236}(T)}{N^{U238}(T)} + \frac{N^{Np237}(T)}{N^{U238}(T)} + \frac{N^{Pu238}(T)}{N^{U238}(T)} \right] - \frac{N_0^{U236}}{N_0^U} + \frac{M_U BU(T)}{E_R N_0^U} \quad (4)$$

$$Z^{238} = 1 - \frac{N_0^{U234}}{N^{U238}(T)} \frac{N^{U238}(T)}{N_0^U} - \frac{N_0^{U236}}{N_0^U} - \frac{N^{U238}(T)}{N_0^U} \quad (5)$$

$$Z^{239} = -\frac{N^{Pu239}(T)}{N^{U238}(T)} \frac{N^{U238}(T)}{N_0^U} + \frac{\bar{\sigma}_\gamma^{U238}}{\bar{\sigma}_a^{U238}} Z^{238} \quad (6)$$

$$Z^{240} = -\frac{N^{Pu240}(T)}{N^{U238}(T)} \frac{N^{U238}(T)}{N_0^U} + \frac{\bar{\sigma}_\gamma^{Pu239}}{\bar{\sigma}_a^{Pu239}} Z^{239} \quad (7)$$

$$Z^{241} = -\frac{N^{Pu241}(T)}{N^{U238}(T)} \frac{N^{U238}(T)}{N_0^U} + \frac{\bar{\sigma}_\gamma^{Pu240}}{\bar{\sigma}_a^{Pu240}} Z^{240}. \quad (8)$$

For most fuels, the initial  $^{236}\text{U}$  concentration is zero, but development of a correlation such as this can determine if a HEU spent fuel recycling capability has been used. Historically only the United States and Russia have separated, down blended, and re-enriched spent HEU fuel which could also aid as information in an identification process. A correlation for  $^{234}\text{U}$  is not developed in this manner, due to variation in  $^{234}\text{U}$  content in nature, potential increased fractional enrichment from a HEU recycling program, and minimal documentation on variable fractional enrichment depending on  $^{235}\text{U}$  enrichment method [10].

Another possible method is to use an already developed correlation based on enrichment and re-enrichment of recycled spent nuclear fuel from nuclear power programs. These correlations were developed using fractional enrichments based on the  $^{235}\text{U}$  enrichment. They are not ideal for usage of HEU fuels, but serve well as an initial guess in the inverse method. The correlation for  $^{234}\text{U}$  for gaseous diffusion enrichment processes is [10]:

$$\left(\frac{N^{U234}}{N^{U235}}\right)_0 = 0.008 \left(\frac{N^{U235}}{N^{U238}}\right)_0 \left(\frac{M^{U238}}{M^{U235}}\right) \quad (9)$$

The correlation for  $^{234}\text{U}$  for gaseous centrifuge enrichment is:

$$\left(\frac{N^{U234}}{N^{U235}}\right)_0 = 0.007731 \left(\frac{N^{U235}}{N^{U238}}\right)_0^{1.0837} \left(\frac{M^{U238}}{M^{U235}}\right)^{1.0837}. \quad (10)$$

Either of these two  $^{234}\text{U}$  correlations can be used. The equations were derived from correlations using low enriched power reactor fuel. They are not accurate at high enrichments and only serve as an initial guess for the numerical method. These correlations are expressed as a ratio to the initial  $^{238}\text{U}$  concentration, which is also unknown, so an iterative procedure is used for convergence. Of all the present uranium isotopes, only the  $^{235}\text{U}$  enrichment is known and an iterative procedure is used to solve for the initial  $^{234}\text{U}$  enrichment. Initially in this  $^{234}\text{U}$  predictor, the  $^{238}\text{U}$  enrichment is set to  $1 - e^{U235} - e^{U236}$ . Then using either Equation 9 or Equation 10, the  $^{234}\text{U}$  enrichment is updated. Then the  $^{238}\text{U}$  enrichment is updated again to  $1 - e^{U234} - e^{U235} - e^{U236}$  and the process is repeated alternating  $^{234}\text{U}$  and  $^{238}\text{U}$  enrichment updates until the  $^{234}\text{U}$  converges with itself sufficiently [9].

If only an analytic enrichment solution is desired, a  $^{236}\text{U}$  correction to the analytic  $^{235}\text{U}$  enrichment can be made. This method is derived analytically by subtracting the initial enrichment equation from itself with and without initial  $^{236}\text{U}$  resulting in:

$$e_0 - e'_0 = \frac{N_0^{U236}}{N_0^U} \quad (11)$$

where  $e_0$  is the initial enrichment with initial  $^{236}\text{U}$  and  $e'_0$  is the initial enrichment without  $^{236}\text{U}$ .

The first step in the inverse analysis performs a forward model reactor simulation using the analytic  $^{235}\text{U}$  enrichment and burnup as initial guesses. Initial  $^{234}\text{U}$  and  $^{236}\text{U}$  are predicted using the techniques described previously. The simulation's results are then compared to the interdicted sample's measured data. The initial uranium isotopic concentrations can now be perturbed and the process is repeated, until their corresponding final concentrations from the forward model's results sufficiently converge with the measured data. The  $^{238}\text{U}$  concentration is not solved for directly, but iteratively updated to the remaining enrichment using:

$$\frac{N_0^{U238}}{N_0^{U234} + N_0^{U235} + N_0^{U236} + N_0^{U238}} = 1 - \frac{N_0^{U234} + N_0^{U235} + N_0^{U236}}{N_0^{U234} + N_0^{U235} + N_0^{U236} + N_0^{U238}} \quad (12)$$

It is desirable to have minimal uncertainties in the measured data and accurate cross sections used in the forward model. A correlation established for the initial  $^{236}\text{U}$  concentration would be highly dependent on burnup, a suitable spectrum collapsed cross-section library (for ORIGEN), and uncertainty in the sample's measured data [9].

A large number of assumptions are embedded into the analytic methods which are summarized below:

- The burnup monitor isotope is stable
- The absorption rate of the burnup monitor isotope is negligible
- The initial isotopic concentration of the burnup monitor isotope is zero
- The cumulative fission yield for the burnup monitor isotope is the same for all fission sources
- $^{234}\text{U}$  radiative capture rate is assumed to be zero
- $^{238}\text{U}$  captures decay instantly to  $^{239}\text{Pu}$
- The only fissile isotopes for reconstructing enrichment are:  $^{235}\text{U}$ ,  $^{238}\text{U}$ ,  $^{239}\text{Pu}$ ,  $^{240}\text{Pu}$ , and  $^{241}\text{Pu}$
- (n,2n), (n,3n) fast reactions are ignored for actinides due to their low probability and contribution

### 3.1.2 Iterative Numerical Optimization

In the inverse analysis, the burnup and initial uranium enrichments are updated together until convergence is achieved. The error associated with each reconstructed parameter,  $z$  as an example, is described in:

$$\epsilon_z = \frac{R^{measured} - R^{iterative}}{R^{measured}} \quad (13)$$

The system global error function is minimized in:

$$\epsilon^2 = \epsilon_{U234}^2 + \epsilon_{U235}^2 + \epsilon_{U236}^2 + \epsilon_{BU}^2 \quad (14)$$

A parameter perturbation algorithm is then performed on each reconstructed parameter. Utilizing a steepest descent inverse method, a linear approximation is performed to estimate the initial fuel parameters that will result in minimization of the global error function, shown below for example parameter vector  $z$ :

$$z^{i+1} = z^i + \alpha p \quad (15)$$

where  $\alpha$  is a chosen step length in direction  $p$  based on optimization of error minimization [9].

The forward model and parameter perturbations are repeated until it is sufficiently minimized, however convergence of all parameters is not guaranteed. Due to the  $^{236}\text{U}$  concentration's dependence on burnup and cross sections, the method may result in unrealistic initial  $^{236}\text{U}$  enrichment. If the sample's measured  $^{236}\text{U}$  enrichment exceeds the iterative enrichment, a flag is raised indicating the cross section set or burnup may need further analysis.

One option is to add the  $^{236}\text{U}$  concentration to the burnup convergence criteria. However, this would cause problems and likely add additional error in the burnup reconstruction. If the measured  $^{236}\text{U}$  final enrichment far exceeds the iterative solution, the system will reconstruct an unrealistic initial enrichment and attention to the cross section set or burnup may be required [9].

### 3.1.3 Fuel Age

After numerical convergence of the sample's burnup and initial enrichment, the cooling time since last shutdown, or fuel age, is determined. A cooling time monitor isotope has a simple production method and low interaction cross sections. The sample's cooling time is calculated using the cooling time monitor isotope and inverting the standard decay equation. The decayed burnup monitor isotopic concentration can be measured with mass or gamma spectrometry, but the isotopic concentration at the time of reactor shut- down is unknown. Two options arise for determining the end of power isotopic concentration, the first option is to use a forward model to predict the concentration using the sample's calculated burnup and initial enrichment. Equation 16 uses a measurable isotopic ratio and an isotopic ratio from the predictor, since the  $^{238}\text{U}$  concentration is approximately the same at shutdown and time of measurement:

$$\Delta T_c = -\frac{1}{\lambda^B} \ln \left( \frac{N^B(T_m)}{N^{U238}(T_m)} \frac{N^{U238}(T_{shut})}{N^B(T_{shut})} \right) \quad (16)$$

The second method utilizes a burnup monitor isotope which is produced from fission and does not decay out of its mass bin. In this case, at the end of power the entire mass bin primarily consists of the monitor isotope. After the monitor isotope beta decays, its mass number remains constant. One example would be  $^{137}\text{Cs}$  which decays to the stable  $^{137}\text{Ba}$ . The sum of the isotopic concentrations of all isotopes with the same mass bin as the burnup monitor is used in the same decay equation:

$$\Delta T_c = -\frac{1}{\lambda^B} \ln \left( \frac{N^B(T_m)}{\sum_i N^{B^i}(T_m)} \right) \quad (17)$$

In the case of research reactors, time away from the core or extended shutdown time causes some of the cooling time monitor isotope to decay prior to final shutdown. This will reduce the concentration of the cooling time monitor isotope, while the total mass bin concentration remains constant. A cooling time monitor with a longer half-life relative to the shutdown or time away from power is ideal, but a monitor with a half-life much longer than the sample cooling time may provide inaccurate results. It has been tested to include the fuel age as an iteratively reconstructed parameter instead of a standalone calculation, but improvements were not observed [9].

### 3.2 Improvements to System Accuracy: Higher Fidelity Forward Models

In this research, the accuracy of the spent fuel forensic analysis system is targeted for improvement by implementation of a higher fidelity forward model. By reducing the model error associated with neutron flux spectra, geometric dependence, fuel shuffling, higher burnup, and other effects, the results from the forward model within the inverse analysis will better represent reality than in previous work. As a result of this improvement, it is expected to have higher accuracy in the reconstructed fuel parameters. A schematic of the new system is shown in Figure 5.

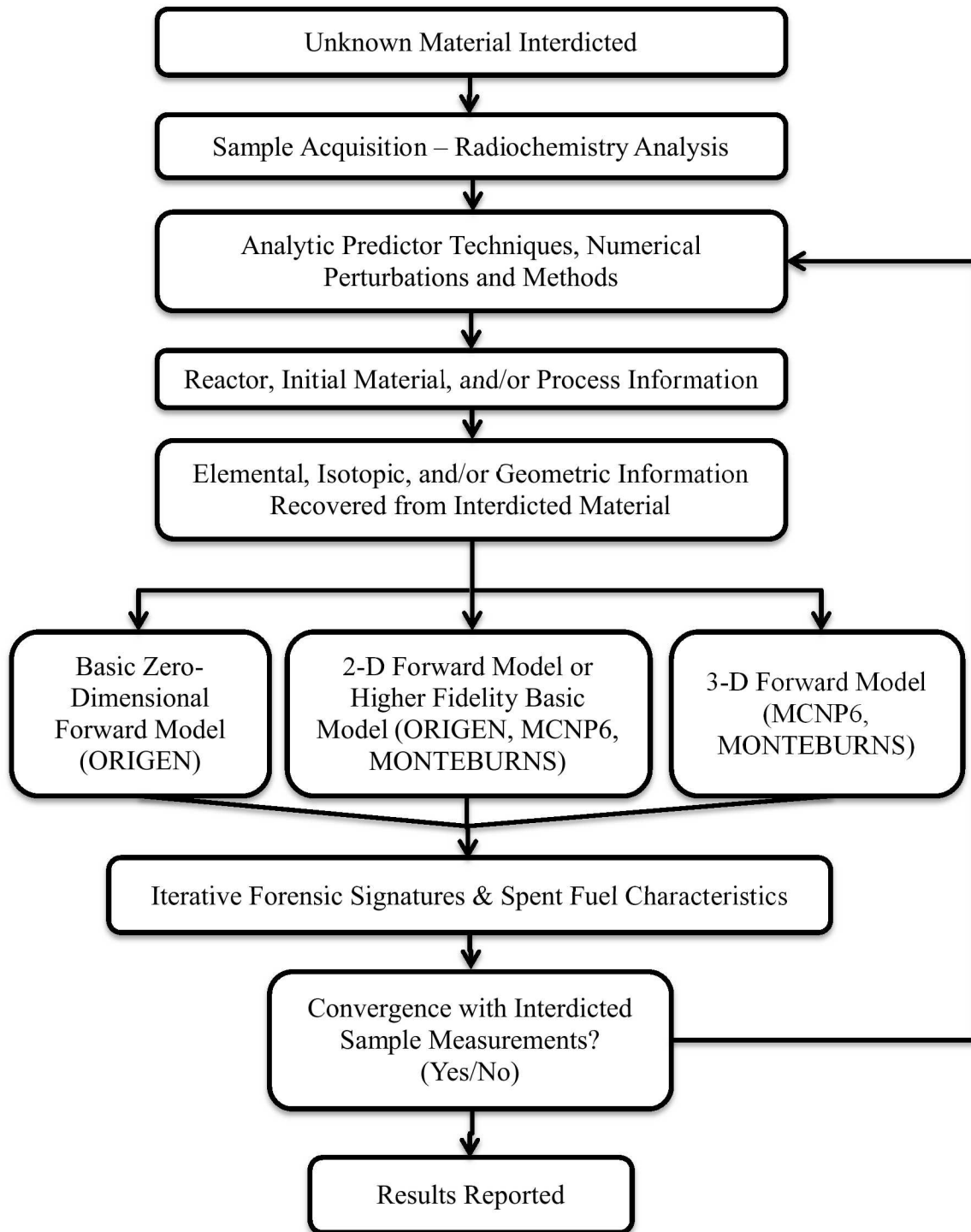


**Figure 5. Schematic of Forensic Inverse Analysis**

## 4 FORWARD MODEL DEVELOPMENT

The goal of this work was to increase accuracy in spent reactor fuel forensic analysis results while minimizing uncertainty. The system developed in previous work utilized ORIGEN 2.2 and was limited to pre-existing nuclear cross-section libraries that came with the code. These 1-group libraries are old, outdated and were developed using conditions that are potentially different than those in operating reactors today.

Within the forensic inverse analysis system, two primary methods were utilized in increasing the forward model fidelity. This included keeping ORIGEN as the forward model, but developing new reactor and condition specific cross-section libraries. This will increase the accuracy of specific forward model calculations by using a neutron flux energy spectrum specific to the system modeled.

The other method to increase the forward model fidelity is to replace the forward model with one that handles geometric information. Depending on the nature of the material interdicted, geometric information may be recovered in a way that will allow either a 2D or 3D reactor depletion simulation to be used as the forward model within the inverse analysis.

### 4.1 ORIGEN Cross-Section Library Development

The reactor depletion code MONTEBURNS, introduced in section 2.1.3, alternates between radiation transport calculations and ORIGEN depletion calculations in user specified time discretization steps. At each of these steps, the code generates a model system specific cross-section library. Upon completion of the code execution, these libraries may be extracted and used with the standard ORIGEN code. This system provides a means to produce reactor specific libraries unavailable with the code's offerings. Creation and extraction of these libraries will enable rapid higher fidelity reactor depletion simulations, otherwise not possible with ORIGEN alone.

However, the code produces a 1-group library based on the neutron flux spectrum at the burnup step it is currently at. Throughout the life of the system modeled, this neutron flux spectrum changes. If a model is to be performed, the burnup level that has the appropriate neutron flux spectrum to model the entire duration of the fuel's life had to be determined.

#### 4.1.1 ORIGEN 2.2 Reactor Libraries Included with Code

The ORIGEN 2.2 code package includes a set of one-group cross-section libraries. These libraries represent specific conditions present in a limited set of reactors. These are described in Table 1.

**Table 1. ORIGEN 2.2 Reactor Cross-Section Libraries**

Library Name	Reactor Type	Description
DECAY	All	Decay properties of radioactive isotopes
GXH2OBRM	All	Photon library: Bremsstrahlung in water
GXUO2BRM	All	Photon library: Bremsstrahlung in $\text{UO}_2$
GXNOBREM	All	Photon library: no Bremsstrahlung
THERMAL	None	0.0253-eV cross sections
PWRU	PWR	$^{235}\text{U}$ enriched $\text{UO}_2$ : 33 GWd/MTHM
PWRPUU	PWR	$^{235}\text{U}$ enriched $\text{UO}_2$ in self-generated Pu recycle reactor
PWRPUPU	PWR	Pu-enriched $\text{UO}_2$ in a self-generated Pu recycle reactor
PWRU3TH	PWR	$\text{ThO}_2$ -enriched with denatured U-233
PWRU50	PWR	$^{235}\text{U}$ enriched $\text{UO}_2$ : 50 GWd/MTHM
PWRD5D35	PWR	$\text{ThO}_2$ -enriched with makeup, denatured $^{235}\text{U}$
PWRD5D33	PWR	$\text{ThO}_2$ -enriched with recycled, denatured $^{233}\text{U}$
PWRUS	PWR	3.2 w/o $^{235}\text{U}$ fuel, 3-cycle PWR to achieve 33 MWd/kg
PWRUE	PWR	4.2 w/o $^{235}\text{U}$ fuel, 3-cycle PWR to achieve 50 MWd/kg
BWRU	BWR	$^{235}\text{U}$ enriched $\text{UO}_2$
BWRPUU	BWR	$^{235}\text{U}$ enriched fuel in a self-generated Pu recycle reactor
BWRPUPU	BWR	Pu-enriched fuel in a self-generated Pu recycle reactor
BWRUS	BWR	3.0 w/o $^{235}\text{U}$ fuel, 4-cycle BWR to achieve 27.5 MWd/kg axial varying moderator density considered
BWRUSO	BWR	3.0 w/o $^{235}\text{U}$ fuel, 4-cycle BWR to achieve 27.5 MWd/kg constant axial moderator density
BWRUE	BWR	3.4 w/o $^{235}\text{U}$ fuel, 4-cycle BWR to achieve 40 MWd/kg
CANDUNAU	CANDU	CANDU with natural uranium
CANDUSEU	CANDU	CANDU with slightly enriched uranium
EMOPUUUC	LMFBR	Early Oxide, LWR-Pu/U/U/U: Core region
EMOPUUUA	LMFBR	Early Oxide, LWR-Pu/U/U/U: Axial blanket region
EMOPUUUR	LMFBR	Early Oxide, LWR-Pu/U/U/U: Radial blanket region
AMOPUUUC	LMFBR	Adv. Oxide, LWR-Pu/U/U/U: Core region
AMOPUUUA	LMFBR	Adv. Oxide, LWR-Pu/U/U/U: Axial blanket region
AMOPUUUR	LMFBR	Adv. Oxide, LWR-Pu/U/U/U: Radial blanket region
AMORUUUC	LMFBR	Adv. Oxide, Recycle-Pu/U/U/U: Core region
AMORUUUA	LMFBR	Adv. Oxide, Recycle-Pu/U/U/U: Axial blanket region
AMORUUUR	LMFBR	Adv. Oxide, Recycle-Pu/U/U/U: Radial blanket region
AMOPUUTC	LMFBR	Adv. Oxide, LWR-Pu/U/U/Th: Core region
AMOPUUTA	LMFBR	Adv. Oxide, LWR-Pu/U/U/Th: Axial blanket region
AMOPUUTR	LMFBR	Adv. Oxide, LWR-Pu/U/U/Th: Radial blanket region
AMOPTTTC	LMFBR	Adv. Oxide, LWR-Pu/Th/Th/Th: Core region
AMOPTTTA	LMFBR	Adv. Oxide, LWR-Pu/Th/Th/Th: Axial blanket region
AMOPTTTR	LMFBR	Adv. Oxide, LWR-Pu/Th/Th/Th: Radial blanket region
AMO0TTTC	LMFBR	Adv. Oxide, Recycle- $^{233}\text{U}$ /Th/Th/Th: Core region
AMO0TTTA	LMFBR	Adv. Oxide, Recycle- $^{233}\text{U}$ /Th/Th/Th: Axial blanket region
AMO0TTTC	LMFBR	Adv. Oxide, Recycle- $^{233}\text{U}$ /Th/Th/Th: Radial blanket region
AMO1TTTC	LMFBR	Adv. Oxide, 14% denatured- $^{233}\text{U}$ /Th/Th/Th: Core region

AMO1TTA	LMFBR	Adv. Oxide, 14% denatured- <sup>233</sup> U /Th/Th/Th: Ax. blanket reg.
AMO1TTTR	LMFBR	Adv. Oxide, 14% denatured- <sup>233</sup> U /Th/Th/Th: Radial blanket region
AMO2TTTC	LMFBR	Adv. Oxide, 44% denatured- <sup>233</sup> U /Th/Th/Th: Core region
AMO2TTTA	LMFBR	Adv. Oxide, 44% denatured- <sup>233</sup> U /Th/Th/Th: Axial blanket region
AMO2TTTR	LMFBR	Adva. Oxide, 44% denatured- <sup>233</sup> U /Th/Th/Th: Radial blanket region
FFTFC	LMFBR	Fast flux test facility: Pu/U
CRBRC	LMFBR	Clinch River Breeder Reactor core
CRBRA	LMFBR	Clinch River Breeder Reactor axial blanket
CRBRR	LMFBR	Clinch River Breeder Reactor radial blanket
CRBRI	LMFBR	Clinch River Breeder Reactor internal blanket

These libraries span a few condition sets of primarily PWR, BWR, and LMFBRs. The data in the libraries origin is shown in Table 2. ORIGEN Cross-Section Data Sources

**Table 2. ORIGEN Cross-Section Data Sources**

Description	Document Number	Date
Summary Report	ORNL-5621	July 1980
(U,Pu) Fuel cycle PWR and BWR	ORNL/TM-6051	September 1978
Alternative fuel cycle PWR	ORNL/TM-7005	February 1980
CANDU models	ORNL/TM-7177	November 1980
LMFBR models	ORNL/TM-7176	October 1981
CRBR models	NUREG/CR-2762	July 1982
Decay and photon libraries	ORNL/TM-6055	February 1979
Revised PWR and BWR models	ORNL/TM-11018	December 1989

All models are relatively dated. In the last 25-30 years reactors have been pushing to higher and higher burnup levels.

#### 4.1.2 Library Creation Algorithm and Code

When a reactor is modeled in the 3D depletion code MONTEBURNS, it is often broken down into individual burnable pieces to generate spatial dependence of reactor burnup. For each material, or piece, of the system modeled and depleted, the code will generate a cross-section library at every burnup step. For systems with many burnable sections and a large number of time steps, a tremendous amount of data is generated. The ORIGEN code has no geometric dependence, so a volume weighted core average of the generated cross sections has to be calculated at every time step.

$$\Sigma_j = \sum_i \frac{\Sigma_{i,j} v_i}{V} \quad (18)$$

A script code was written to perform these calculations effortlessly regardless of the complexity of the original model. A schematic of this process is in Figure 6.

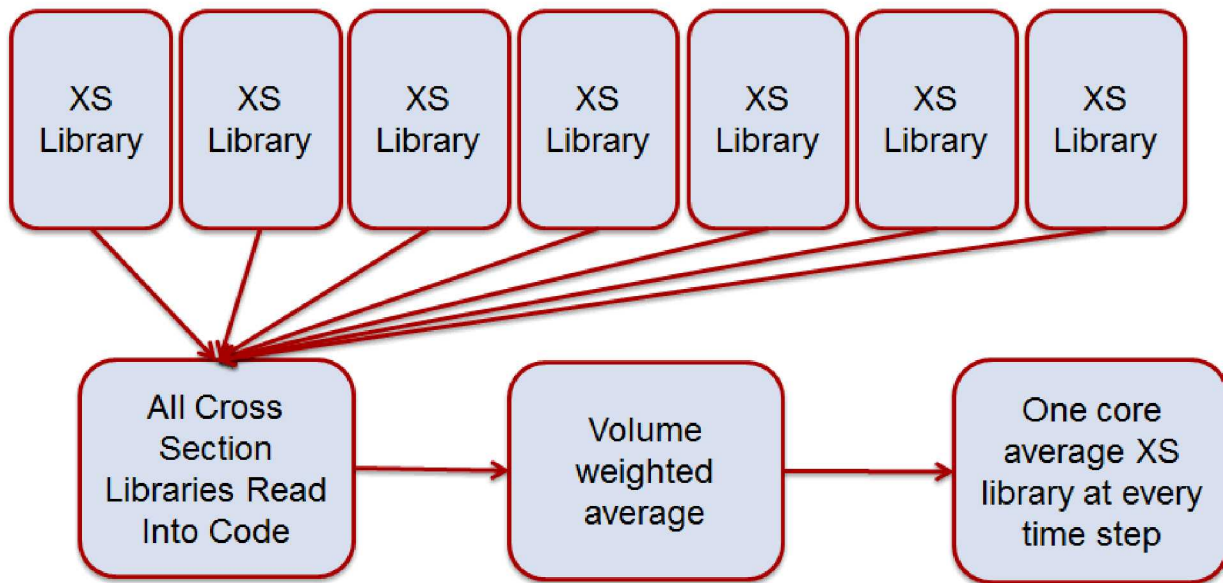


**Figure 6.** Cross-section Library Development Schematic

In order to effectively perform these calculations, an understanding of the ORIGEN cross-section library format was required. The libraries are split into 3 primary sections, including activation products, actinides & daughters, and fission products. Each section has a different number of parameters per isotope and may not include the same number of isotopes as other libraries. An adaptive system was required for any number of isotopes in each section.

The cross-section data for section has similarities and differences. In general, the first line of an isotope's data contains cross-section information. The second line contains fission product yields, which only exists for fission products. However, there were inconsistencies in the data and some isotopes in the fission product section did not include fission yields. The code written had to search for and adapt for the existence of a second line of data for every isotope. An isotope's data is characterized as following:

First card of each library segment:

NLB TITLE

First card for each nuclide:

NLB NUCLID SNG SN2N SN3N (or SNA) SNF (or SNP) SNGX SW2NX YYN

Optional second card for each nuclide:

NLB Y(<sup>232</sup>Th) Y(<sup>233</sup>U) Y(<sup>235</sup>U) Y(<sup>238</sup>U) Y(<sup>239</sup>Pu) Y(<sup>241</sup>Pu) Y(<sup>245</sup>Cm) Y(<sup>249</sup>Cf)

Where:

- NLB = the number of this cross-section and fission product yield library segment
- TITLE = a 72-character alphanumeric cross-section and fission product yield library segment title beginning in column 11
- NUCLID = a six-digit nuclide identifier corresponding to the data on these 1-2 cards

- SNG = the effective, one-group (n,y) cross section of nuclide NUCLID leading to a ground state
- SN2N = the effective (n,2n) cross section of nuclide NUCLID leading to a ground state
- SN3N = the effective (n,3n) cross section of nuclide NUCLID leading to the ground state; actinide segment only
- SNA = the effective, one-group (n,a) cross section of nuclide NUCLID leading to a ground state; activation product and fission product segments only
- SNF = the effective, one-group (n,f) cross section of nuclide NUCLID; actinide segment only
- SNP = the effective, one-group (n,p) cross section of nuclide NUCLID leading to a ground state; activation product and fission product segments only
- SNGX = the effective one-group (n,y) cross section of nuclide NUCLID leading to an excited state of the daughter
- SN2NX = the effective, one-group (n,2n) cross section of nuclide NUCLID leading to an excited state of the daughter
- YYN = a control character indicating whether or not a fission yield card follows
  - YYN > 0.0 = fission yield card follows
  - YYN < 0.0 = no fission yield card follows

This data was read into a script using Perl, then volume weighted averaged, and saved for each burnup step. Using this system generates one group cross-section libraries at various burnup levels. Benchmarks would be needed to determine which library is best suitable for performing simulations using only one library. Using the library that corresponds to the total burnup of the simulation may not produce the most accurate results.

#### **4.1.3 Data Management and Compilation**

The system developed has the ability to produce tremendous amounts of data. The goal was to run ORIGEN using the same model for every cross-section library produced, then compile the results only collecting data for isotopes of interest for analysis. For example, a model with 100 time steps would require 100 ORIGEN code executions with slightly different perturbations on the neutron spectrum and generates 100 sets of results to analyze and compare. Two codes were written to execute and then compile the data for analysis.

The ORIGEN execution script was written in Windows Batch, which iterates a user specified model and repeatedly executes based on the number of cross section libraries. A screen shot of the code is shown in Figure 7. ORIGEN Execution ScriptFigure 7.

```

1 echo off
2 rem Matthew R. Sternat
3 rem Sandia National Laboratory
4 rem ORIGEN Execution script
5 echo ***** running *****
6
7 rem Remove existing tape and output files
8 del tape* output*
9
10 rem Initial Parameters
11 rem -----
12 SET XSDIR=AP1000
13 SET MODEL=prob_0.U5
14 SET /a i=1
15 SET /a j=1
16 SET /a k=53
17 SET /a l=4
18
19 rem Beginning of loop
20 :LOOP
21 copy %MODEL% tape5.inp >nul
22 IF %i%==%k% GOTO END1
23
24 echo This is iteration %i%
25 copy %XSDIR%\TAPE9_%j%.I%i% tape9.inp >nul
26 copy gxuo2brm.lib tape10.inp >nul
27
28 rem ORIGEN execution
29 origentwo
30
31 rem combine and save files from run
32 copy TAPE6.out output%j%_%i%.txt
33 del tape*
34 SET /a i=%i%+1
35 GOTO :LOOP
36
37 rem End of inner loop
38 :END1
39
40 SET /a i=1
41 echo ***** done with mat %j% *****
42 SET /a j=%j%+1
43 IF %j%==%l% GOTO END2
44 GOTO :LOOP
45
46 rem End of outer loop
47 :END2
48 echo ***** done *****
49 echo on
50

```

Figure 7. ORIGEN Execution Script

The next code written compiles all of the data generated from execution. This was written in Perl and extracts the data from a user specified isotope list.

```

1  #!/C:/mb/perl/bin
2  # Matthew Sternat
3  # Sandia National Laboratory
4  # Perl script to converge initial enrichment and burnup values using ORIGEN
5  # Version 1 November 2014
6  use File::Copy;
7  use File::Path;
8  use File::Find;
9  use IO::Select;
10
11 print "Running script...\n";
12 $k=53;
13 $l=4;
14 $y=16;
15
16 @isotope1=("-U234", "U235", "U236", "U238", "CS137", "BA137", "ND148", "LA139", "ND145", "ND146", "NP237", "PU238", "PU239", "PU240", "PU241");
17
18 $filename="results.txt";
19
20 $spaces=119;
21
22 open (output, ">", $filename);
23 select (output);
24
25 # ORIGEN Loops reading all outputs and extracting $isotope's data
26
27 $x=1;
28
29 while ($x<$y) {
30     $j=1;
31     print "Output data for isotope $isotope1[$x]\n";
32     while ($j<$l) {
33         $i=1;
34         while ($i<$k) {
35             $file="output$j\_$_i.txt";
36             #print $stdout "$file\n";
37             open (origen, "<", $file);
38             #print $stdout "test\n";
39             while ($lines = <origen>) {
40                 read(origen, $isotope2, 11);
41                 if ($isotope2 eq $isotope1[$x]) {
42                     read(origen, $isotope3, $spaces);
43                     #print $stdout "test\n";
44                 }
45                 last;
46             }
47             close (origen);
48             printf output "$isotope3\n";
49             $isotope3="";
50             $i++;
51         }
52         $j++;
53     }
54     $x++;
55 }
56
57
58
59
60
61
62
63
64
65
66
67
68

```

Figure 8. ORIGEN Data Compilation Code

## 4.2 2D and 3D Forward Model Implementation

### 4.2.1 Input Parameter Analysis

To execute a 2D or 3D depletion code, many input parameters are required. Geometric information is required to build the model. This information will come from measurements on the unknown fuel sample. Depending on the nature of the sample, there may be enough information to create a 2D or 3D model. The 2D model in this case is actually a 1cm tall 3D model that uses reflective conditions in one dimension, creating the effect of a 2D simulation. Using the geometric information, the fuel meat density and volume can be calculated and are required for the 2D or 3D model.

To fill the spatial regions of the model, material compositions are required. These will come from a series of laboratory measurements and analysis. In particular, the chemical form of the fuel meat is important. The reactor fuel meat may be a mixture of metals, oxides, metals and oxides, or other forms. The system implemented allows for non-heavy metal fuel constituents to be normalized per unit kilogram fuel material. This system allows for iterative updates of the uranium isotopic constituents, while preserving the proper chemical form. Using the fuel meat's material composition, the heavy metal density is required to execute the code. The heavy metal density is used for burnup normalization when combined with the volume of the fuel to calculate its mass.

Other materials include cladding, structural materials, and coolant. The coolant will be difficult to characterize as it may be different in a shipping or transport container than while operating. There also may not be any coolant required to transport an old fuel sample. Expert analysis may be required to determine what operating coolant is used based on an identifiable reactor fuel type.

Additional information is required to approximate the system power. If the reactor type is identifiable from determining the coolant type and geometric information, the approximate average specific power density can be determined. The inverse analysis requires this for 2D and 3D models specified in the units of GW/MTHM. In these units, ORIGEN can be run directly and utilizing other measured information will allow for the 2D or 3D model power to be calculated using Equation 19,

$$P = p_m \rho_{HM} V \quad (19)$$

where,  $P$  is the model power,  $p_m$  is the specific power for the reactor type,  $\rho_{HM}$  is the heavy metal fuel density, and  $V$  is the fuel meat volume. Using this form allows the modeled reactor power to be calculated. An example of each input file is shown in Figure 9 and Figure 10.

```

1 Input file for example
2 PC.....Operating system (PC or UNIX) (reads 4 chars)
3 MB.....Forward model used (ORIGEN/MCNP6/MB) (reads 5 char)
4 2.54.....!U234 measured signature
5 0.00.....!U234 relative uncertainty
6 133.....!U235 measured signature
7 0.000.....!U235 relative uncertainty
8 26.2.....!U236 measured signature
9 0.00.....!U236 relative uncertainty
10 16.0.....!U238 measured signature
11 0.000.....!U238 relative uncertainty
12 0.168.....!Pu239 measured signature
13 0.0.....!Pu239 relative uncertainty
14 0.0992.....!Pu240 measured signature
15 0.0.....!Pu240 relative uncertainty
16 0.0116.....!Pu241 measured signature
17 0.00.....!Pu241 relative uncertainty
18 2.52.....!Cs137 measured signature (gamma spec)
19 0.000.....!Cs137 relative uncertainty (gamma spec)
20 1.41.....!Nd148 measured signature
21 0.00.....!Nd148 relative uncertainty
22 4.54.....!137 mass bin signature
23 0.00.....!137 mass bin relative uncertainty
24 12.....!Number of burnsteps
25 Cs137.....!Burnup method (Nd148 or Cs137)
26 3.4315.....!Power density [GW/MTHM]
27 3.02.....!Measured fuel meat volume
28 0.84437.....!Measured fuel meat HM density
29 1.....!signatures unit [1=mass, 0=atom densities]
30

```

Figure 9. Spent Fuel Forensics Main Input File

```

1 One Group Cross Section file MTRHEU
2 33.3.....!U234 Capture Cross Section
3 0.457.....!U234 Fission Cross Section
4 17.7.....!U235 Capture Cross Section
5 88.5.....!U235 Fission Cross Section
6 15.9.....!U236 Capture Cross Section
7 0.384.....!U236 Fission Cross Section
8 7.09.....!U238 Capture Cross Section
9 0.0972.....!U238 Fission Cross Section
10 87.1.....!Pu239 Capture Cross Section
11 172.....!Pu239 Fission Cross Section
12 250.....!Pu240 Capture Cross Section
13 0.574.....!Pu240 Fission Cross Section
14 70.6.....!Pu241 Capture Cross Section
15 200.....!Pu241 Fission Cross Section
16

```

Figure 10. Spent Fuel Forensics Cross-Section File

## 4.2.2 Code Execution

Several additional files are required in order to execute the inverse analysis using MONTEBURNS as the forward model. Using ORIGEN as a forward model, there are two required inputs; the main input containing the sample measurement information and another containing cross-section data to be used for analytic calculations. Using MONTEBURNS as the forward model, two additional files are required; a skeleton MCNP file that is created using the measured geometric information and material composition and a skeleton MONTEBURNS “.inp” file that includes additional reactor depletion information and isotope tracking. Both of these skeleton files have missing information where placeholder text is present. As the inverse analysis is performed, the code will create copies of these skeleton files. During iterative execution, the placeholder text is replaced with the iterative system information, such as uranium

isotopic information and burnup. Examples of the placeholder text from both skeleton files are shown in Figure 11 and Figure 12.

```

1 ORR 2D XY burnup profile
2 PC ..... ! Type of operating system
3 1 ..... ! Number of MCNP materials to burn
4 11 ..... ! MCNP material number #01 (must be less than 100)
5 sysvol ..... ! Material #01 volume (cc), input 0 to use mcnp value (if exists)
6 syspwr ..... ! Power in MWT (for the entire system modeled in mcnp deck)
7 -200 ..... ! Recov. energy/fis (MeV); if negative use for U235, ratio other isos
8 0 ..... ! Total number of days burned (used if no feed)
9 nsteps ..... ! Number of outer burn steps
10 50 ..... ! Number of internal burn steps (multiple of 10)
11 1 ..... ! Number of predictor steps (+1 on first step), 1 usually sufficient
12 0 ..... ! Step number to restart after (0=beginning)
13 THERMAL ..... ! number of default origin2 lib - next line is origin2 lib location
14 E:/SF_forensics_code
15 .0001 ..... ! fractional importance (track isos with abs,fis,atom,mass fraction)
16 0 ..... ! Intermediate keff calc. (0) No (1) Yes
17 10 ..... ! Number of automatic tally isotopes, followed by list.
18 55137.70c
19 56137.70c
20 60148.70c
21 92234.70c
22 92235.70c
23 92236.70c
24 92238.70c
25 94239.70c
26 94240.70c
27 94241.70c

```

Figure 11. Placeholder Text Example from MONTEBURNS ".inp" File

```

146 c.fuel.meat-----
147 m11 92234 -twothirtyfour
148 ... 92235 -twothirtyfive
149 ... 92236 -twothirtysix
150 ... 92238 -twothirtyeight
151 ... 8016 -181.3278
152 ... 13027 -2839.767
153 ... nlib=70c

```

Figure 12. Placeholder Text Example from MCNP File

Similar to using ORIGEN as the forward model, the number of burnup steps to be used in the time discretization is specified in the main input file. In both MONTEBURNS and ORIGEN power history creation algorithms, a 30 day decay step is inserted after the final power step to allow for time for short lived isotopes that are produced to decay.

With all of the required information, the code may be executed. Post execution, the resulting isotopic information must be read from the output files. An algorithm was written to look at a specific temporary file containing the isotopic compositions from the last step. The file is always stored in the “tmpfile” directory the code is being executed from and is called “mb5x\_t.out”. This file contains the fuel information with eight digit precision, which is notably higher than the 3 digits of precision in the code’s main output file. While several of these digits may be

insignificant due to model error and statistical variance, accuracy greater than 3 digits was desired.

## 5 BENCHMARKS AND RESULTS

Two reactors were used for benchmarks in this project. To span a wide global variety of reactor types a research reactor and a power reactor were chosen, the Westinghouse AP1000, a pressurized water reactor (PWR), and the Oak Ridge Research Reactor, a materials test reactor (MTR).

### 5.1 Materials Test Reactor – Oak Ridge Research Reactor

The research reactor chosen for analysis in this work was the Oak Ridge Research Reactor (ORR). The ORR was fueled by 93.1% enriched HEU in the form of  $U_3O_8$  in an aluminum matrix. The assemblies are of the MTR type which for this reactor consist of 21 thin, aluminum-cladded, curved fuel plates attached to aluminum side plates [11,12].

#### 5.1.1 ORR Information

Spent fuel documentation for fuel at Savannah River National Laboratory was used to create a model for this reactor. Figure 13 shows the assembly cross-sectional dimensions in the XY plane.

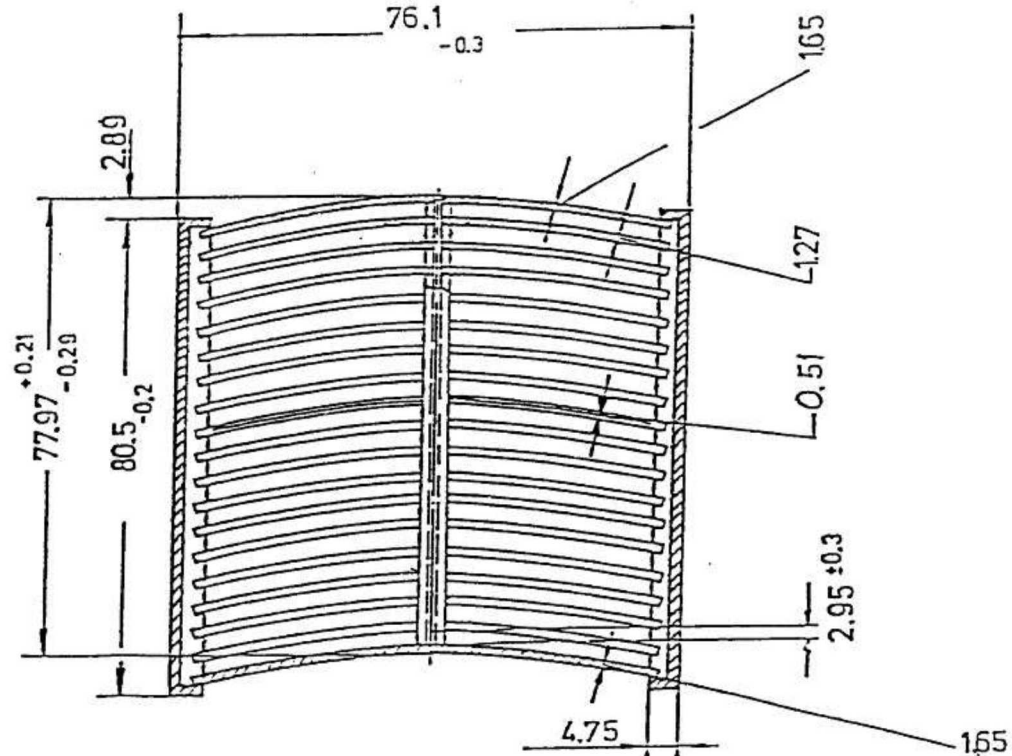


Figure 13. ORR XY Plane Assembly Dimensions (Expressed in mm)

The axial profile of an assembly consists of much more than only fuel. There are extended grid plate spacers on either end of the assembly. There is another piece called the comb, which sits across into the fuel plates for support. These features can be viewed in Figure 14.

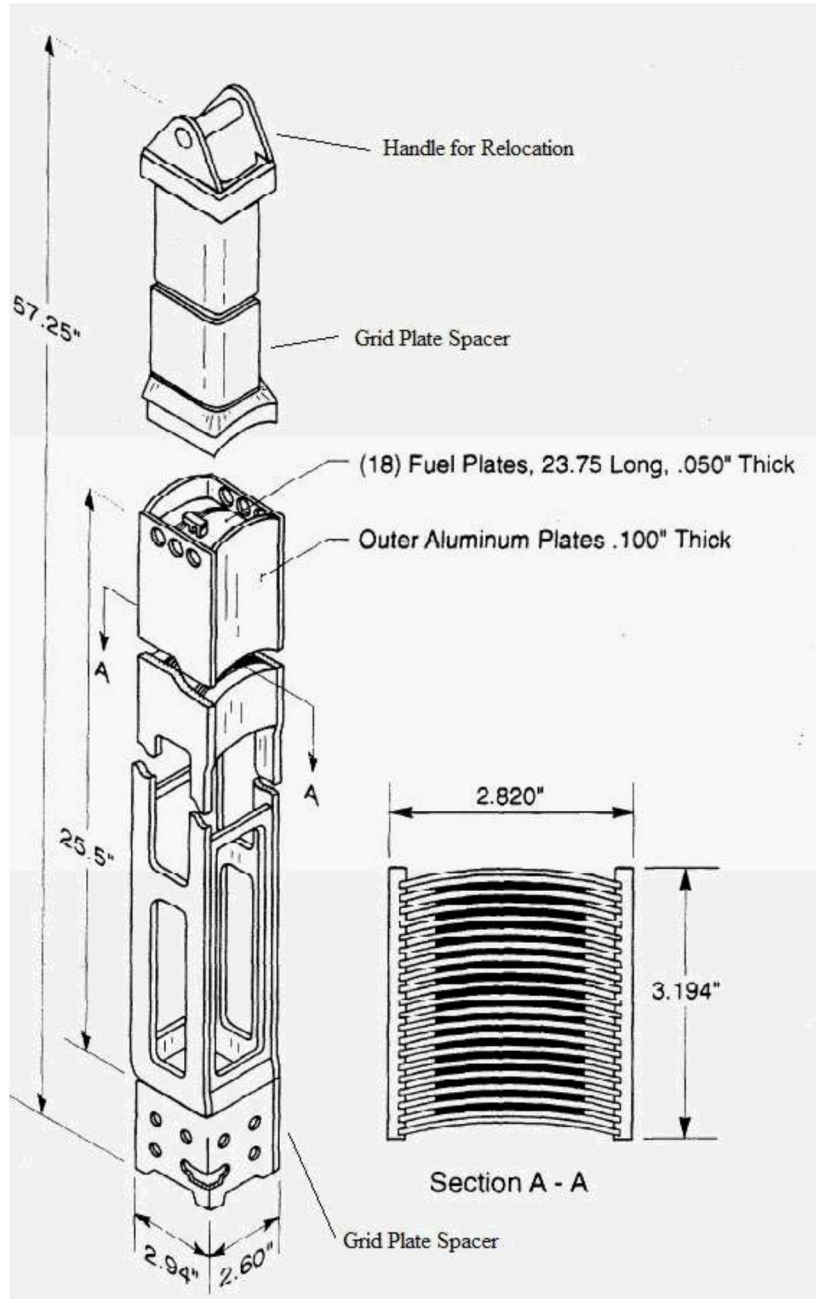


Figure 14. ORR Axial Assembly Profile

The ORR changed core configurations several times through the active 3 year life of assembly T-397. The core configuration consists of a 9 by 7 grid spacing system that can be filled with different types of elements including: fuel elements, beryllium reflector elements, aluminum shelled experimentation tubes, fuel followed control elements, or empty water locations. An

example of a core configuration is in Figure 15, which also displays some beam ports and external features.

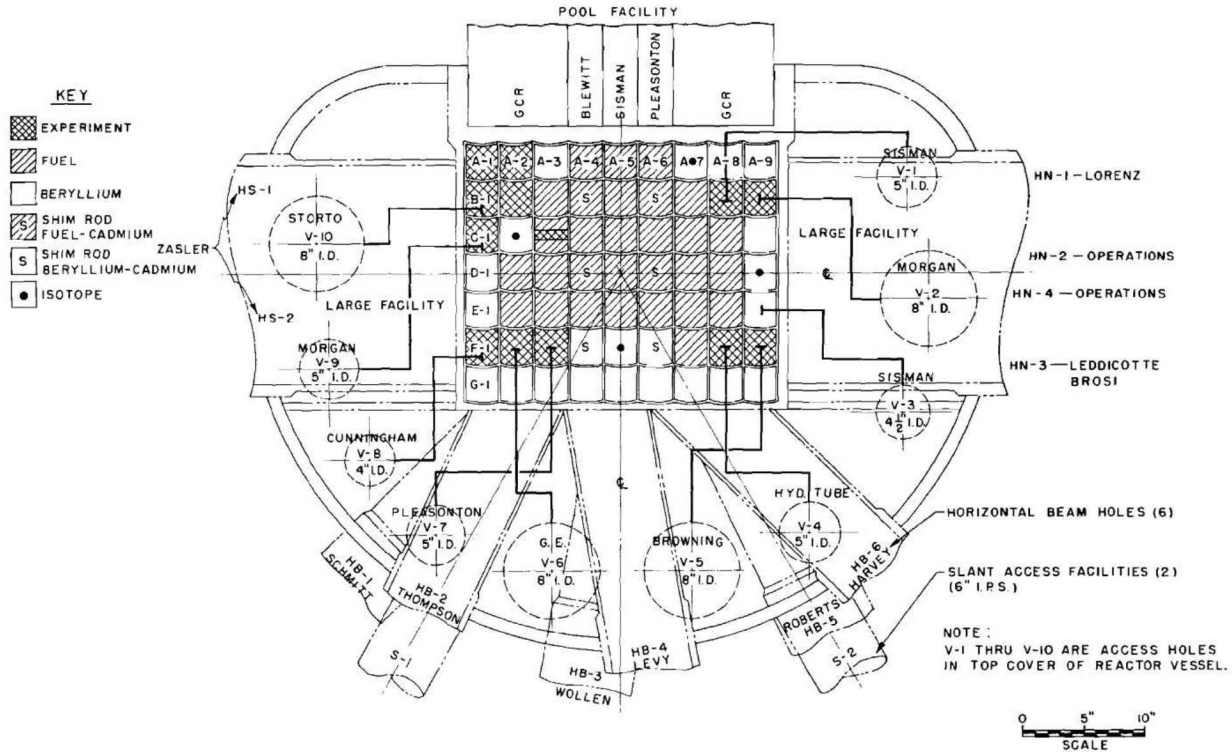


Figure 15. ORR Example Core Configuration

Assembly T-397 spent only 108.9 d (approximately 10%) of its active 1198 d life at power. This time at power consisted of five cycles operating at 3.62 MW/kgHM. The rest of the time the assembly was either out of the core or the reactor was shutdown. In a cooling pool area, there was an extensive inventory of active fuel that could be swapped into the core at any time. Frequent core shuffling, swapping fuel out of the core, and frequent shutdowns provide a large amount of facility operation data to keep track of and will affect the accuracy of the information provided in the Appendix-A documentation [11].

The fresh fuel contained 306 g of 93.1% enriched uranium fuel (285 g  $^{235}\text{U}$ ) in the material form of  $\text{U}_3\text{O}_8$  mixed in an aluminum matrix. The fuel density was 3.396 g/cc and was enclosed in an aluminum cladding with a density of 2.70 g/cc [11,12].

### 5.1.2 MTR Cross-Section Library Forward Model Benchmarks

A full core model was developed for ORR and consisted of a reactor of all fresh fuel. An image of the XY plane of the full core model is in Figure 16. There is a large surrounding sphere of water which is cropped in the image. The green material represents beryllium reflector elements, the yellow material represents an aluminum core enclosure, and the purple material is water. The fuel followed control elements are located at core positions D2, D4, D6, E2, E4, and E6.

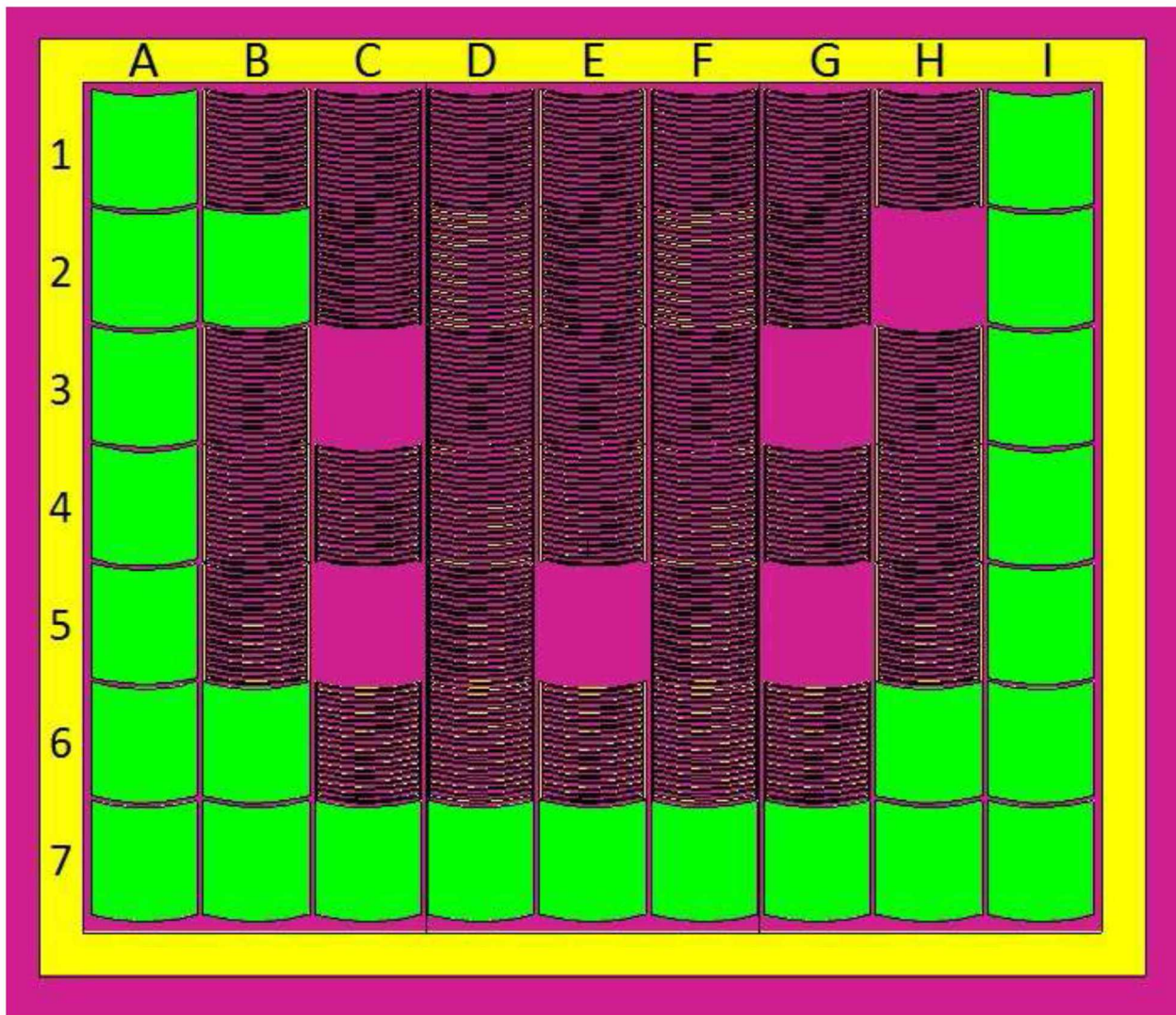


Figure 16. ORR MTR Reactor Full Core Model XY-Plane at Z=0

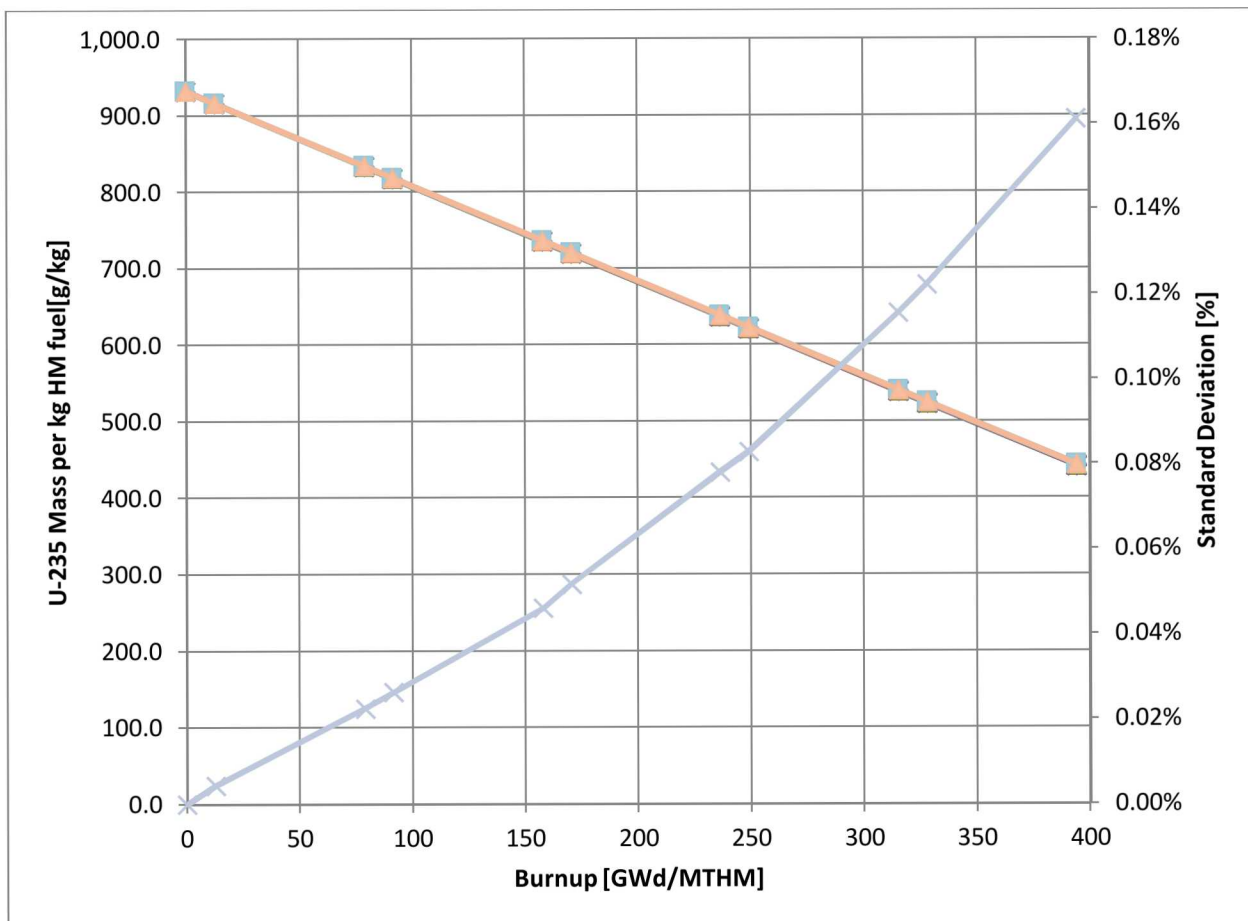
This model was depleted using one material to create core average neutron spectra at various burnup levels. The core was depleted using one documented fuel cycle load where the fuel had a capacity factor similar to assembly T-397 at approximately 10%. The burn time was broken into 30 time steps shown in Table 3, each of which creates a one-group cross-section library with the current neutron spectrum.

Table 3. ORR MTR Simulation Power History

Step	Duration [d]	Power [%]	Cumulative Burnup [GWd/MTHM]
1	0.5	100	1.813
2	1.0	100	5.437
3	2.0	100	12.69
4	8.0	100	41.71
5	15.07	100	79.02
6	213.01	0	79.02

7	0.5	100	80.83
8	1.0	100	84.45
9	2.0	100	91.71
10	8.0	100	120.7
11	15.07	100	158.0
12	213.01	0	158.0
13	0.5	100	159.8
14	1.0	100	163.4
15	2.0	100	170.7
16	8.0	100	199.7
17	15.07	100	237.0
18	213.01	0	237.0
19	0.5	100	238.8
20	1.0	100	242.4
21	2.0	100	249.6
22	8.0	100	278.6
23	15.07	100	315.9
24	213.01	0	315.9
25	0.5	100	317.7
26	1.0	100	321.3
27	2.0	100	328.5
28	8.0	100	357.5
29	15.07	100	394.7
30	8738.10	0	394.7

Each of these libraries was then extracted and used with ORIGEN 2.2 by itself. The same basic ORIGEN 2.2 model was then simulated by burning 1000g of heavy metal, and associated oxygen and aluminum, for the same documented burnup using each of the model generated cross-section libraries. Compiling the final results of all of these rapid 0D ORIGEN simulations would then enable a comparison to determine the burnup and spectrum that optimally achieves the closest isotopic compositions to a full 3D simulation results. The resulting  $^{235}\text{U}$  concentrations at every burnup step for the ORIGEN simulations are shown below.



**Figure 17. MTR  $^{235}\text{U}$  mass variance based on beginning to end of life neutron spectrum changes**

All 30 of the ORIGEN simulation's results produce very similar results, regardless of neutron spectrum. A more in-depth look at the error compared to the MONTEBURNS simulation was performed next. The comparison of the full core model's results for  $^{235}\text{U}$  is shown in Figure 18.

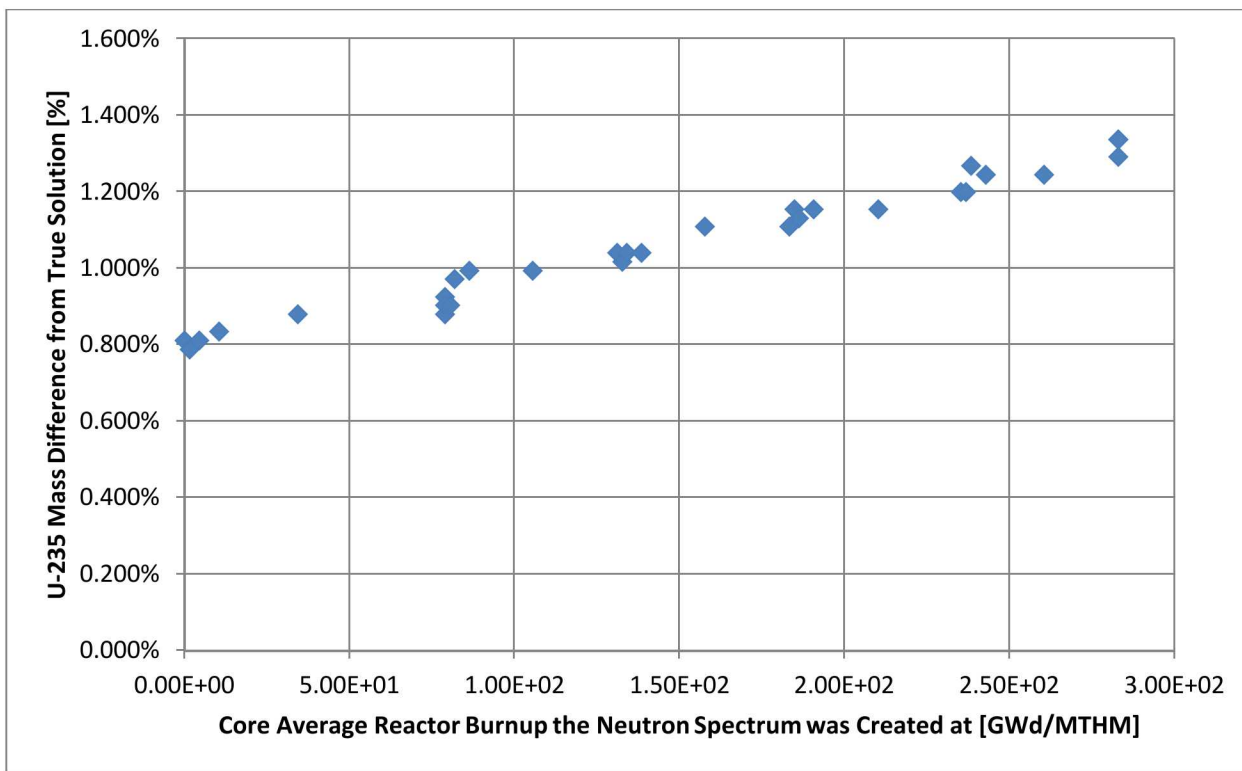


**Figure 18. MTR  $^{235}\text{U}$  mass difference between ORIGEN simulations using 1-group cross-section libraries created at various burnups in MONTEBURNS 3D model, resulting standard deviation is 0.161%**

It was expected that there would be a minimum error achieved somewhere in the middle of the data set. As Figure 18 shows, all of the ORIGEN simulations resulted in a higher spent  $^{235}\text{U}$  composition than the initial MONTEBURNS simulation that created the ORIGEN cross-section libraries. Part of this difference is likely attributed to variations in the burnup of  $^{235}\text{U}$  associated with the way conservation of energy is accounted for in either code. In MONTEBURNS, a series of constant flux irradiations are performed, while in ORIGEN the reactor power is held constant. In MONTEBURNS, the power conversion is handled by a user specified total system reactor power and associated power per nuclear fission event. In ORIGEN, the power is specified as specific power, normalized to the mass of material in the 0D model. The standalone ORIGEN models did create similar results with all neutron spectra though; the average spent fuel  $^{235}\text{U}$  mass was precisely the midpoint of a linear fit of the data. The ORIGEN  $^{235}\text{U}$  results had a standard deviation of 0.16%, proving the error had minimal dependence on variations in the neutron spectrum and primarily was attributed to model error.

Aside from minor differences in the burned  $^{235}\text{U}$ , the effects on the other spent fuel nuclear forensic signature isotopes were observed.  $^{238}\text{U}$  was analyzed next and a similar analysis was performed. The ORIGEN simulation results for  $^{238}\text{U}$  are shown in Figure xx.

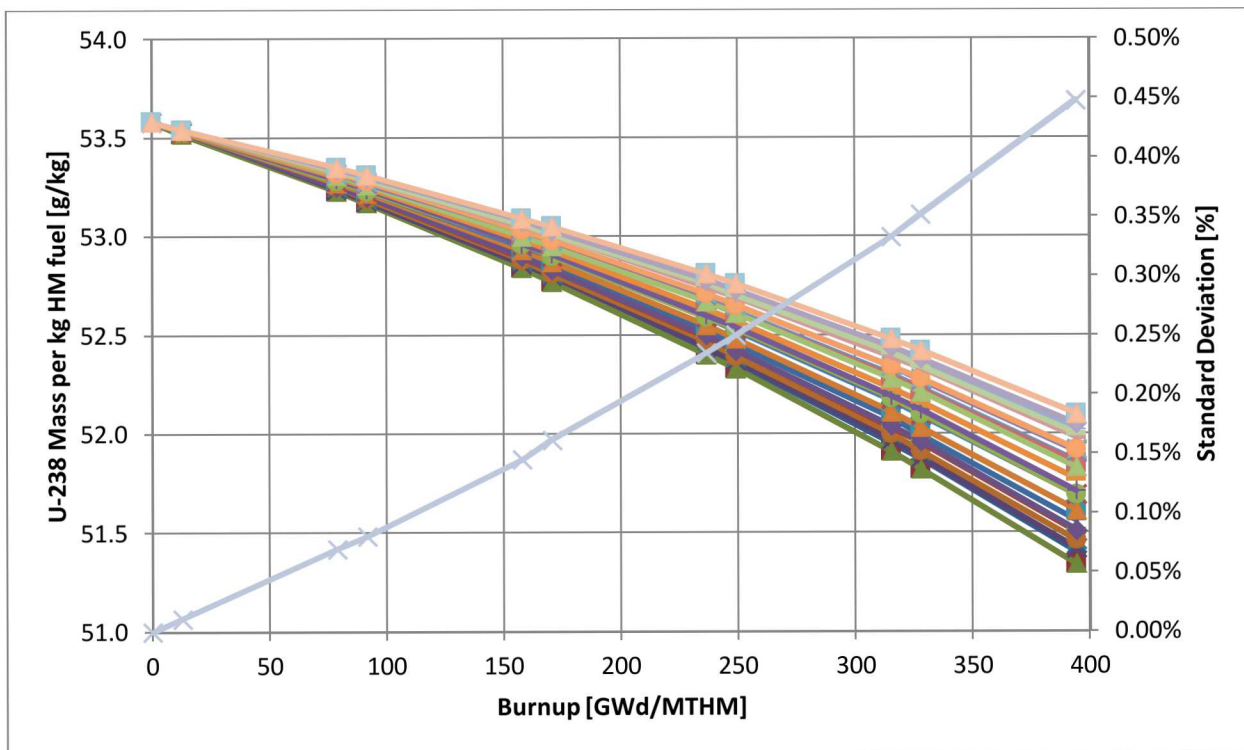


Figure 19. MTR  $^{238}\text{U}$  mass variance based on beginning to end of life neutron spectrum changes

$^{238}\text{U}$  typically either absorbs a neutron to induce fission or capture to form  $^{239}\text{Pu}$  down the decay chain. The  $^{238}\text{U}$  fission and radiative capture cross sections do have energy dependence, with fission probability increasing at higher energies. However at higher energies, the total absorption probability is still lower. It was expected and demonstrated that the more thermal spectrum toward the end of life would deplete the  $^{238}\text{U}$  faster than the higher energy spectrum at the beginning of life. In Figure 19, the result with the largest and smallest amount of  $^{238}\text{U}$  corresponds to the data from the spectrum present at lowest and highest burnup levels. The MONTEBURNS simulation resulted in a core average of 52.4 [g/kg]  $^{238}\text{U}$  per kg of heavy metal fuel, slightly higher than the ORIGEN results. Similar differences were observed as in the  $^{235}\text{U}$  results, as the same 0.16% standard deviation resulted.

Another important set of isotopes is  $^{137}\text{Cs}$  and  $^{137}\text{Ba}$ . Together these cumulatively account for the 137 mass bin when performing mass spectrometry analysis on spent fuel.  $^{137}\text{Cs}$  decays into the stable  $^{137}\text{Ba}$  and this isotope set is useful for reconstructing a fuel sample's burnup and time since discharge. Both of these isotopes have low absorption cross sections and should result in negligible effect by slight spectrum changes. Their ORIGEN results are shown in Figure 20 and Figure 21 for  $^{137}\text{Cs}$  and  $^{137}\text{Ba}$  respectively.

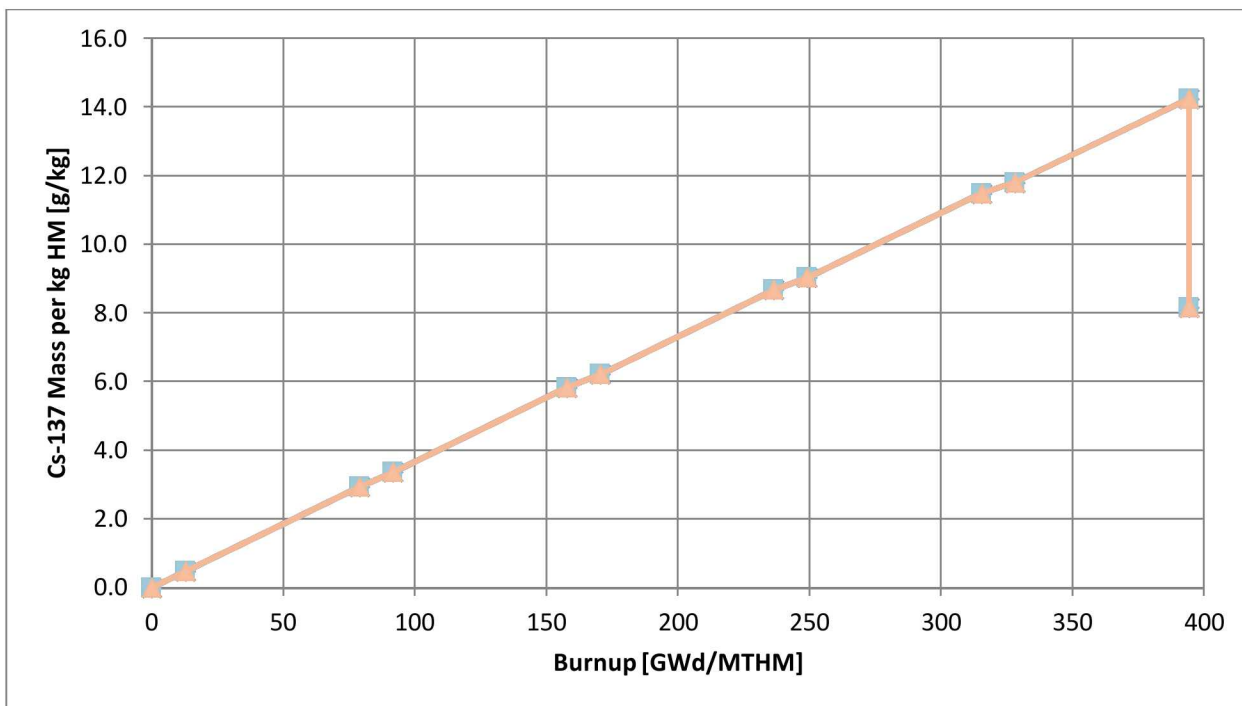


Figure 20. MTR  $^{137}\text{Cs}$  mass variance based on beginning to end of life neutron spectrum changes

The  $^{137}\text{Cs}$  results were identical for all of the ORIGEN simulations. These small spectrum perturbations had no effect on  $^{137}\text{Cs}$  that was within ORIGEN's reported significant digits. All 30 simulations produced the exact same results to a thousandth of a gram, therefore having a standard deviation of 0.0%.

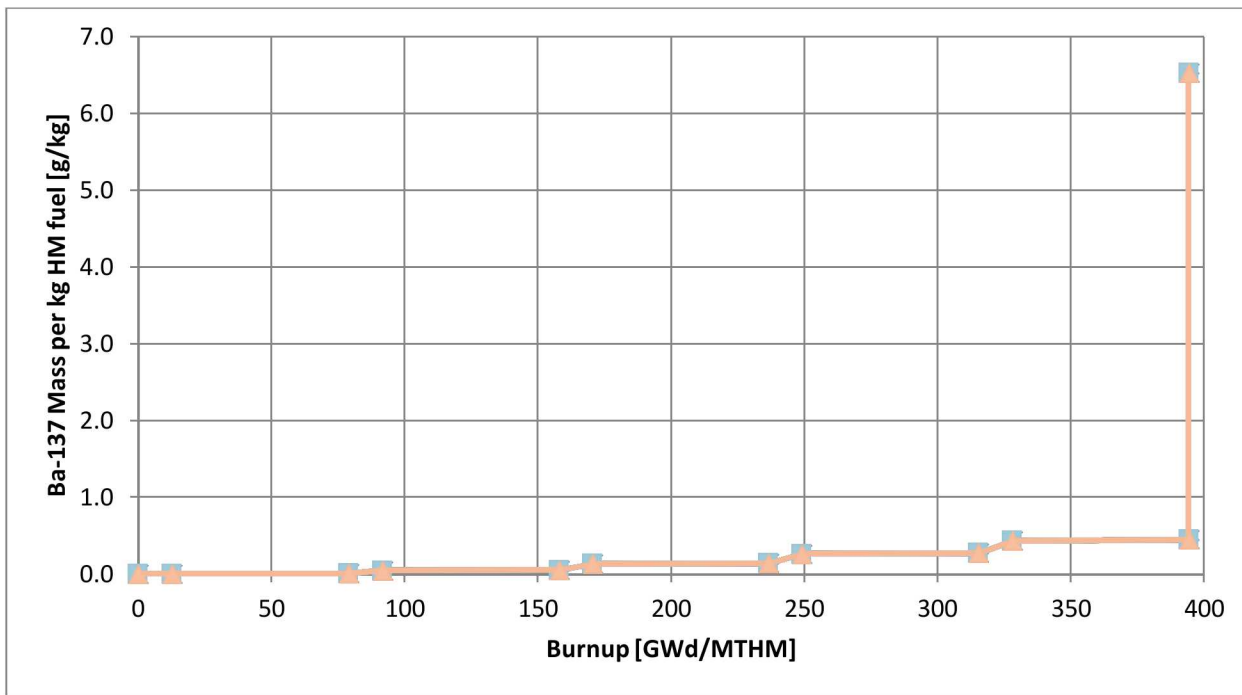


Figure 21. MTR  $^{137}\text{Ba}$  mass variance based on beginning to end of life neutron spectrum changes

$^{137}\text{Ba}$  had similar results as  $^{137}\text{Cs}$ , which was expected since it is its decay product. There was a small amount of variance present however all results were within a thousandth of a gram of each other. The resulting standard deviation was 0.0038%.

$^{148}\text{Nd}$  was analyzed next and is perhaps the most common used isotope to calculate spent fuel burnup. Previous work has indicated that in dynamically operated research reactors, accumulation of  $^{148}\text{Sm}$  due to decay from  $^{148}\text{Pm}$ , that is created from neutron absorption of  $^{147}\text{Pm}$ , during extended shutdown time poisons the 148 mass bin. This effect causes over prediction of a sample's burnup due to excess previously unaccounted for mass in the 148 chain. Both  $^{148}\text{Nd}$  and  $^{148}\text{Sm}$  results are shown in Figure 22 and Figure 23 respectively.

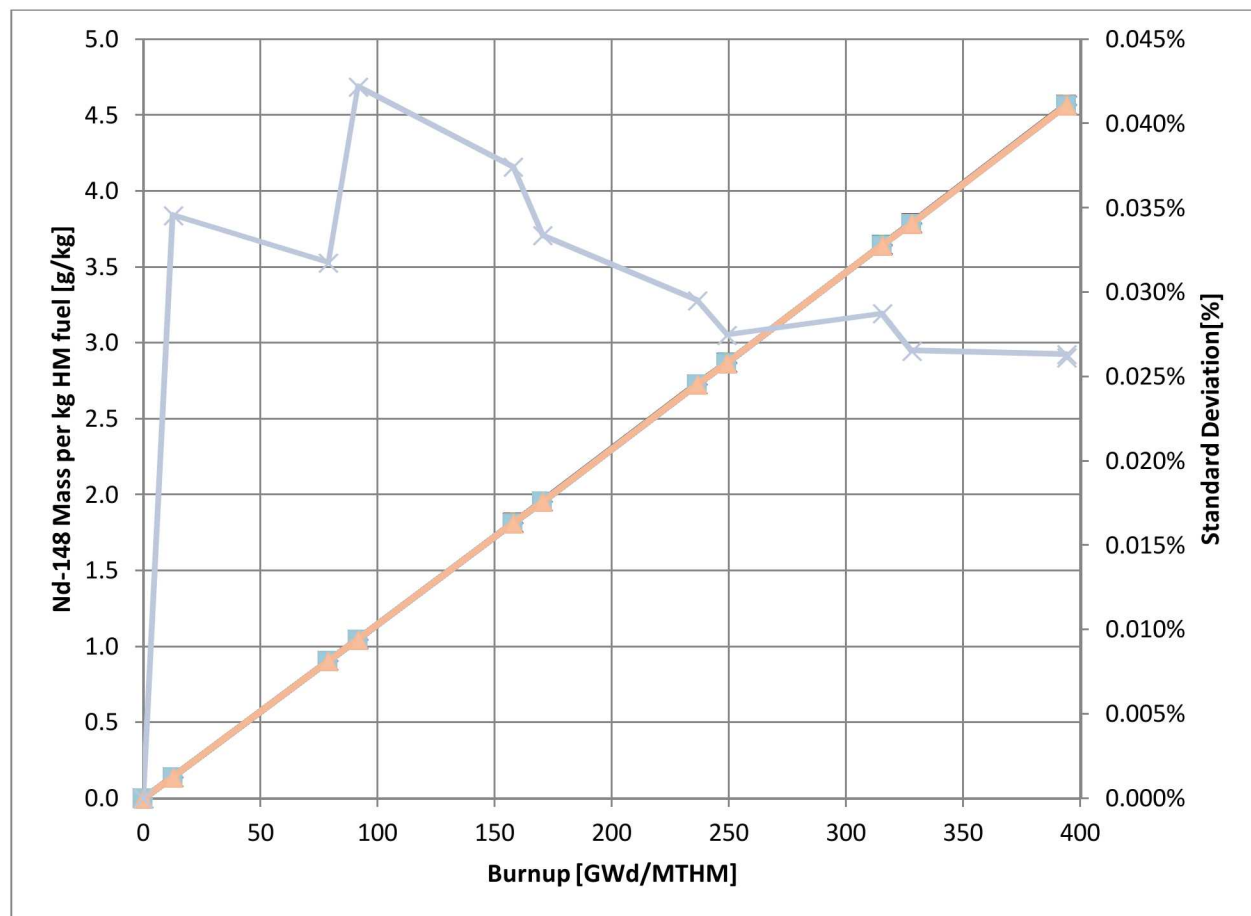
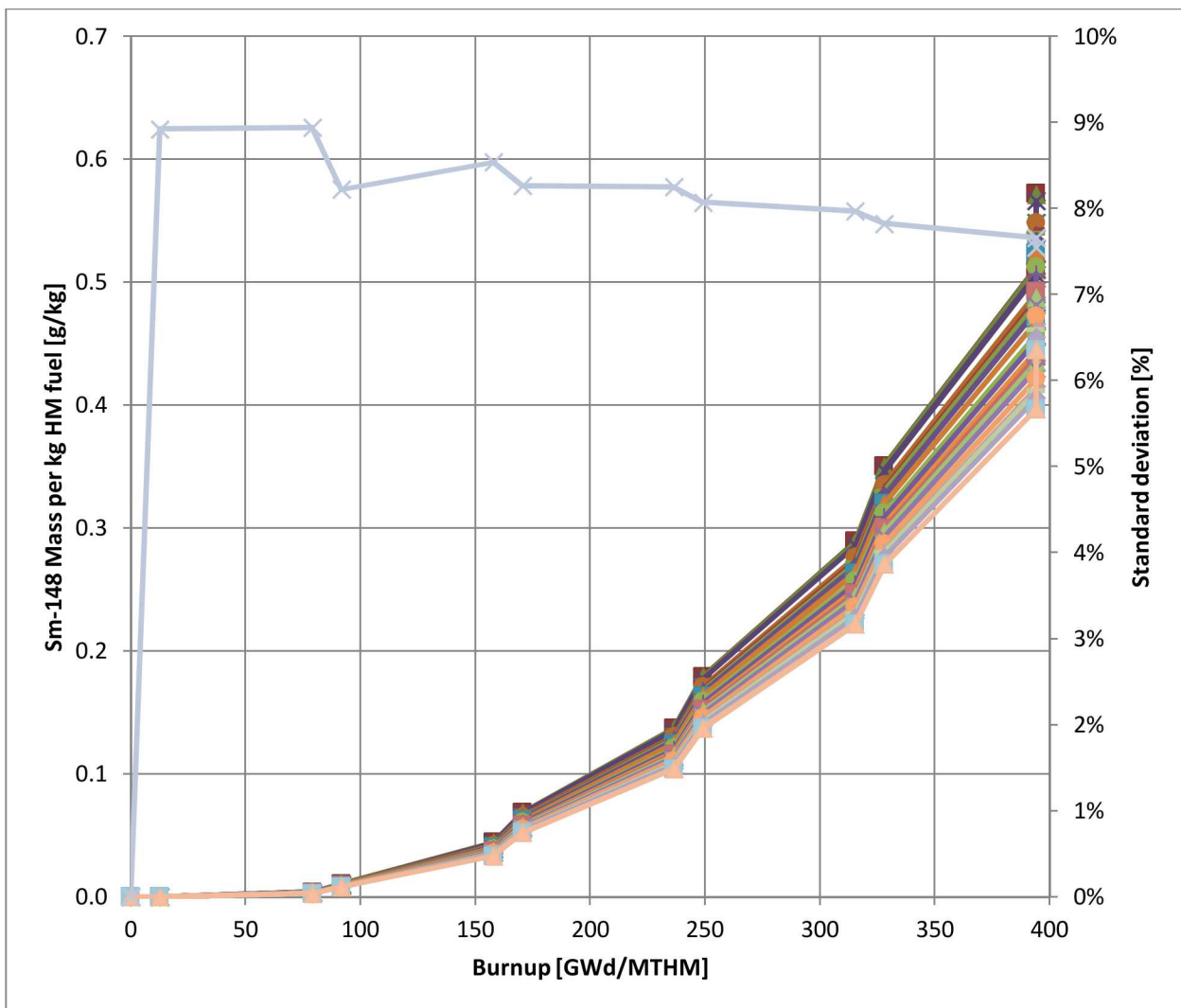


Figure 22. MTR  $^{148}\text{Nd}$  mass variance based on beginning to end of life neutron spectrum changes

$^{148}\text{Nd}$  produced similar results to  $^{137}\text{Cs}$ , due to its direct production from fission and low absorption cross section. It has negligible effect due to small neutron flux perturbations. The results for all 30 simulations lay atop each other in Figure 22. The resulting standard deviation for  $^{148}\text{Nd}$  was 0.026%.  $^{148}\text{Sm}$  has a significantly more complicated production chain. It originates from fission into the 147 mass chain, then when  $^{147}\text{Pm}$  absorbs a neutron to form the strong neutron absorber  $^{148}\text{Pm}$  or  $^{148\text{m}}\text{Pm}$ , there is a chance to decay to  $^{148}\text{Sm}$  prior to absorption. During shutdown time or extended time that fuel is away from power, provides significant time for the isotopes to decay to  $^{148}\text{Sm}$ . It was expected that changes in the neutron spectrum would be noticed here due to the dependence on the absorption cross sections.



**Figure 23. MTR 1<sup>48</sup>Sm mass variance based on beginning to end of life neutron spectrum changes**

<sup>148</sup>Sm had much more variance than other isotopes, resulting in a standard deviation of 7.55%. The beginning of life neutron spectrum produced the least amount of <sup>148</sup>Sm and the more thermal end-of-life spectrum produced the most. The more thermal the fuel's neutron spectrum was produced greater <sup>148</sup>Sm concentrations in the spent fuel. SRNL had a project in 2012 that involved samarium and neodymium chemical separation techniques which could be considered for analysis of spent fuel. In addition to dynamic operation, spectrum perturbations will change the <sup>148</sup>Sm concentration and will potentially change burnup reconstruction results using the 148 mass bin. Utilization of a cross-section library that minimizes the model error in the neutron flux will directly improve the accuracy of this method.

Other effective burnup reconstruction methods involve <sup>139</sup>La or the cumulative <sup>145</sup>Nd and <sup>146</sup>Nd concentrations. These isotopes were analyzed next.

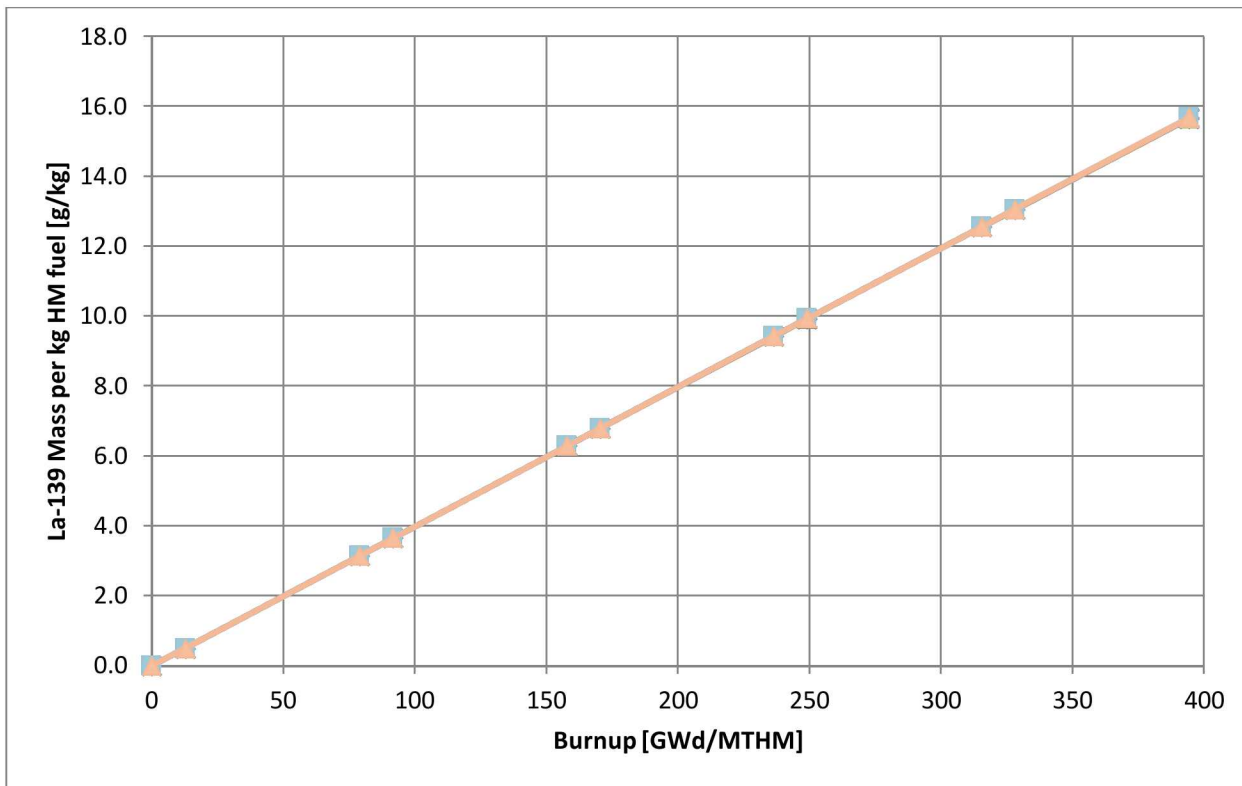


**Figure 24. MTR  $^{139}\text{La}$  mass variance based on beginning to end of life neutron spectrum changes**

The stable  $^{139}\text{La}$  has a small absorption cross section and was expected to produce similar results as  $^{137}\text{Cs}$ . All 30 simulation results fall atop each other in this case too and had a resulting standard deviation of 0.032%. Small spectrum perturbations had minimal to no effect on  $^{139}\text{La}$  concentrations. The standard deviation was not reported at every burnup step in

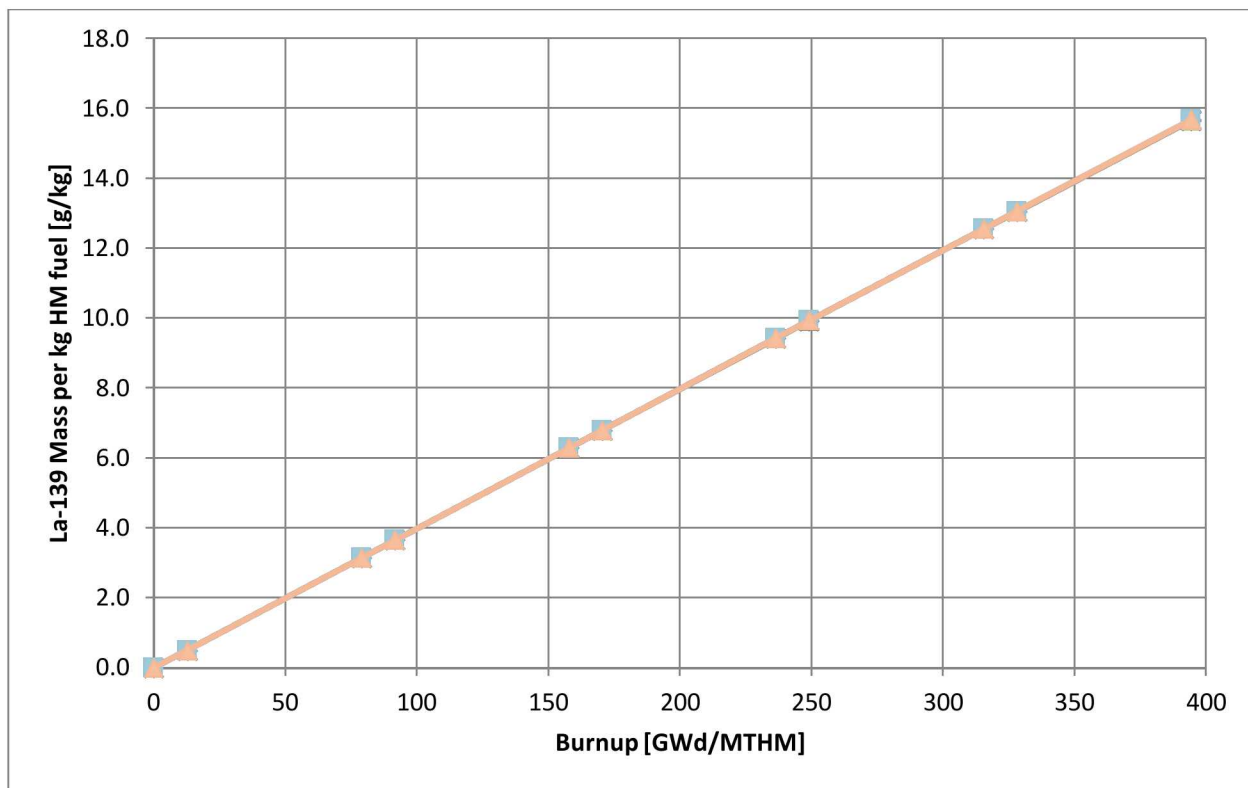


Figure 24, due to rounding effects it is zero at several low burnup points.

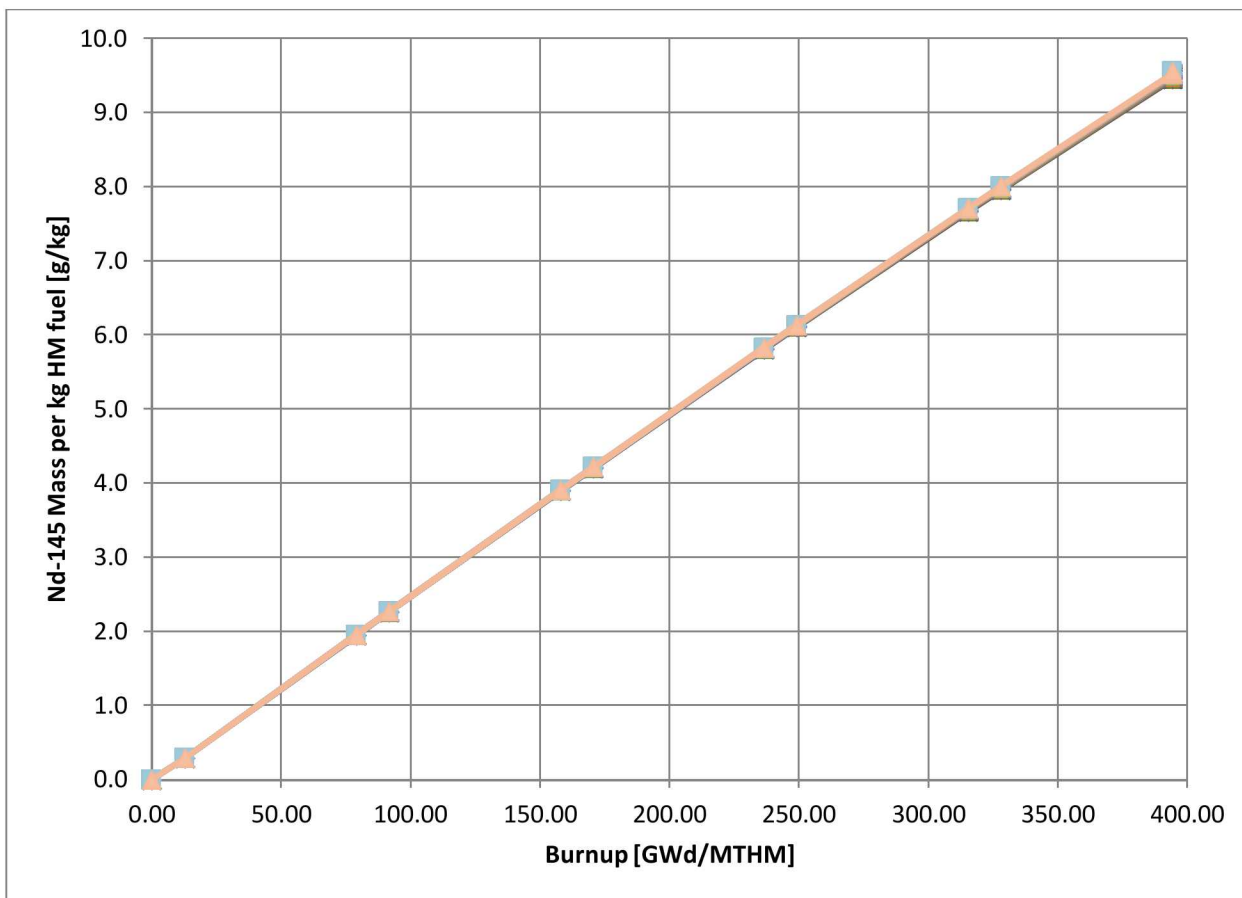


Figure 25. MTR  $^{145}\text{Nd}$  mass variance based on beginning to end of life neutron spectrum changes

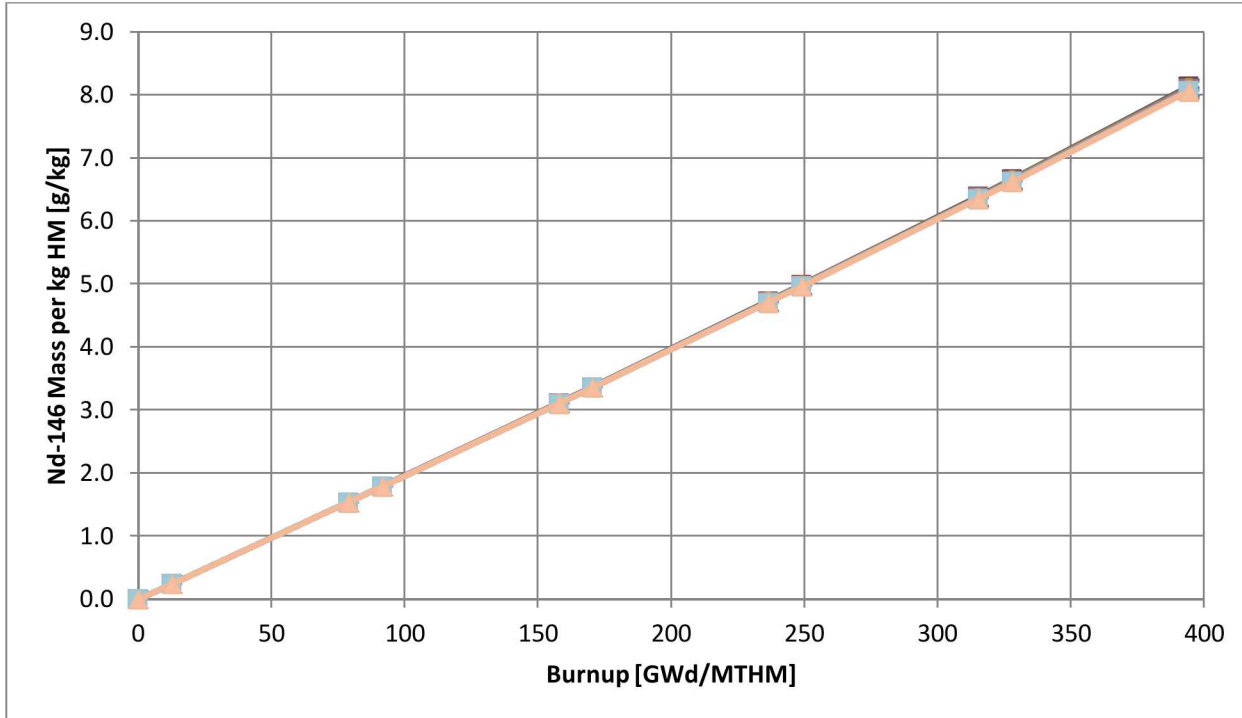


Figure 26. MTR  $^{146}\text{Nd}$  mass variance based on beginning to end of life neutron spectrum changes

$^{145}\text{Nd}$  and  $^{146}\text{Nd}$  showed slightly more variance than the other fission products and  $^{235}\text{U}$ . These simulations resulted in standard deviations of 0.24% and 0.26% for  $^{145}\text{Nd}$  and  $^{146}\text{Nd}$  respectively. Both of these are higher which is driven by the  $^{145}\text{Nd}$  neutron absorption cross section. This reaction causes additional loss of  $^{145}\text{Nd}$  and production of  $^{146}\text{Nd}$ , however the cumulative sum of these two isotopes is very stable and not sensitive to slight spectrum changes. The standard deviation in the sum was 0.0086%, significantly lower than the isotopes individually. The result's standard deviation for  $^{145}\text{Nd}$ ,  $^{146}\text{Nd}$ , and the sum of  $^{145}\text{Nd}$  and  $^{146}\text{Nd}$  is shown in Figure 27.

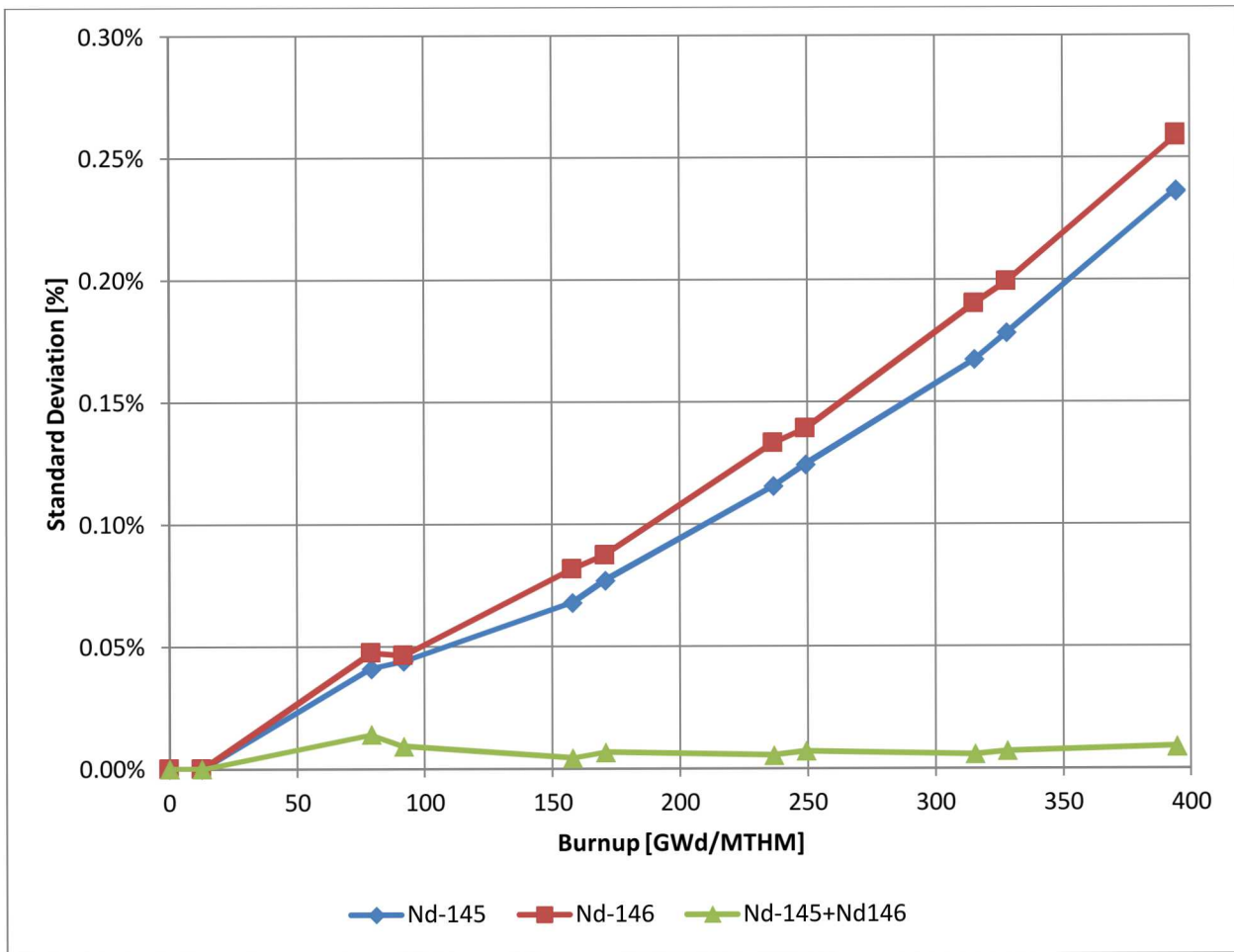


Figure 27. MTR  $^{145}\text{Nd}$  and  $^{146}\text{Nd}$  mass standard deviations from spectrum perturbations.

### 5.1.3 MTR 0D Inverse Analysis Results

The cross-section libraries that were generated were then benchmarked using the inverse analysis to determine the best suitable for usage. Each library was created at different burnup levels and represents the neutron spectrum present at that time. The benchmarked cases for MTR fuel

consist of thermal cross sections that come with ORIGEN and then the new cross sections at burnup levels of 79.02, 158.0, 237.0, 315.9, and 394.7 all in units of GWd/MTHM.

**Table 4. MTR Inverse Analysis Results Using 0D Forward Model with Thermal Cross Sections**

	True Solution	Reconstructed Result	Error [%]
Analytic Burnup [GWd/MTHM]	394.7	389.9	1.22%
Analytic $^{235}\text{U}$ Enrichment [%]	93.148%	93.73	0.62%
Numerical Burnup [GWd/MTHM]	394.7	399.5	1.21%
Numerical $^{234}\text{U}$ Enrichment [%]	1.001%	0.9361%	6.70%
Numerical $^{235}\text{U}$ Enrichment [%]	93.148%	92.320%	0.89%
Cooling Time [a]	23.94	25.28	5.44%
Cooling Time [a]	23.94	25.54	6.47%

The thermal cross-section library that comes with the ORIGEN code produced the least accurate results. In particular, the reconstructed initial  $^{234}\text{U}$  enrichment had an error of 6.7%.

**Table 5. MTR Inverse Analysis Results Using 0D Forward Model with 79.02 GWd/MTHM Cross Sections**

	True Solution	Reconstructed Result	Error [%]
Analytic Burnup [GWd/MTHM]	394.7	389.9	1.22%
Analytic $^{235}\text{U}$ Enrichment [%]	93.148%	93.76	0.65%
Numerical Burnup [GWd/MTHM]	394.7	398.3	0.91%
Numerical $^{234}\text{U}$ Enrichment [%]	1.001%	1.0156	1.45%
Numerical $^{235}\text{U}$ Enrichment [%]	93.148%	93.148	0.00%
Cooling Time [a]	23.94	25.27	5.41%
Cooling Time [a]	23.94	25.54	6.47%

Using the neutron spectrum with at low burnup, 79.02 GWd/MTHM, greater accuracy was achieved. Burnup,  $^{234}\text{U}$  enrichment, and  $^{235}\text{U}$  enrichment all resulted in lower errors using this cross-section library. Most notably,  $^{234}\text{U}$  enrichment error dropped from 6.7% to 1.45% and the  $^{235}\text{U}$  enrichment error was reconstructed exactly to within round off error.

**Table 6. MTR Inverse Analysis Results Using 0D Forward Model with 158.0 GWd/MTHM Cross Sections**

	True Solution	Reconstructed Result	Error [%]
Analytic Burnup [GWd/MTHM]	394.7	389.91	1.22%
Analytic $^{235}\text{U}$ Enrichment [%]	93.148%	93.76	0.65%
Numerical Burnup [GWd/MTHM]	394.7	398.3	0.91%
Numerical $^{234}\text{U}$ Enrichment [%]	1.001%	1.007	0.60%
Numerical $^{235}\text{U}$ Enrichment [%]	93.148%	93.122	0.03%
Cooling Time [a]	23.94	25.29	5.48%
Cooling Time [a]	23.94	25.54	6.47%

Increasing the burnup that the neutron spectrum originated initially decreased the error further. However, the error in burnup maintained approximately the same level, but in all cases was lower than when using the thermal cross-section library.

**Table 7. MTR Inverse Analysis Results Using 0D Forward Model with 237.0 GWd/MTHM Cross Sections**

	True Solution	Reconstructed Result	Error [%]
Analytic Burnup [GWd/MTHM]	394.7	389.91	1.22%
Analytic $^{235}\text{U}$ Enrichment [%]	93.148%	93.76	0.65%
Numerical Burnup [GWd/MTHM]	394.7	398.6	0.98%
Numerical $^{234}\text{U}$ Enrichment [%]	1.001%	1.002	0.10%
Numerical $^{235}\text{U}$ Enrichment [%]	93.148%	93.114	0.04%
Cooling Time [a]	23.94	25.31	5.56%
Cooling Time [a]	23.94	25.54	6.47%

**Table 8. MTR Inverse Analysis Results Using 0D Forward Model with 315.9 GWd/MTHM Cross Sections**

	True Solution	Reconstructed Result	Error [%]
Analytic Burnup [GWd/MTHM]	394.7	389.91	1.22%
Analytic $^{235}\text{U}$ Enrichment [%]	93.148%	93.76	0.65%
Numerical Burnup [GWd/MTHM]	394.7	398.6	0.98%
Numerical $^{234}\text{U}$ Enrichment [%]	1.001%	0.9953	0.57%
Numerical $^{235}\text{U}$ Enrichment [%]	93.148%	93.084	0.07%
Cooling Time [a]	23.94	25.29	5.48%
Cooling Time [a]	23.94	25.54	6.47%

**Table 9. MTR Inverse Analysis Results Using 0D Forward Model with 394.7 GWd/MTHM Cross Sections**

	True Solution	Reconstructed Result	Error [%]
Analytic Burnup [GWd/MTHM]	394.7	389.91	1.22%
Analytic $^{235}\text{U}$ Enrichment [%]	93.148%	93.76	0.65%
Numerical Burnup [GWd/MTHM]	394.7	398.77	1.03%
Numerical $^{234}\text{U}$ Enrichment [%]	1.001%	0.9894	1.17%
Numerical $^{235}\text{U}$ Enrichment [%]	93.148%	93.061	0.09%
Cooling Time [a]	23.94	25.28	5.44%
Cooling Time [a]	23.94	25.54	6.47%

There was no improvement to the cooling time reconstruction using the existing methods. The cooling time was consistently over predicted due to excess shutdown time during operation.

The resulting error in burnup,  $^{234}\text{U}$ , and  $^{235}\text{U}$  enrichment was analyzed as a function of the neutron spectrum. This enables identification of the ideal cross-section library, which corresponds to the spectrum that produces the minimal error, for future 0D inverse analyses for this fuel type.

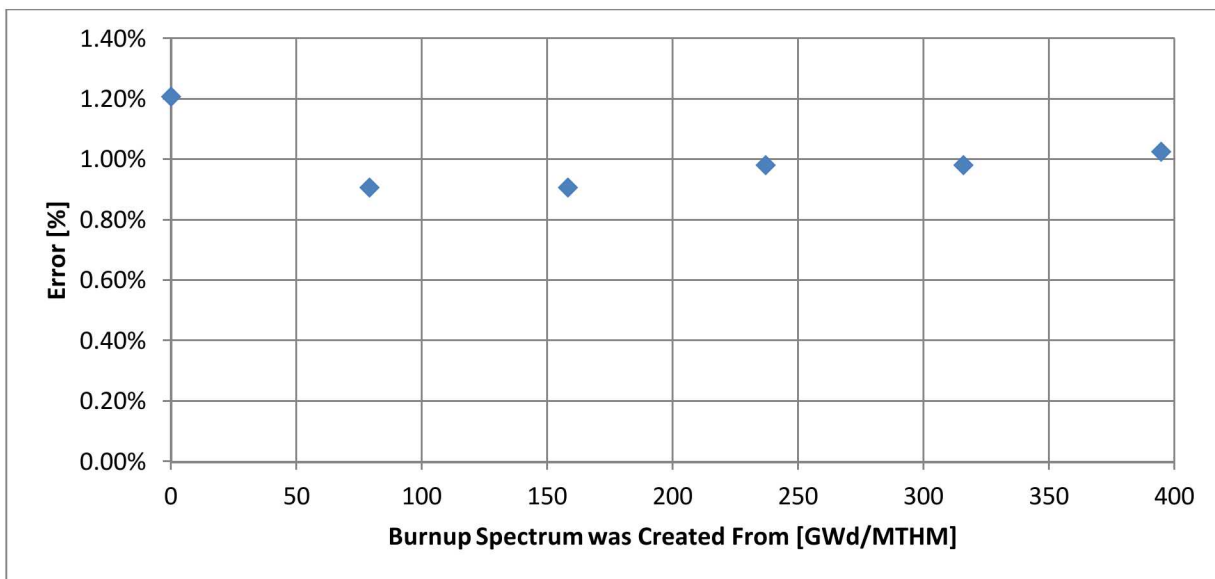


**Figure 28. Error in Reconstructed Burnup using Neutron Spectra at Various Burnup Levels\***

\*Burnup of 0.0 represents the ORIGEN code's thermal cross section used

After branching from the ORIGEN code's included libraries, the error in the reconstructed burnup was lowered. The level of error in the reconstructed burnup maintained a consistent level using spectra from all burnup levels and ranged between 0.91% and 1.05%, where the lowest error was achieved at lower burnup spectra.

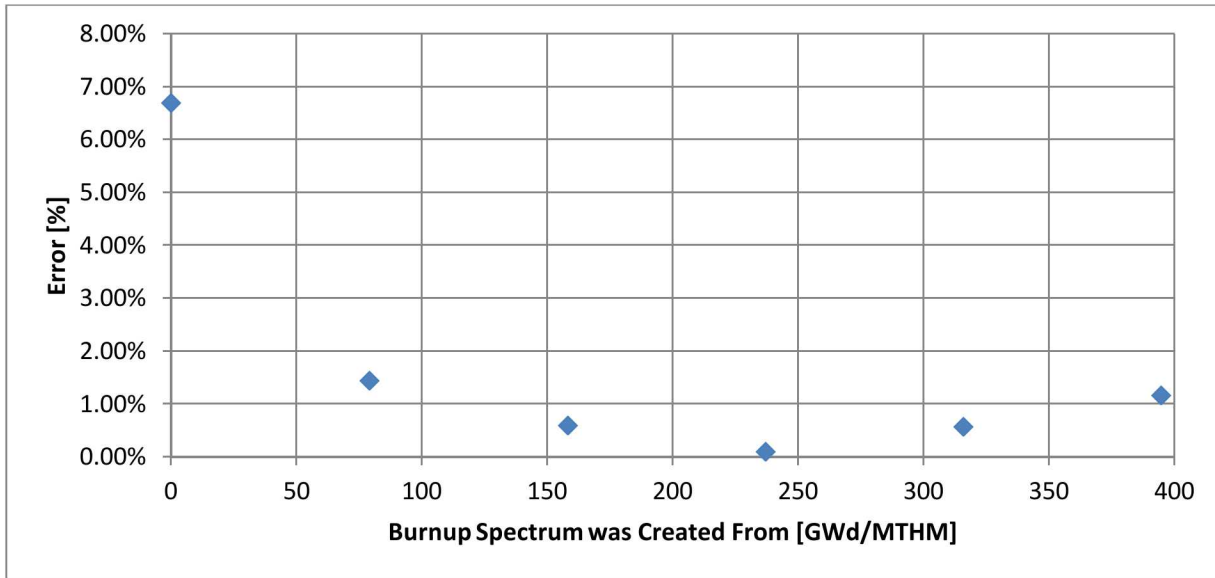


**Figure 29. Error in Reconstructed  $^{234}\text{U}$  Enrichment using Neutron Spectra at Various Burnup Levels\***

\*Burnup of 0.0 represents the ORIGEN code's thermal cross section used

The reconstructed  $^{234}\text{U}$  enrichment has high error when using the thermal cross-section library. Utilization of the model-specific libraries significantly reduced this error to range between 0.10% and 1.45%. The minimum error occurs when using the spectrum present when the fuel is halfway spent.

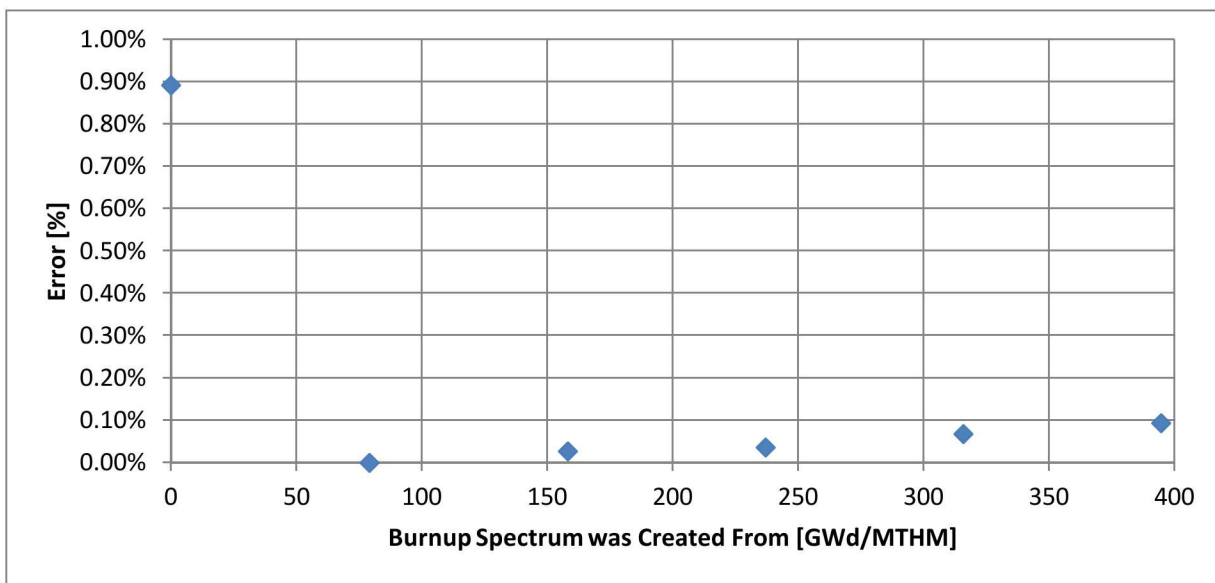


**Figure 30. Error in Reconstructed  $^{235}\text{U}$  Enrichment using Neutron Spectra at Various Burnup Levels\***  
 \*Burnup of 0.0 represents the ORIGEN code's thermal cross section used

The reconstructed  $^{235}\text{U}$  enrichment also has high error when using the thermal cross-section library and was also reduced when utilizing these reactor type specific libraries. Using the newly developed libraries reduced the error from 0.89% to a range between 0.0% and 0.09%.

The system developed proved to enable higher accuracy in reconstructed parameters from an unknown fuel sample than using ORIGEN's default cross-section libraries. These results are expected to be replicated for any reactor type that differs drastically from the existing library types.

#### 5.1.4 MTR 2D/3D results

A 2D and a 3D benchmark were performed using the developed system for MTR fuel. The 2D model consisted of a 1cm tall XY plane cutout of a single fuel assembly. This model was placed into an infinite lattice configuration after being simplified with reflective conditions. An image of the XY plane is shown in Figure 31.

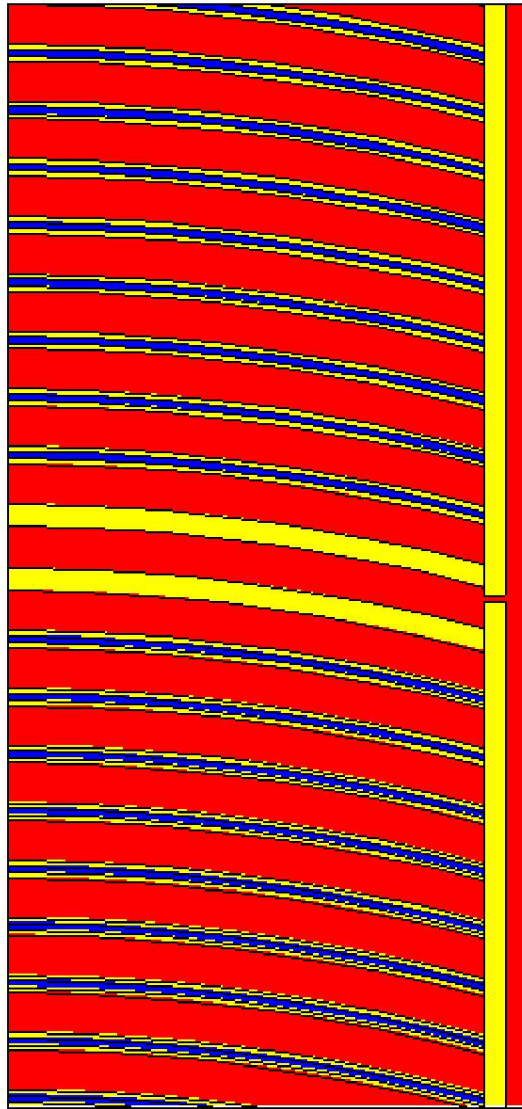


**Figure 31. 2D ORR MTR Type Reactor Model XY Plane**

This model has periodic conditions at axial planes of heights  $z=0\text{cm}$  and  $z=1\text{cm}$  and also at the upper and lower Y planes, creating a system infinite in the z-axis due to homogeneity. The Y dimension requires periodic conditions instead of reflective conditions due to non-symmetry. There is also a reflective condition in the X dimension as the model was cut in half to optimize reflector savings.

This system was benchmarked against the simulation results from a full assembly model that was designed and experimentally benchmarked to true operating conditions. In this analysis the total error,  $\epsilon$  from Equation 14, was driven below 0.001. This analysis converged in 8 iterations and the results are shown in Table 4.

**Table 10. MTR Inverse Analysis Results Using 2D Forward Model**

	True Solution	Reconstructed Result	Error [%]
Analytic Burnup [GWd/MTHM]	394.7	389.91	1.22%
Analytic $^{235}\text{U}$ Enrichment [%]	93.148%	93.76	0.65%
Numerical Burnup [GWd/MTHM]	394.7	395.6	0.23%
Numerical $^{234}\text{U}$ Enrichment [%]	1.001%	1.006%	0.50%
Numerical $^{235}\text{U}$ Enrichment [%]	93.148%	93.175%	0.03%
Cooling Time [a]	23.94	25.26	5.37%
Cooling Time [a]	23.94	25.54	6.47%

This 2D model proved to provide significantly higher accuracy than both the 0D models with new and previously existing cross section libraries. Expansion to a 3D model was performed next.

The 3D model consisted of a full assembly, placed into an infinite lattice configuration. The XY cross section of this model looks similar to the 2D model, except there is not a reflective boundary at the plane of  $X=0$ . This model has periodic conditions across the X and Y boundaries, simulating an infinite lattice of assemblies. There is 1m of water above and below the assembly and void surrounding the water.

**Table 11. MTR Inverse Analysis Results using 3D Forward Model**

	True Solution	Reconstructed Result	Error [%]
Analytic Burnup [GWd/MTHM]	394.7	389.91	1.22%
Analytic $^{235}\text{U}$ Enrichment [%]	93.148%	93.73%	0.62%
Numerical Burnup [GWd/MTHM]	394.7	395.55	0.22%
Numerical $^{234}\text{U}$ Enrichment [%]	1.001%	1.005%	0.40%
Numerical $^{235}\text{U}$ Enrichment [%]	93.148%	93.174	0.03%
Cooling Time [a]	23.94	25.44	6.08%
Cooling Time [a]	23.94	25.54	6.47%

The 3D model produced the most accurate results, driving burnup and initial uranium enrichment errors below 0.5%. This system proved to significantly reduce model error and reconstruct the most accurate results.

## 5.2 Pressurized Water Reactor – AP1000

The AP1000 is a Westinghouse Electric Company reactor design and is the first Generation III+ reactor to receive final design approval from the NRC. The AP1000 is a two-loop PWR planned to produce around 1000 MW<sub>e</sub>. The design is built on proven technology from over 35 years of PWR operating experience. Major improvements over earlier generation reactors include the utilization of passive safety technology, overall system simplification, and modular construction.

These improvements make the AP1000 safer, simpler and less expensive to build, operate, and maintain.

The major design parameters for the AP1000 are similar to that of other PWRs. The thermal power is rated at 3415 MW<sub>th</sub> and with a thermodynamic efficiency of 33%, it can produce a usable electrical power of 1161 MW<sub>e</sub>. The fuel type is enriched UO<sub>2</sub> and the coolant/moderator is light water. A listing of the AP1000 design parameters are provided in Table 12.

**Table 12. AP1000 Design Parameters**

Thermal power (MW <sub>th</sub> )	3415
Electrical power (MW <sub>e</sub> )	1161
Thermodynamic efficiency (%)	33
Fuel	UO <sub>2</sub>
Average Fuel enrichment (wt %)	4.8
Type of fuel assembly	17x17
Number of fuel assemblies	157
Active fuel length (m)	4.3
Equivalent core diameter (m)	3.04
Operating cycle length (months)	18
Linear heat rating (kW/m)	18.7
Operating pressure (Mpa)	15.5
Coolant	Light Water
Coolant inlet temperature (°C)	280.7
Coolant outlet temperature (°C)	321.1

### **5.2.1 AP1000 Information**

A whole-core 3D benchmark model was designed based on the AP1000 Design Control Documentation [13] provided by the US NRC. The report provided the multiplication factor ( $k_{eff}$ ) for cold, zero power, beginning of cycle, and zero soluble boron core conditions. MCNP was used to model the reactor at the specified core conditions in order to benchmark the  $k_{eff}$  value against published results.

The reactor core consists of 157 fuel assemblies that are arranged to form a right circular cylinder. Each fuel assembly contains 264 fuel rods, 24 guide tubes for control rod clusters, and one centrally located guide tube for in-core instrumentation, all of which are arranged in a 17 x 17 square lattice array. Figure 32 shows a cross-sectional view of the fuel assembly and related fuel rod and guide tube placements.

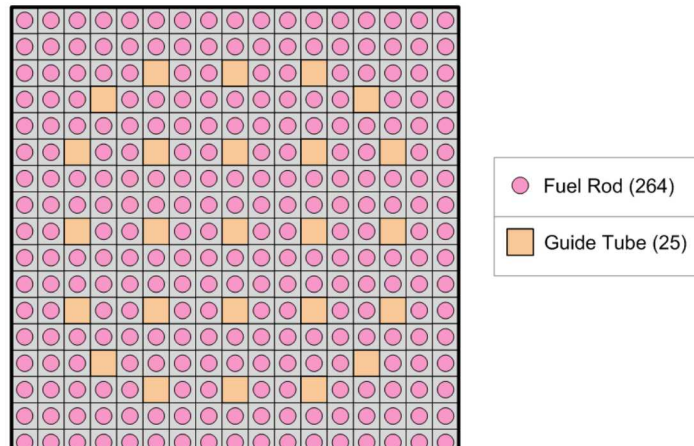


Figure 32. AP1000 Fuel Assembly

The model design is based on the initial core loading, in which the fuel rods within any given assembly have the same uranium enrichment in both the radial and axial planes. Fuel assemblies of three different enrichments are used to establish a favorable radial power distribution.

Figure 33 shows the fuel assembly loading pattern used for the AP1000 model. It also shows the placement of the assemblies containing the Discrete Burnable Absorber (PYREX) rods and Integral Fuel Burnable Absorber (IFBA) rods within the core.

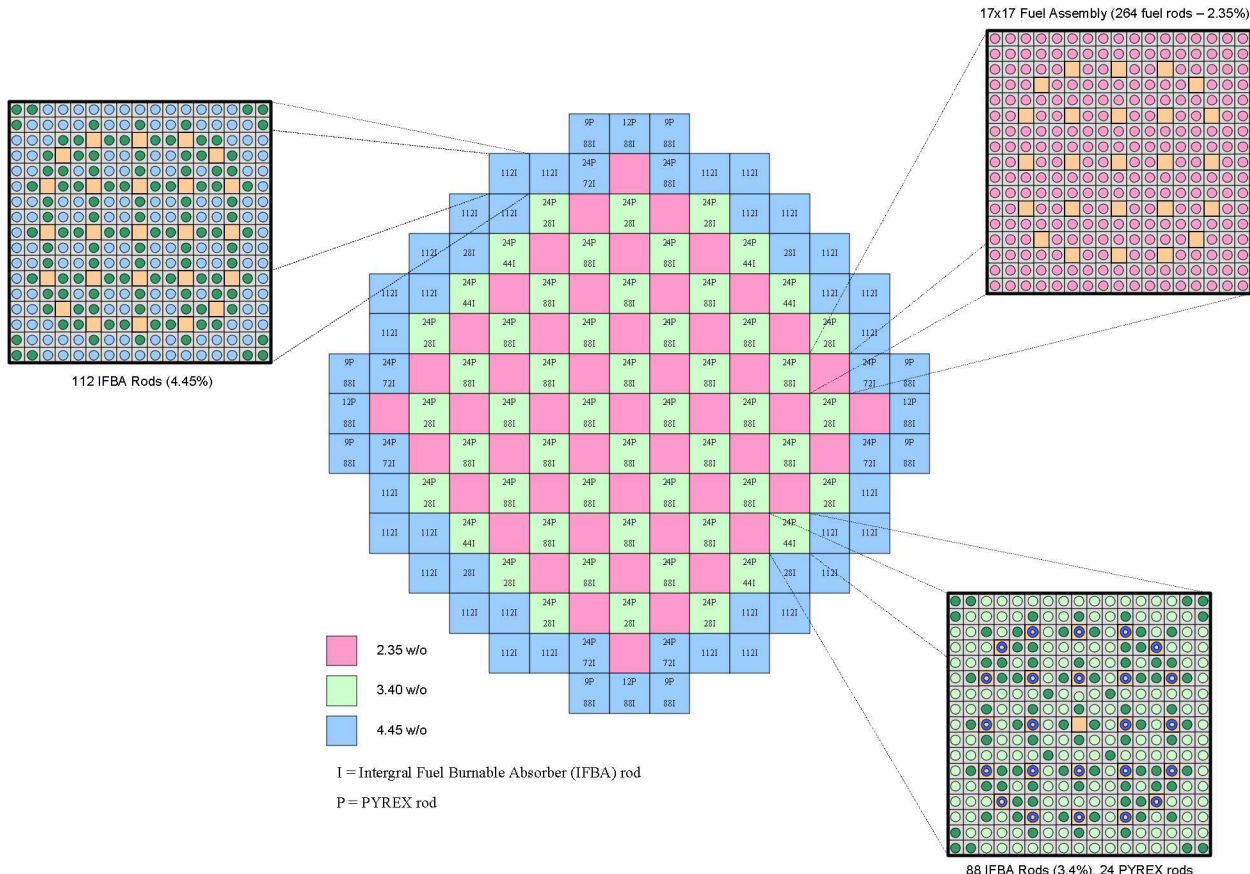


Figure 33. AP1000 Reactor Core Map

Burnable absorbers in the form of PYREX and IFBA rods are used to provide partial control of the excess reactivity present during the fuel cycle. Their main function is to limit peaking factors and prevent the moderator temperature coefficient from being positive at normal operating conditions. A description of the reactor core, including dimensions and core materials, is provided in Table 13.

**Table 13. AP1000 Reactor Core Dimensions**

<b>Active Core</b>	
Equivalent diameter (cm)	304.04
Active fuel height (cm)	426.72
Height-to-diameter ration	78.14
Total cross section area (m <sup>2</sup> )	7.26
Fuel weight, as UO <sub>2</sub> (g)	9.76x10 <sup>7</sup>
<b>Fuel Assembly</b>	
Number	157
Rod array	17x17
Rods per assembly	264
Rod pitch (cm)	1.26
Overall transverse dimensions (cm)	21.40
<b>Fuel Rods</b>	
Number	41448
Outside diameter (cm)	0.9500
Gap diameter (cm)	0.0165
Clad thickness (cm)	0.0572
Clad material	ZIRLO
<b>Fuel Pellets</b>	
Material	UO <sub>2</sub> sintered
Density (% theoretical)	95.5
Fuel Enrichments (weight percent)	
Region 1	2.35
Region 2	3.40
Region 3	4.45
Diameter (cm)	0.819
Length (cm)	0.983
<b>Discrete Burnable Absorber Rods (PYREX)</b>	
Number	1558
Material	Borosilicate Glass
Outside diameter (cm)	0.968
Inner diameter (cm)	0.461
Clad material	Stainless Steel
B <sub>10</sub> content (Mg/cm)	6.24
Absorber length (cm)	368.30
<b>Integral Fuel Burnable Absorbers (IFBA)</b>	
Number	8832
Type	IFBA
Material	Boride Coating

B <sub>10</sub> content (Mg/cm)	0.772
Absorber length (cm)	386.08
Absorber coating thickness (cm)	0.00256

Results for the whole-core 3D MCNP benchmark model are listed in Table 14. As indicated, the MCNP calculation was very accurate when compared to the published results, giving a difference of only 0.0498% between  $k_{\text{eff}}$  values, thus providing high confidence in the MCNP model used for simulations.

**Table 14. AP1000 Multiplication Factor Results**

Multiplication Factor Origin	$k_{\text{eff}}$	% difference (published-to-code)
AP1000 Design Control Documentation	1.2050	na
MCNP Code System (version 5 1.51)	1.2044	0.0498

In order to accurately simulate the time evolution of an operating AP1000 a fuel shuffling scheme was incorporated. To account for this the core was divided into zones and a three batch shuffling scheme was applied. The initial core matches the model used for the benchmark analysis described above. After the initial core is depleted the first core shuffle removes zone 3 from the reactor replacing it with the fuel from zone 2. The fuel in zone 1 is moved to zone 2, and fresh fuel is added to zone 1, as shown in Figure 34. Each subsequent fuel shuffle follows this same pattern.

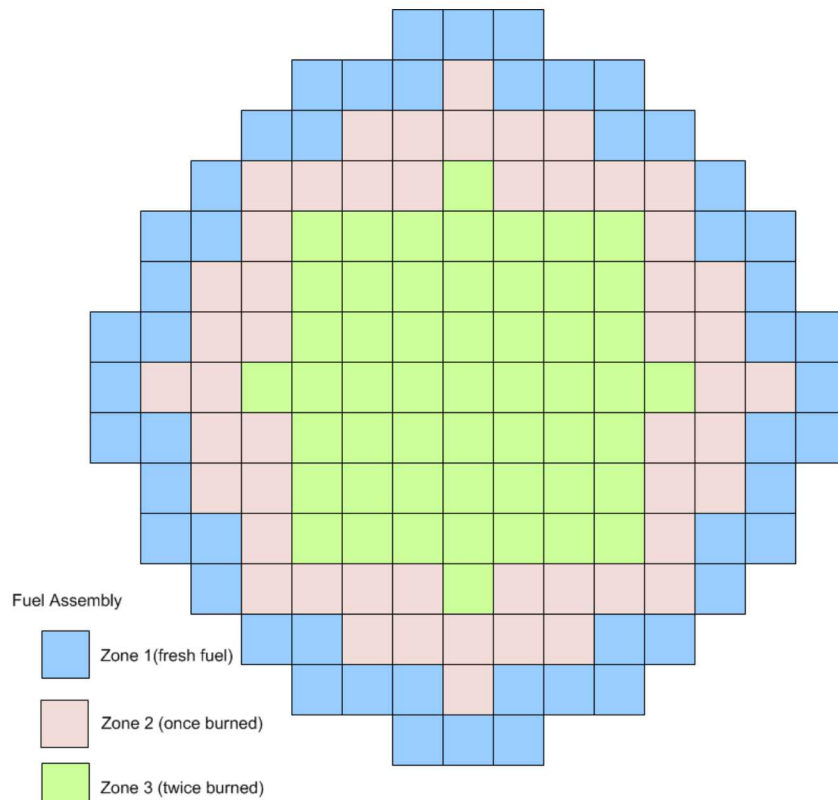


**Figure 34. AP1000 Fuel Shuffling Scheme**

The fresh fuel added to the core has a  $^{235}\text{U}$  enrichment of 4.8%. The shuffling scheme was applied for multiple cycles until an equilibrium core was reached. Comparisons of the isotopic compositions at the end of the 4<sup>th</sup> and 5<sup>th</sup> shuffling step indicated an equilibrium core had been reached, whereas nearly all fission products and actinides showed only fractional differences. Figure 35 shows the core multiplication factor as a function of time for several fuel shuffles. A five day down time was included between each core shuffle and a capacity factor of 93% was applied. The fuel burnup for the equilibrium core was calculated to be 52.8 GWd/MTHM, with a 470 day batch cycle duration, indicating a fuel resident time of 1410 power producing days within the core. Table 15 lists the defining characteristics for the AP1000 equilibrium fuel shuffling case.

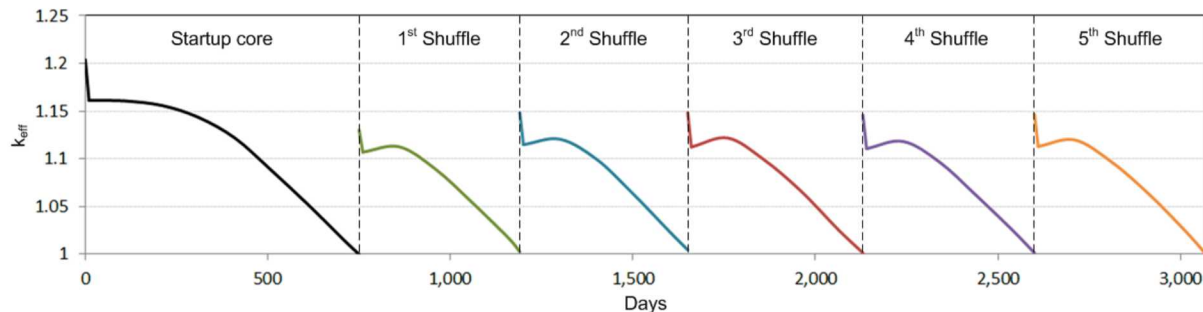


Figure 35. Depletion Sequence for AP1000 Equilibrium Core

Table 15. Burnup and Batch Duration Results for AP1000 Equilibrium Core

Enrichment (%)	Capacity Factor (%)	Batch Duration (days)	Burnup (GWd/MTHM)
4.8	93	470	52.8

## 5.2.2 PWR Cross-Section Library Forward Model Benchmarks

The AP1000 equilibrium model was simulated in MONTEBURNS for one cycle to generate cross-section libraries in each of the three regions at many burnup points. The cycle was discretized in time into 47 steps of 10 days each. The spent fuel was then decayed in several steps. The power history information is shown below.

Table 16. AP1000 PWR Simulation Power History

Step	Duration [d]	Power [%]
1-47	10.0	100
48	5.0	0.0
49	360.0	0.0
50	730.0	0.0
51	2555.0	0.0
52	7300.0	0.0

This system generated a cross-section library at every step, for all three materials, totaling 156 ORIGEN libraries. Each of these 156 cross-section libraries were then used in an ORIGEN simulation, with the same burnup and material parameters as the original model, to observe the

effects of small flux perturbations on isotopes of interest. The results, beginning with  $^{235}\text{U}$ , are shown below.

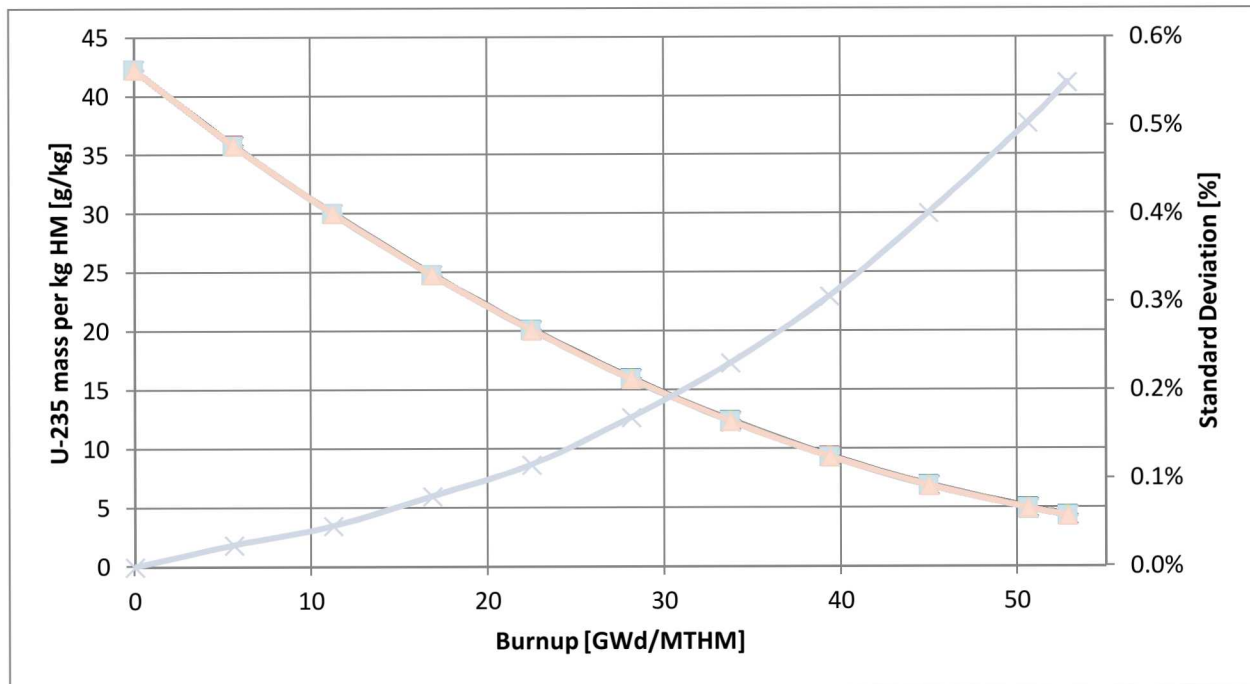
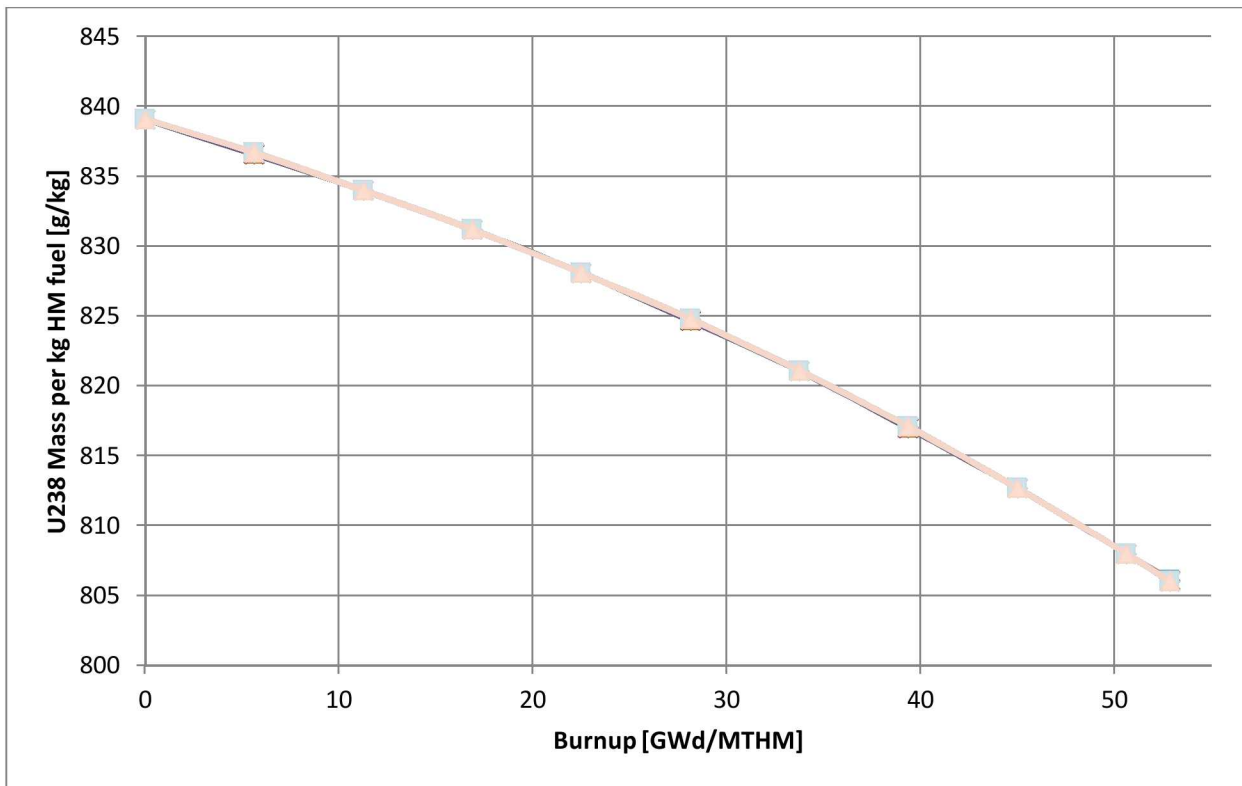


Figure 36. PWR  $^{235}\text{U}$  mass variance based on beginning to end of life neutron spectrum changes

The AP1000 cross sections generated more variance in  $^{235}\text{U}$  than the MTR full core model did, ending with 0.548% standard deviation. This difference is likely attributed to the larger quantity of plutonium produced with this LEU fuel compared to the MTR type. The spectrum perturbations would alter the amount of plutonium produced and therefore the amount of power that plutonium generates. While holding burnup constant, this changes the amount of  $^{235}\text{U}$  burned as well.



**Figure 37. PWR  $^{238}\text{U}$  Mass variance based on beginning to end of life neutron spectrum changes**

The AP1000's  $^{238}\text{U}$  results had negligible variance which was on the order of round off error. The standard deviation for  $^{238}\text{U}$  results ranged between 0.0% and 0.006%. Due to the large  $^{238}\text{U}$  content in the fuel, this variance was on the order of 0.1g per kg fuel, which is still significant to show changes in  $^{238}\text{U}$  activation products such as plutonium.

$^{137}\text{Cs}$  and  $^{137}\text{Ba}$  had low variance, similar to the MTR fuel, due to their low neutron cross sections.  $^{137}\text{Cs}$  had low standard deviation at all burnup levels ranging 0.0% to 0.027%, on the order of round off error.

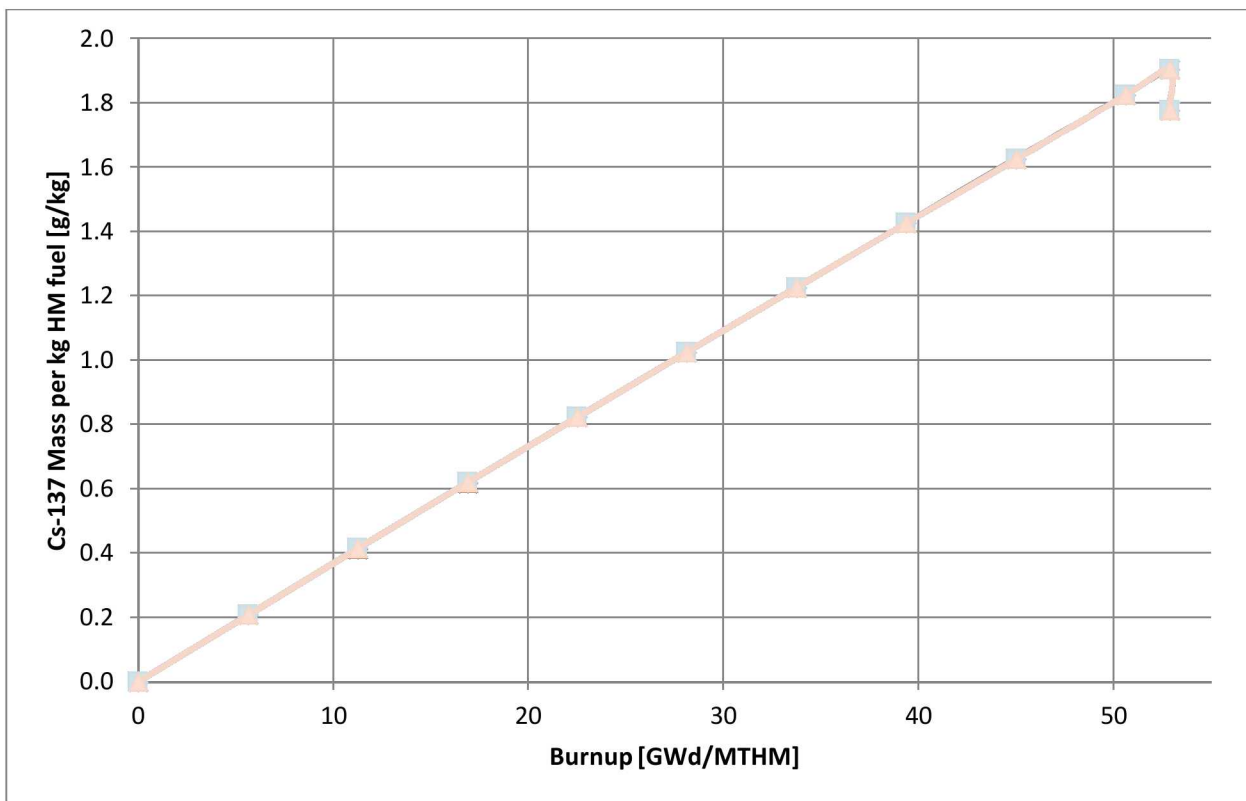


Figure 38. PWR  $^{137}\text{Cs}$  Mass variance based on beginning to end of life neutron spectrum changes

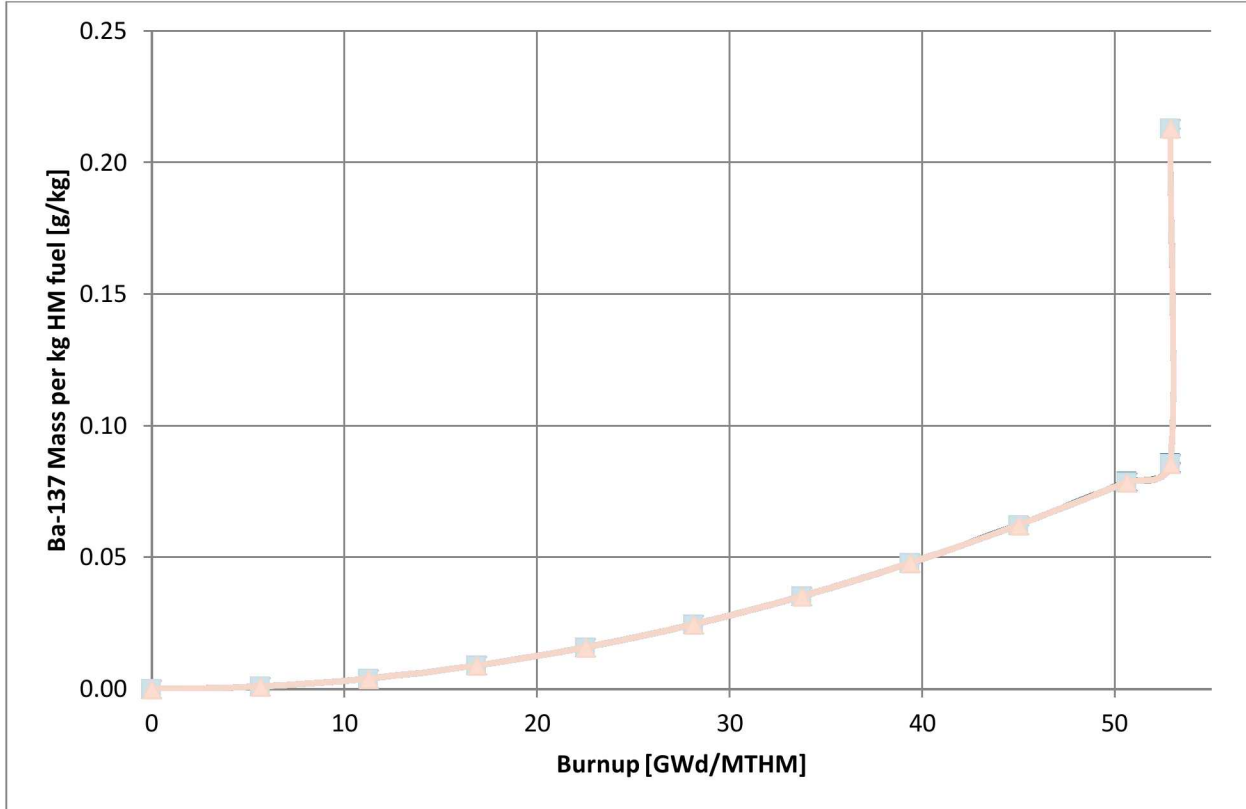


Figure 39. PWR  $^{137}\text{Ba}$  Mass variance based on beginning to end of live neutron spectrum changes

$^{137}\text{Ba}$  had standard deviations slightly higher than  $^{137}\text{Cs}$  ranging from 0.0% to 0.046%, which was on the order of round off error.

$^{148}\text{Nd}$  had higher variance than the 137 mass chain and the results are shown in

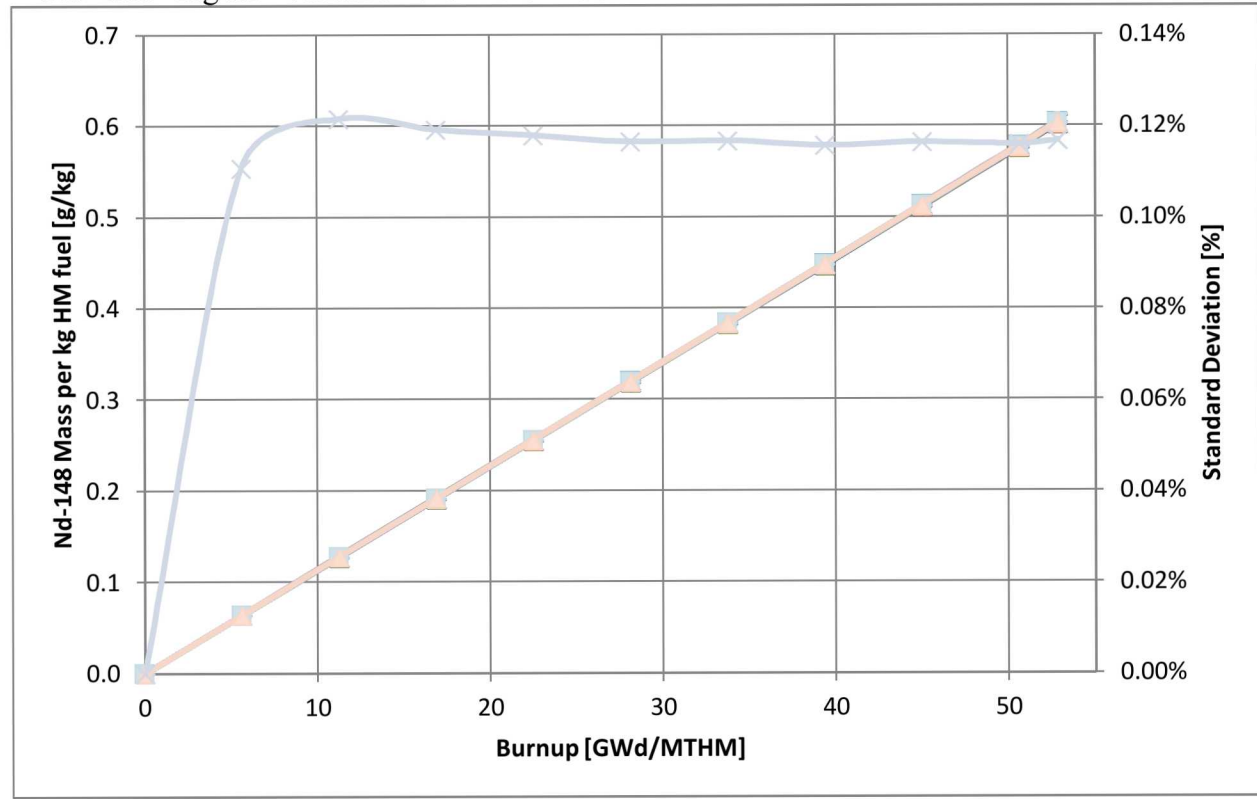
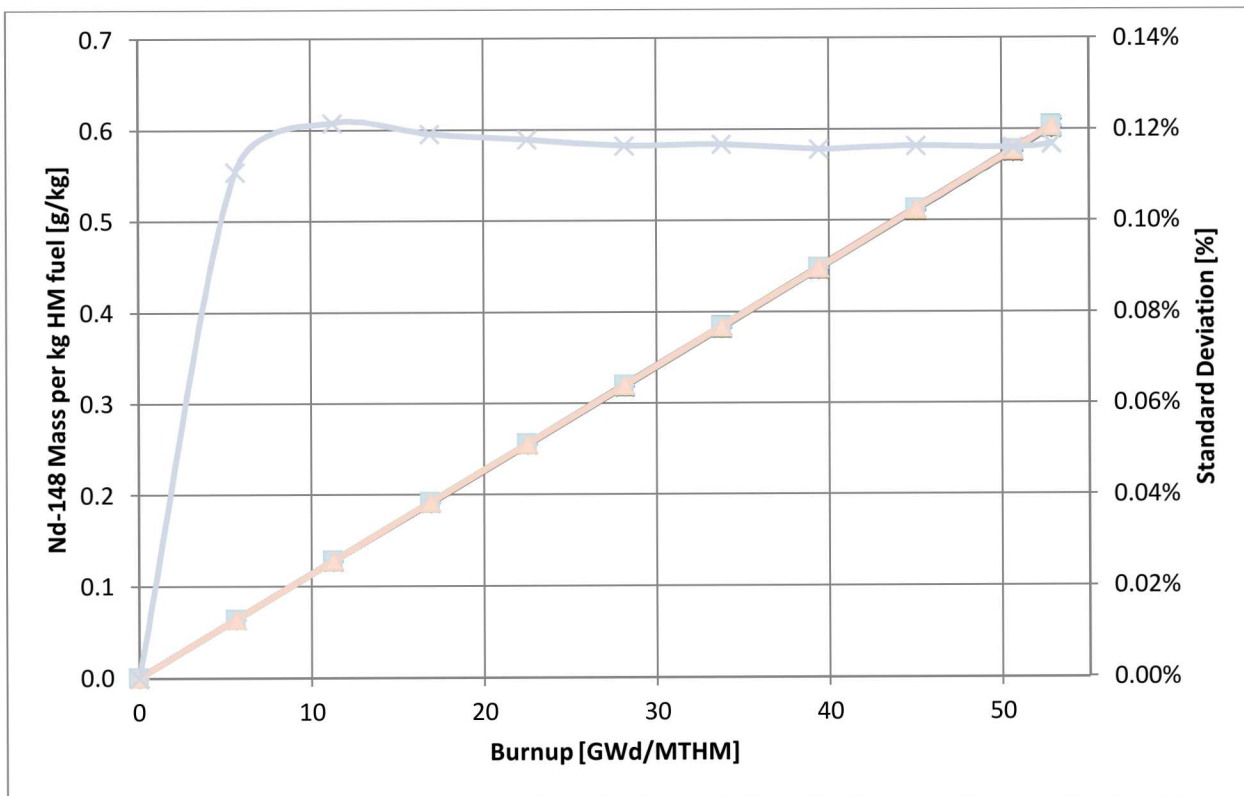
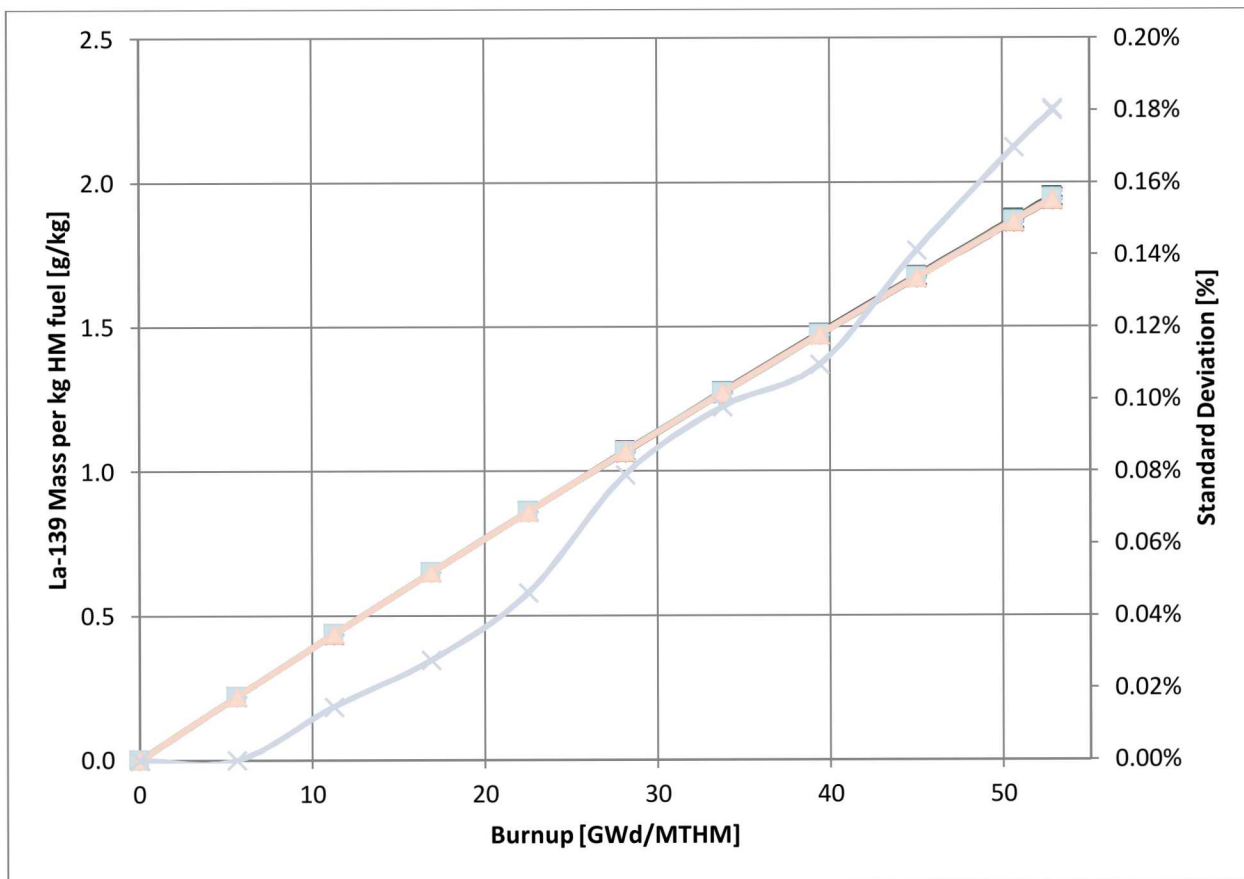


Figure 40. The  $^{148}\text{Nd}$  standard deviation was pretty consistent independent of burnup, at approximately 0.12% throughout the life of the fuel.



**Figure 40. PWR  $^{148}\text{Nd}$  Mass variance based on beginning to end of life neutron spectrum changes**

$^{139}\text{La}$  resulted with higher variance in the PWR model than MTR. In the MTR model, the standard deviations were on the order of round off error, often zero, while in the PWR model these steadily increased as a function of burnup with a final value of 0.18% at the end of life for the fuel. This is still low variance, but more sensitive to spectrum changes than in the MTR environment.



**Figure 41. PWR  $^{139}\text{La}$  Mass variance based on beginning to end of life neutron spectrum changes**

$^{145}\text{Nd}$  and  $^{146}\text{Nd}$  were analyzed and had similar results to the MTR fuel. As  $^{145}\text{Nd}$  accumulated, its absorption cross section is attributed for variance as the neutron spectrum was perturbed. These absorptions created additional variance in  $^{146}\text{Nd}$ .

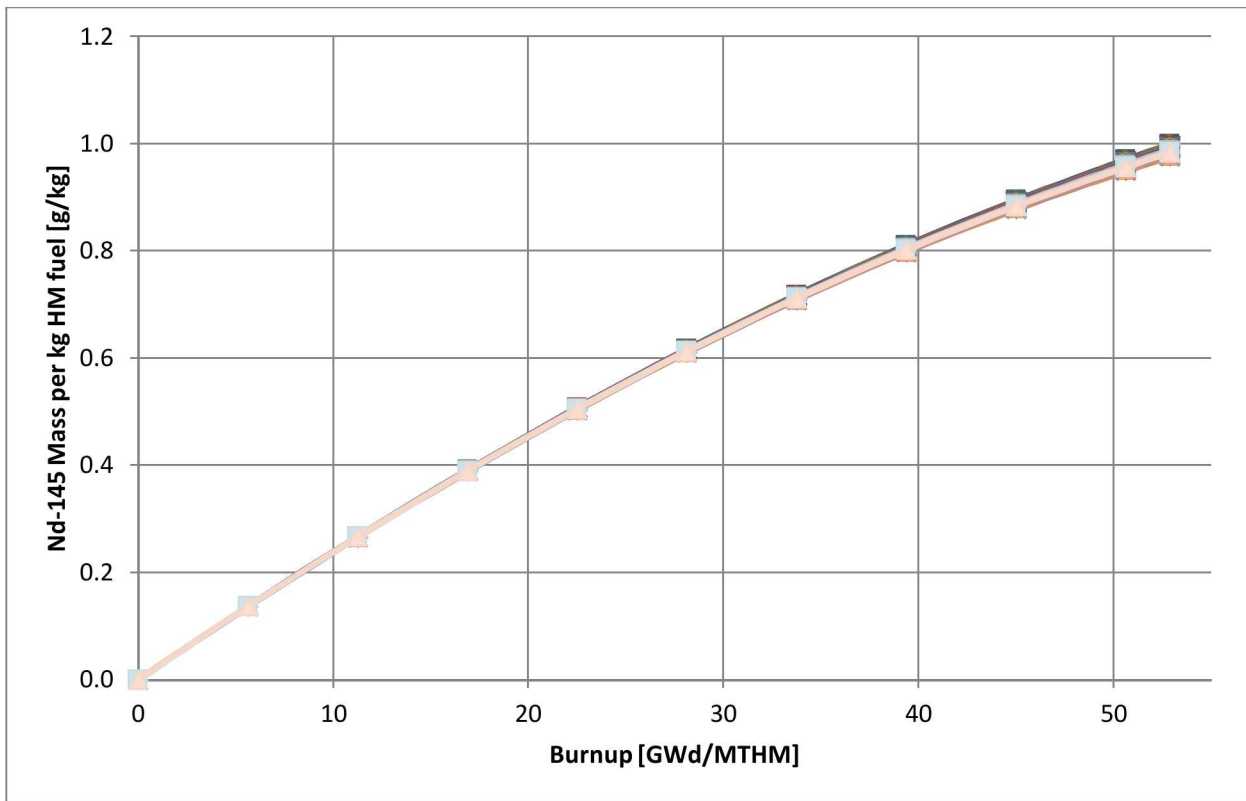


Figure 42. PWR  $^{145}\text{Nd}$  Mass variance based on beginning to end of life neutron spectrum changes

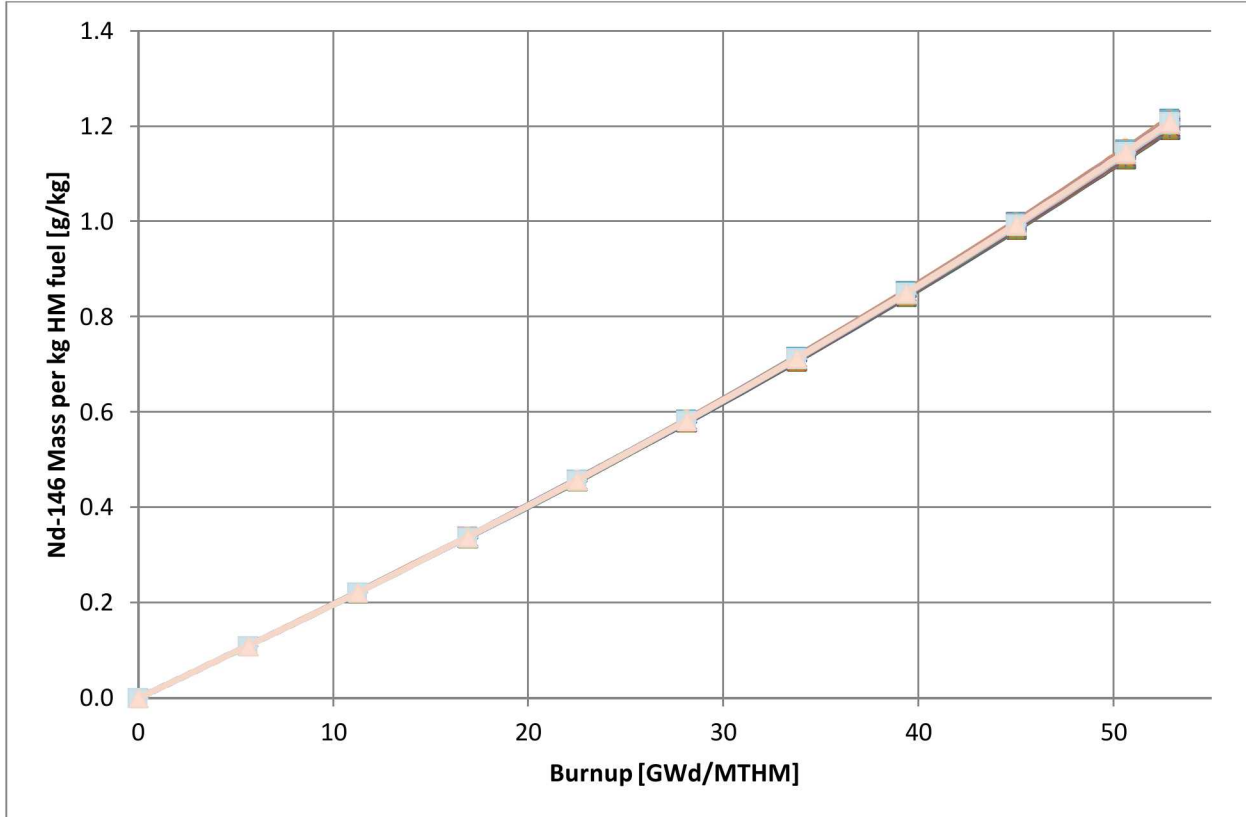


Figure 43. PWR  $^{146}\text{Nd}$  Mass variance based on beginning to end of life neutron spectrum changes

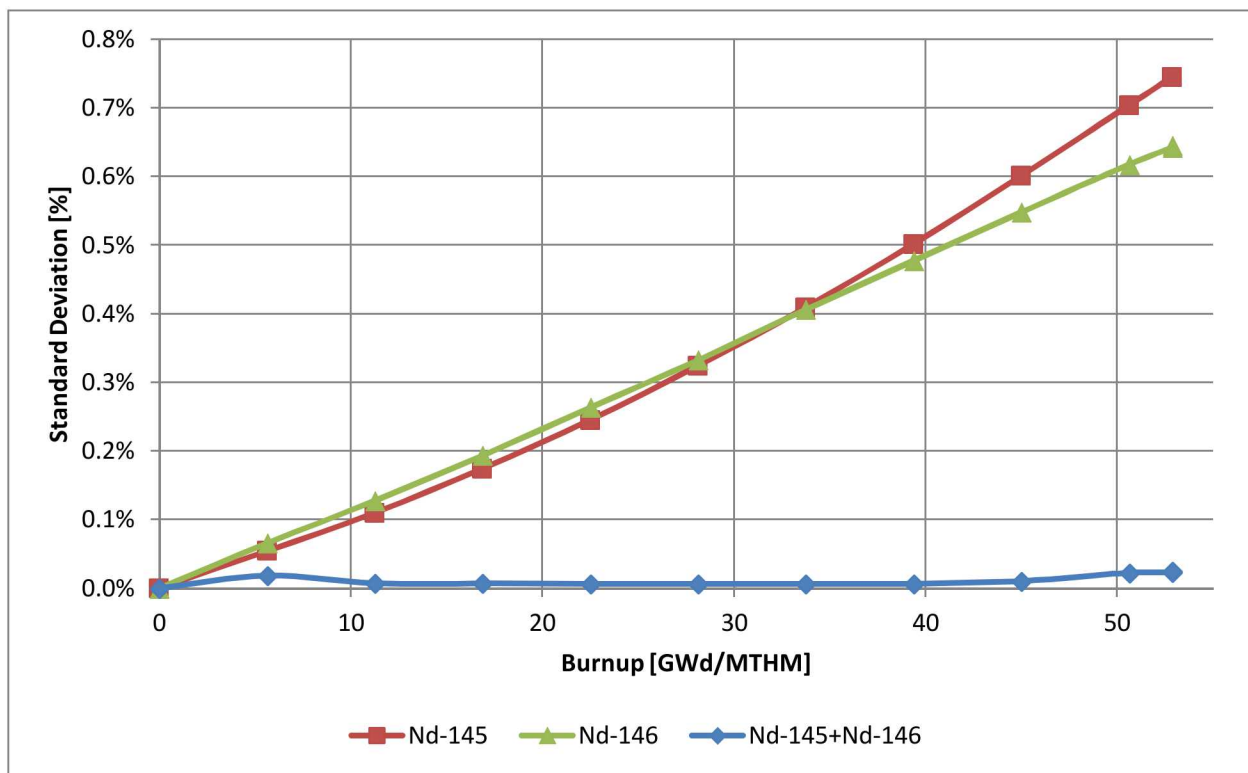


Figure 44. PWR  $^{145}\text{Nd}$  and  $^{146}\text{Nd}$  resulting standard deviations

None of the AP1000 cross-section library benchmarks showed high standard deviations. In general, the isotopes of interest were not sensitive to small spectrum perturbations.

### 5.2.3 PWR 0D Inverse Analysis Results

The developed AP1000 PWR cross-section libraries were benchmarked in the iterative forensic analysis system. The libraries benchmarked were created from the spectra at burnup levels of 4.995, 19.53, 29.81, 47.32, and 52.84 all in units of GWd/MTHM. The simulated measured data originates from a detailed full core analysis with 3 zone fuel shuffling. The  $^{234}\text{U}$  content was not tracked in the benchmark data, so it was omitted.

Table 17. PWR Inverse Analysis Results Using 0D Forward Model with PWRU Cross Sections

	True Solution	Reconstructed Result	Error [%]
Analytic Burnup [GWd/MTHM]	52.8	50.02	5.41%
Analytic $^{235}\text{U}$ Enrichment [%]	4.80	6.140	24.50%
Numerical Burnup [GWd/MTHM]	52.8	51.05	3.37%
Numerical $^{235}\text{U}$ Enrichment [%]	4.80	4.728	1.51%
Cooling Time [a]	30.0	30.35	1.16%
Cooling Time [a]	30.0	32.28	7.32%

The PWRU cross-section library that comes with the ORIGEN code produced results with more error than the MTR benchmarks. The fundamental difference is the lower enrichment. For enrichments under 75% in  $^{235}\text{U}$ , the system uses isotopic ratios for burnup to  $^{238}\text{U}$  and for enrichments over 75% in  $^{235}\text{U}$ , the system uses  $^{235}\text{U}$ . This increases stability in the system. Another difference is that the PWR shuffling pattern exposes the fuel to different neutron flux spectrum environments throughout the life of the fuel; it is more difficult to replicate the final isotopic composition using only one spectrum.

**Table 18. PWR Inverse Analysis Results Using 0D Forward Model with 4.995 GWd/MTHM Cross Sections**

	True Solution	Reconstructed Result	Error [%]
Analytic Burnup [GWd/MTHM]	52.8	50.02	5.41%
Analytic $^{235}\text{U}$ Enrichment [%]	4.80	6.140	24.50%
Numerical Burnup [GWd/MTHM]	52.8	51.06	3.35%
Numerical $^{235}\text{U}$ Enrichment [%]	4.80	4.707	1.96%
Cooling Time [a]	30.0	30.34	1.13%
Cooling Time [a]	30.0	32.28	7.32%

The next cross-section library was created in the inner third of the reactor core at a burnup level of 19.53 GWd/MTHM.

**Table 19. PWR Inverse Analysis Results Using 0D Forward Model with 19.53 GWd/MTHM Cross Sections**

	True Solution	Reconstructed Result	Error [%]
Analytic Burnup [GWd/MTHM]	52.8	50.02	5.41%
Analytic $^{235}\text{U}$ Enrichment [%]	4.80	6.140	24.50%
Numerical Burnup [GWd/MTHM]	52.8	51.07	3.33%
Numerical $^{235}\text{U}$ Enrichment [%]	4.80	4.707	1.96%
Cooling Time [a]	30.0	30.35	1.16%
Cooling Time [a]	30.0	32.28	7.32%

The next cross-section library was created in the inner third of the reactor core at a burnup level of 29.81 GWd/MTHM.

**Table 20. PWR Inverse Analysis Results Using 0D Forward Model with 29.81 GWd/MTHM Cross Sections**

	True Solution	Reconstructed Result	Error [%]
Analytic Burnup [GWd/MTHM]	52.8	50.02	5.41%
Analytic $^{235}\text{U}$ Enrichment [%]	4.80	6.140	24.50%
Numerical Burnup [GWd/MTHM]	52.8	51.07	3.33%
Numerical $^{235}\text{U}$ Enrichment [%]	4.80	4.710	1.89%
Cooling Time [a]	30.0	30.35	1.16%
Cooling Time [a]	30.0	32.28	7.32%

The next cross-section library was created in the middle third of the reactor core, after the fuel had been shuffled outward. This library represents the neutron spectrum at a burnup of 47.32 GWd/MTHM.

**Table 21. PWR Inverse Analysis Results Using 0D Forward Model with 47.32 GWd/MTHM Cross Sections**

	True Solution	Reconstructed Result	Error [%]
Analytic Burnup [GWd/MTHM]	52.8	50.02	5.41%
Analytic $^{235}\text{U}$ Enrichment [%]	4.80	6.140	24.50%
Numerical Burnup [GWd/MTHM]	52.8	51.06	3.35%
Numerical $^{235}\text{U}$ Enrichment [%]	4.80	4.725	1.57%
Cooling Time [a]	30.0	30.35	1.16%
Cooling Time [a]	30.0	32.28	7.32%

The final cross-section library was created in the outer third of the reactor core, after the fuel had been shuffled outward once again. This library represents the neutron spectrum at the full burnup of 52.84 GWd/MTHM.

**Table 22. PWR Inverse Analysis Results Using 0D Forward Model with 52.84 GWd/MTHM Cross Sections**

	True Solution	Reconstructed Result	Error [%]
Analytic Burnup [GWd/MTHM]	52.8	50.02	5.41%
Analytic $^{235}\text{U}$ Enrichment [%]	4.80	6.140	24.50%
Numerical Burnup [GWd/MTHM]	52.8	51.06	3.35%
Numerical $^{235}\text{U}$ Enrichment [%]	4.80	4.722	1.64%
Cooling Time [a]	30.0	30.35	1.16%
Cooling Time [a]	30.0	32.28	7.32%

At all burnup levels benchmarked, very similar results were produced. The slight perturbations in the neutron spectra had little to no effect on the reconstruction accuracy for this model. In some cases, the libraries created more error in the reconstruction results. It is recommended for PWR fuel to simply use the PWRU library that comes with the ORIGEN code.

### 5.2.4 PWR 2D Reconstruction results

A 2D pin cell model was developed for the AP1000 fuel. The model is a basic 1cm tall pin in water and uses reflective boundary conditions in all X, Y, and Z edges. This simulates an infinite lattice of pins that is infinite in the z-dimension, creating a 2D model. Figure 45 is a graphic representation of the model.

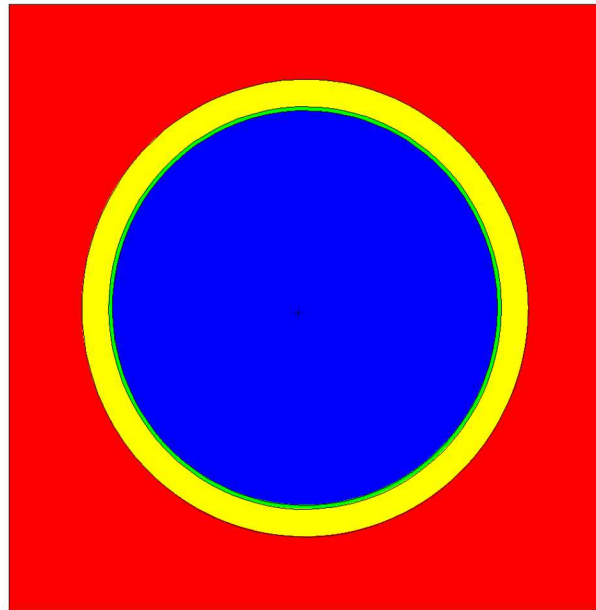


**Figure 45. 2D AP1000 PWR Pincell Model XY plane**

In Figure 45Figure 1, the blue represents the fuel meat, thin green layer represents a helium air gap, and the yellow represents the zircaloy cladding. The red material is the water and is surrounded by void.

The same measured data from the 0D inverse analysis models was used and reconstruction results are shown in Table 23.

**Table 23. PWR Inverse Analysis Results Using 2D Forward Model**

	True Solution	Reconstructed Result	Error [%]
Analytic Burnup [GWd/MTHM]	52.8	50.02	5.41%
Analytic $^{235}\text{U}$ Enrichment [%]	4.80	6.140	24.50%
Numerical Burnup [GWd/MTHM]	52.8	58.75	10.67%
Numerical $^{235}\text{U}$ Enrichment [%]	4.80	4.795	0.10%
Cooling Time [a]	30.0	30.34	1.13%
Cooling Time [a]	30.0	32.28	7.32%

Using the 2D model in the inverse analysis produced similar results to the 0D simulations with the exception of burnup. The burnup in the 2D model was over predicted by approximately 10%. There are two potential contributors to this over prediction, adjustments needed for fissioning  $^{239}\text{Pu}$ . The recoverable energy per fission in the MONTEBURNS skeleton file may need adjustment to account for accumulation of burning  $^{239}\text{Pu}$ . The 2D model did produce greater accuracy in reconstructed initial  $^{235}\text{U}$  enrichment result.

## 6 CONCLUSIONS

The fidelity of forward models within a spent fuel forensic analysis system was improved by using two methods. The first method consisted of developing a system to create accurate one-group neutron cross-section libraries for any user specified model. These libraries could be housed in a database and then used for analyzing unknown fuel samples. The forensic analysis system for spent fuel resulted in higher accuracy at predicting the initial uranium isotopic compositions and burnup from spent fuel samples.

The second method consisted of implementing 2D/3D reactor depletion codes as the forward model within the system's framework. This method would allow the usage of potentially recoverable geometric information from an unknown sample. No predetermined cross-section library is required for the system using this method, therefore potentially reducing model error associated with the neutron flux spectrum. The accuracy of the recovered initial uranium isotopic compositions and burnup from spent fuel samples was also improved using this method, even more so than the first. However, additional research may be required to determine the ideal fission yield and recoverable energy per fission for cases where significant amounts of  $^{239}\text{Pu}$  are bred and burned throughout the life of the fuel.

## 7 REFERENCES

1. International Atomic Energy Agency, IAEA Research Reactor Status July 2011, Technical Report, International Atomic Energy Agency, July 2011.
2. Pablo Adelfang and Iain G. Ritchie, Overview of the status of research reactors worldwide, In *Proceedings from 2003 International Meeting on Reduced Enrichment for Research and Test Reactors*, Chicago, Illinois, 2003.
3. World Nuclear Association, Nuclear Power Reactors, <http://www.world-nuclear.org/info/Nuclear-Fuel-Cycle/Power-Reactors/Nuclear-Power-Reactors>, January 2015.
4. Michael M. May and Donald A. Barr, *Nuclear forensics role, state of the art, and program needs*, Technical Report, Joint Working Group of the American Physical Society and the American Association for the Advancement of Science, Washington, DC, February 2008.
5. F. Pointurier, N. Baglan, and P. Hmet, Ultra low-level measurement of actinides by sector field ICP-MS, *Applied Radiation and Isotopes*, 60(2-4):561-566, 2004.
6. Oak Ridge National Laboratory, *ORIGEN 2.2: Isotope Generation and Depletion Code Matrix Exponential Method*, Oak Ridge: Department of Energy, RSICC, 2002.
7. *MCNP User Manual*, Version 6, LA-CP-00634, rev0, Los Alamos National Laboratory, May 2013.
8. David I. Poston and Holly R. Trellue, *User's Manual, Version 1.0 for MONTEBURNS, Version 3.01*, 1998.
9. Matthew R. Sternat, Development of Technical Nuclear Forensics for Spent Research Reactor Fuel, Ph.D. dissertation, Texas A&M University, 2012.
10. Adrienne M. LeFleur and William S. Charlton, A method for determining material attributes from post-detonation fission product measurements of an HEU device, In *Proceedings from Institute of Nuclear Materials Management 2006 Annual Conference*, Nashville, Tennessee, 2006.
11. Oak Ridge National Laboratory, Oak Ridge Research Reactor: Appendix A, Technical Report, United States Department of Energy, 1997.
12. Oak Ridge National Laboratory, Oak Ridge Research Reactor Appendix F: Evaluation of Fuel Element Powers,  $^{235}\text{U}$  Masses, and Burnups from the Gamma Scanning of Full-Sized Fuel Elements, Technical Report, United States Department of Energy, 1997.

13. "Westinghouse AP1000 Design Control Documentation Rev. 16," Tier 2, Chapter 4, Reactor Section 4.3, Nuclear Design. ML071580897 (2007).

## 9 DISTRIBUTION LIST

1	MS1136	David Ames, 6221
1	MS1371	Dianna Blair, 06832
1	MS1373	Kent Biringer, 06834
1	MS1373	Matthew Sternat, 6832
1e	MS0899	D. Chavez, LDRD Office, 1911
1e	MS0899	Techincal Library, 9536

THIS PAGE INTENTIONALLY LEFT BLANK



**Sandia National Laboratories**